Dynamics of microbial pollution in aquatic systems

Matthew Richard Hipsey

B.Sc (Hons) (Environmental Science)
M.Eng.Sc (Environmental Engineering)

This thesis is presented for the degree of
Doctor of Philosophy of
The University of Adelaide

School of Earth and Environmental Sciences
May 2007

Table of Contents

List of Figures

List of Tables

Abstract

Microbial pollution of surface waters and coastal zones is one of the foremost challenges facing the water industry and regulatory authorities. Yet despite the concern and increasing pressures on water resources in both developed and developing countries, understanding of microbial pollutants in the aquatic environment is fairly scattered. There is a need for an improved ability to quantify the processes that control the fate and distribution of enteric organisms to support decision-making and risk-management activities. The aim of this thesis has been to advance the understanding of the dynamics of microbial pollution in aquatic systems through review, experimentation and numerical modelling.

Initially, a new module for simulating the protozoan pathogen, *Cryptosporidium*, was developed and implemented within a three-dimensional (3D) coupled hydrodynamic-water quality model (ELCOM-CAEDYM). The coupled 3D model was validated against a comprehensive dataset collected in Myponga Reservoir (South Australia), and without calibration, performed to a high degree of accuracy. The investigation then sought to examine the experimental dataset in more detail and found a significant difference between protozoan pathogens and the bacterial and viral indicators. To examine the role of bacterial association with particles in more detail, a second experimental campaign was carried out in Sugarloaf Reservoir (Victoria). This campaign was used to gain insights into the association of coliform bacteria with suspended sediment and to quantify their sedimentation dynamics based on *in situ* measurements. Using an inverse technique, particle profile data was used to create a simple Lagrangian model that was applied to back-calculate the sedimentation rates of the coliform bacteria and the fraction that were attached to the particles. The results indicated that 80 – 100% were associated with a small-sized clay fraction. This result was in contrast with the *Cryptosporidium* dynamics in Myponga Reservoir, where it was concluded that oocysts did not settle with the inorganic particles.

These findings indicated the current models for simulating the array of organisms of interest to regulatory authorities are inadequate to resolve the level of detail necessary for useful predictions and risk management. Large differences between the protozoa, bacteria and phages were being observed due to different particle association rates and sedimentation dynamics, order of magnitude differences in natural mortality rates, and different sensitivity to sunlight bandwidths. The original model implemented within CAEDYM was therefore rewritten to be more complete and generic for all microbial pollutants and different types of aquatic systems. The model was built using a generic set of parameterizations that describe the dynamics of most protozoan, bacterial and viral organisms of interest. The parameterizations dynamically account for sensitivities to environmental conditions, including temperature, salinity, pH, dissolved oxygen, sunlight, nutrients and turbidity, on the growth and mortality of enteric organisms.

The new model significantly advances previous studies in several areas. First, inclusion of the growth term allows for simulation of organisms in warm, nutrient rich environments, where typical die-off models tend to over-predict loss rates. Second, the natural mortality term has been extended to independently account for the effects of salinity and pH, in addition to temperature. The salinity–mediated mortality has also been adapted to account for the nutrient status of the medium to simulate the importance of nutrient starvation on the ability of an organism to survive under osmotic stress. Third, a new model for sunlight-mediated mortality is presented that differentially accounts for mortality induced through exposure to visible, UV-A and UV-B bandwidths. The new expression has capacity to simulate the photo-oxidative and photo-biological mechanisms of inactivation through included sensitivities to dissolved oxygen and pH. Fourth, the model allows for organisms to be split between free and attached pools, and sedimented organisms may become resuspended in response to high shear stress events at the water-sediment interface caused by high velocities or wind-wave action. Fifth,

the enteric organism module has been implemented within the bio-geochemical model CAEDYM, thereby giving it access to dynamically calculated concentrations of dissolved oxygen, organic carbon, and suspended solids, in addition to pH, shear stress and light climate information.

Without adjustment of the literature derived parameter values, the new model was validated against a range of microbial data from three reservoirs that differed in their climatic zone, trophic status and operation. The simulations in conjunction with the experimental data highlighted the large spatial and temporal variability in processes that control the fate and distribution of enteric organisms. Additionally, large differences between species originate from variable rates of growth, mortality and sedimentation and it is emphasized that the use of surrogates for quantifying risk is problematic. The model can be used to help design targeted monitoring programs, examine differences between species and the appropriateness of surrogate indicators, and to support management and real-time decision-making. Areas where insufficient data and understanding exist are also discussed.

This work contains no material which has been accepted for the award of any other degree or diploma in any university or other tertiary institution and, to the best of my knowledge and belief, contains no material previously published or written by another person, except where due reference has been made in the text.

I give consent to this copy of my thesis being made available in the University Library.

The author acknowledges that copyright of published works contained within this thesis (as listed below) resides with the copyright holder(s) of those works.

Signed …….. Date……..

Acknowledgements

Numerous people have been either directly or indirectly instrumental in enabling the completion of this thesis. This would not have been possible without the patience and help of my two main advisors Dr. Justin Brookes and Dr. Jason Antenucci. I am also grateful to Jason for the freedom he has given me, whilst juggling the dual demands of working and completing this thesis. I would also like to offer a special thanks to Assoc. Prof. George Ganf at the University of Adelaide for facilitating my candidature whilst working remotely at CWR.

Much of the work and data presented in this thesis was made possible through a grant from the American Water Works Association Research Foundation (AwwaRF), under project #2752 "Hydrodynamic distribution of pathogens in lakes and reservoirs" (view project summary online at: http://www.awwarf.org/research/topicsandprojects/execSum/2752.aspx). In addition to AwwaRF, I would like to acknowledge the contribution by the project Chief Investigator, Mike Burch, from the Australian Water Quality Centre in Adelaide for his very competent management of this ambitious research project. The project also was supported with additional cash and in-kind funding support from the following organizations:

CRC for Water Quality and Treatment
Melbourne Water Corporation
Sydney Catchment Authority
South Australian Water Corporation

The advice of the Project Advisory Committee (PAC) – including Rhea Williamson, Ronald Coss, Robin Oshiro, Thomas Mahin and particularly Linda Reekie, the AwwaRF Project Manager, is also greatly appreciated.

Although much of the thesis focuses on modelling and numerical prediction of enteric organisms, a significant component relies on field data collected during two intensive field campaigns. Both the field campaigns were logistically challenging and involved a large effort from numerous people. For their contribution in making these campaigns successful, I would like to acknowledge: Peter Hobson for input into various aspects of the project, including assistance with the preparation of the QA Plan, and during field work for the validation studies; Leon Linden who made a significant contribution to the field work at Myponga Reservoir; Melita Stevens, Kathy Cinque and Karyn Hunter from Melbourne Water were instrumental in assisting to plan and carry out field work for model verification at Sugarloaf Reservoir; Warwick Grooby, Kerry Cabaretta and the Microbiology and Protozoology Laboratories at the Australian Water Quality Centre for their efforts in processing massive numbers of microbiological samples over a short period of time collected as part of model validation exercises; Rod Boothy, Alan Brown and Viv Allan provided excellent logistical support for field work at Myponga Reservoir. Data from Billings Reservoir in Brazil was provided courtesy of Companhia de Tecnologia de Saneamento Ambiental (CETESB).

At the Centre for Water Research at the University of Western Australia, I wish to acknowledge the contribution of Prof. Jörg Imberger and Dr. José Romero for their advice and input regarding model development and application. My thanks are also given to Jörg for his seemingly endless enthusiasm and support and for helping facilitate my completion of this thesis whilst still working at CWR. I also wish to acknowledge the opportunity offered to me early in my career, which was the custodianship of the model CAEDYM - much of this thesis would not have been possible if it was not for years of experience developing such a multi-disciplinary model and daily exposure to the CAEDYM source code.

Finally, I would like to thank my family; to my parents for teaching me curiosity and commitment, to my wife, Van, who has always been supportive, patient and forgiving, and to my son Daniel, who always knows how to make me smile.

Preface

The main body of this thesis is comprised of six chapters (2-7). Chapter 2 is preliminary hydrodynamic modelling work conducted on several reservoirs proposed for use during the research program. Although it may seem somewhat peripheral to the main focus of the thesis, it forms the backbone of many of the predictions presented later on since all the systems simulated depend on the integrity of the 3D hydrodynamic predictions. Additionally, this work was performed prior to the field campaigns, and so these simulations served as virtual environmental laboratories and enabled testing of hypotheses and sampling regimes prior to committing to the field experiments.

The remaining chapters (3-7) are independent papers written for journal publication. Each of these papers contains an introduction that includes a review of the relevant literature. To avoid unnecessary duplication, Chapter 1 does not seek to provide a comprehensive review of the literature pertaining to the entire thesis, but rather to place the individual papers in the context of the overall work. Similarly, Chapter 8 draws together the conclusions from each of the individual papers and serves to synthesize the individual chapters into a single body of work.

Chapter 3 has been published in the *International Journal for River Basin Management* as "A three dimensional model of *Cryptosporidium* dynamics for lakes and reservoirs – a new tool for risk management", by M.R. Hipsey, J.P. Antenucci, J.D. Brookes, M.D. Burch, R.H. Regel and L. Linden, Volume 2(3), pp. 181-197 (2004). Copyright for this paper belongs to the International Association for Hydraulic Research.

Chapter 4 has been published in the journal *Environmental Science and Technology* as "The relative value of surrogate indicators for detecting pathogens in lakes and reservoirs", by J.D. Brookes, M.R. Hipsey, M.D. Burch, R.H. Regel, L. Linden, C.M. Ferguson and J.P. Antenucci, Volume 39(22), pp. 8614-8621 (2005). Copyright for this paper belongs to the American Chemical Society.

Chapter 5 has been published in the *Journal of Water, Air and Soil Pollution* as "*In situ* evidence for the association of Total Coliforms and *Escherichia coli* with suspended inorganic particles in an Australian reservoir" by M.R. Hipsey, J.D. Brookes, R.H. Regel, J.P. Antenucci and M.D. Burch, Volume 170(1-4), pp. 191-209 (2006). Copyright of this article belongs to Springer Publishers.

Chapter 6 is in preparation for submission to the journal *Water Research* as "A generic, process-based model of microbial pollution in aquatic systems" by M.R. Hipsey, J.P. Antenucci and J.D. Brookes.

Chapter 7 is a brief summary article aimed at lake and reservoir engineers, and outlines the tools and options available for assisting with microbial pollution problems. It appeared in the periodical *LakeLine* as "Decision support tools for managing microbial pollution in lakes and reservoirs", by M.R. Hipsey, J.P. Antenucci, and J.D. Brookes, Volume 24(4), pp. 25-28 (2004).

Various components of the work have also been presented in other papers and at conferences, but have not been included in the thesis directly. These include:

- Antenucci, J.P., Brookes, J.D. and Hipsey, M.R. A simple model for quantifying *Cryptosporidium* transport, dilution and potential risk in reservoirs. *J. AWWA*, 97(1): 86-93 (2005).
- Brookes, J.D., Antenucci, J.P., Hipsey, M.R., Burch, M.D., Ashbolt, N.J. and Ferguson, C.M. Fate and transport of pathogens in lakes and reservoirs, *Environ. Intl.*, 30: 741-759 (2004).

- Brookes, J.D., Davies, C.M., Hipsey, M.R. and Antenucci, J.P. Association of *Cryptosporidium* with bovine faecal particles and implications for risk reduction by settling within water supply reservoirs. *Water and Health*, 4(1): 87-98 (2006).
- Hipsey, M.R., Antenucci, J.P. and Brookes, J.D. Coupling a *Cryptosporidium* fate model to a 3D hydrodynamic model: results from Myponga Reservoir, SA. *Australian Water Association 20th Convention - 2003 OzWater Conf.*, Perth, Western Australia, 2003.
- Hipsey, M.R., Brookes, J.D. Antenucci, J.P. and Burch, M.D. Field and modelling evidence for pathogen behaviour in drinking water reservoirs. *Australian Society for Limnology Annual Conf*., Warnambool, Victoria, Australia, 2003.
- Hipsey, M.R., Antenucci, J.P., Brookes, J.D., Burch, M.D. and Regel, R.H. Simulation tools for minimizing pathogen risk in drinking water reservoirs. *6th International Conf. on Hydroinformatics*, Singapore, 2004.
- Hipsey, M.R., Antenucci, J.P. and Brookes, J.D. A new process-based model of enteric organism dynamics in natural waters. *7th International Conf. on Hydroscience and Engineering*, Philadelphia, USA, 2006.

CHAPTER 1

INTRODUCTION

An Emerging Threat

Pathogen contamination of water systems has become a frequent occurrence in both developing and developed countries across the globe (Herwaldt *et al*., 1992; Moore *et al*., 1994; MacKenzie *et al*., 1994; Lisle and Rose, 1995; Zuckerman *et al*., 1997; Gibson *et al*., 1998; Hsu *et al*., 2000; Howe *et al*., 2002; Belkin and Colwell, 2006). The pathogens of concern vary between systems depending on the nature of their source and the intended use of the water. Due to their longetivity and resistance to conventional treatment technologies the (oo)cysts of the protozoan organisms *Cryptosporidium* spp. and *Giardia* spp. are a typical concern in water bodies used for drinking water (Robertson *et al*., 1992). In poorly treated drinking water stores and recreational waters (both fresh and marine), other problem organisms include bacteria such as *Salmonella* spp., *Shigella* spp., *Vibrio* spp. *Clostridium* spp. and *Staphylococcus aureus,* and numerous human enteric viruses such as those from the genera *Enterovirus*, *Hepatovirus*, *Rotavirus* and *Norovirus* (Fong and Lipp, 2006). Accordingly, the nature of disease caused by these organisms is also widely variable, and Table 1.1 lists the most common forms.

Most concern is given to the allochthonous enteric microorganisms, which enter via an external loading, although in certain locations some autochthonous pathogens may also be important (*e.g. Vibrio cholerae*). The allochthonous sources typically occur when heavy rains washing infected material from surrounding agricultural or urban catchments into the floodwaters that supply the waterbody, or when effluent is discharged directly into watercourses (Figure 1.1). These two major sources present a risk to humans through three main routes of exposure: direct consumption of microorganisms within drinking water (fresh only), recreational contact (fresh, estuarine and marine), and consumption of microorganisms that have bio-accumulated within the tissues of consumable shellfish (estuarine and marine) (Figure 1.2).

Table 1.1: Summary of common water-borne diseases.

Disease	Agent	Symptoms
Amebiasis	Protozoan (*Entamoeba histolytic*)	Abdominal pain, fatigue, weight loss, diarrhoea
Campylobacteriosis	Bacterium (*Campylobacter jejuni*)	Fever, Abdominal pain, fatigue, diarrhoea
Cholera	Bacterium (*Vibrio cholerae*)	Fever, Abdominal pain, vomiting, diarrhoea
Cryptosporidiosis	Protozoan (*Cryptosporidium parvum*)	Abdominal pain, vomiting, diarrhoea
Diarrhoeagenic *Escherichia coli*	Bacterium (*Escherichia coli* O157:H7)	Acute bloody diarrhoea, abdominal cramps
Giardiasis	Protozoan (*Giardia lamblia*)	Abdominal pain, vomiting, diarrhoea
Hepatitis	Virus (Hepatitis A)	Fever, chills, abdominal pain, jaundice
Salmonellosis	Bacterium (*Salmonella* sp.)	Fever, abdominal cramps, bloody diarrhoea
Shigellosis	Bacterium (*Shigella* sp.)	Fever, diarrhoea, bloody stools
Viral Gastroenteritis	Virus (rotavirus etc.)	Vomiting, diarrhoea, headache, fever

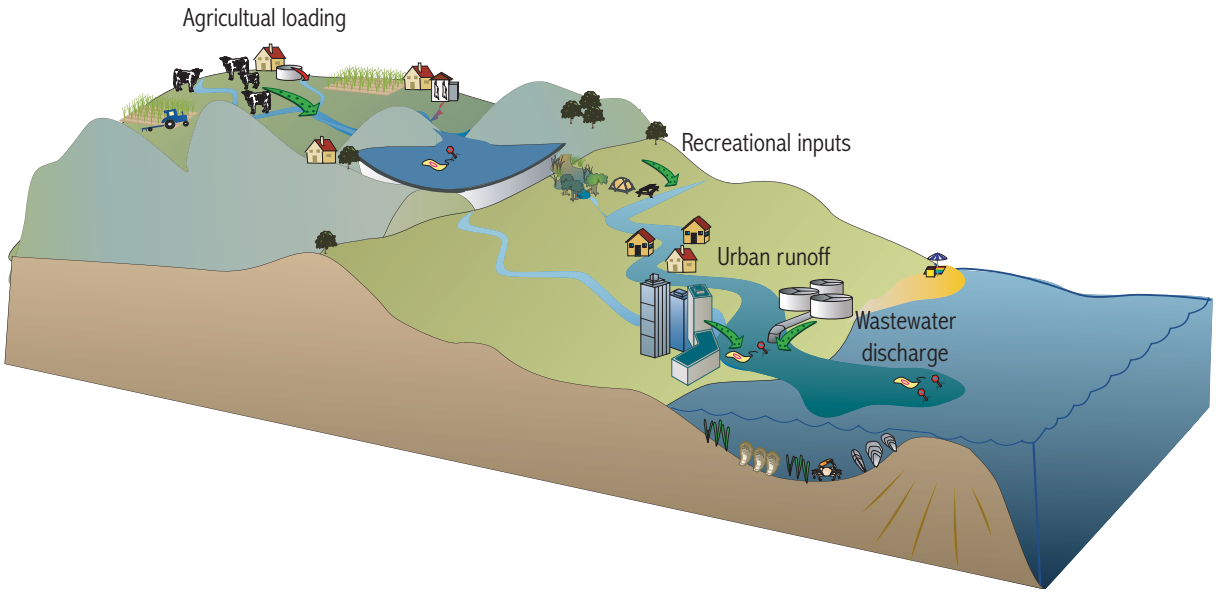

Figure 1.1: Schematic overview of allochthonous microbial sources and receiving aquatic environments from the catchment to the ocean.

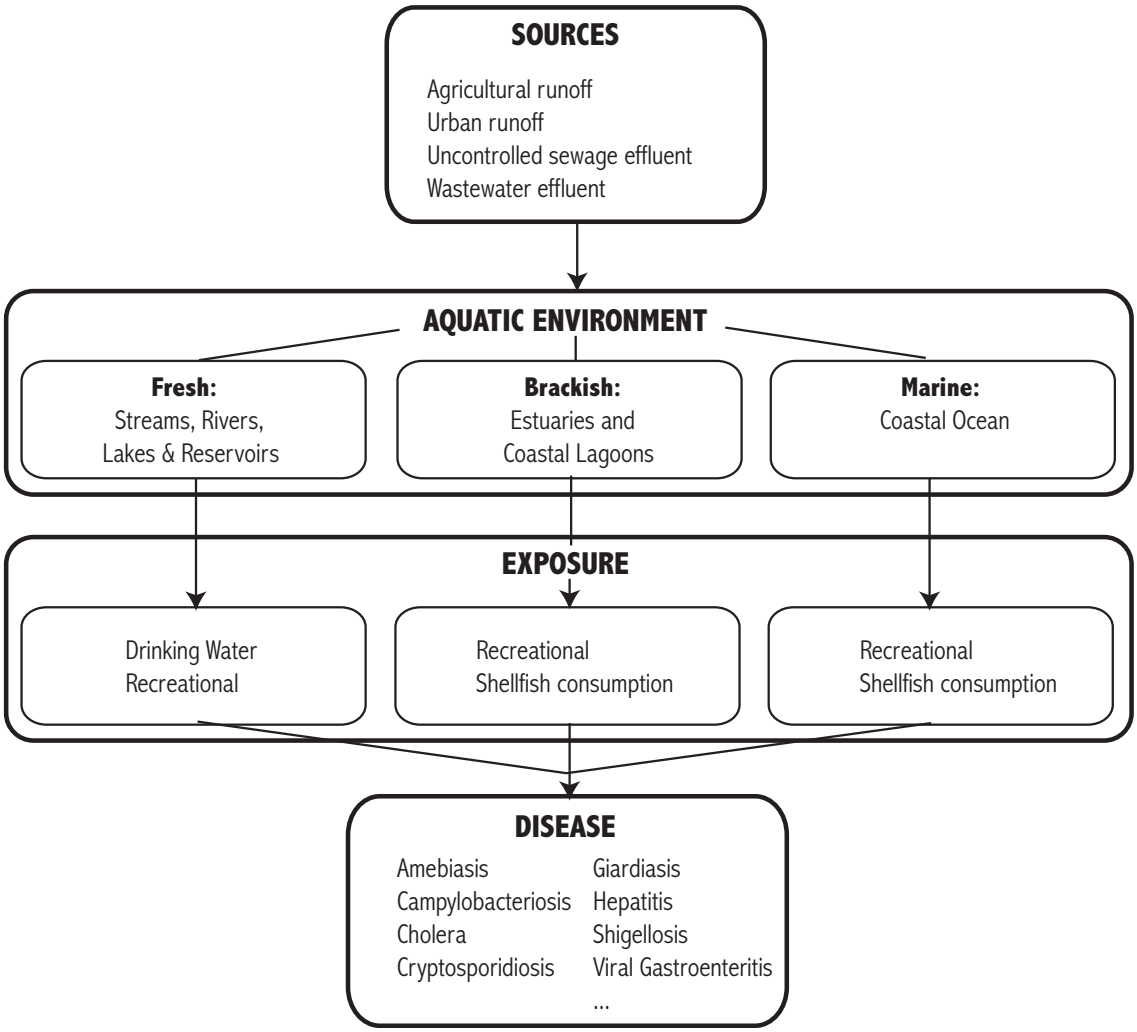

Figure 1.2: Conceptual breakdown of routes of exposure of microbial pollutants.

Surrogates for Indicating Pathogen Threats

The complexity, cost and time constraints associated with the direct enumeration of pathogens to identify their distribution in large water bodies, frequently limits the ability of water managers to detect the intrusion of poorer quality water inflows into the aquatic environment. As a result, there is considerable discussion in regulatory organizations and water utilities as to the value of using surrogates, such as microbial indicator organisms or even physical properties such as turbidity, as a way of detecting the presence of microbial contamination and hence the threat of actual pathogenic organisms. Microbial indicators have the advantage of being low-risk, present in high concentrations relative to other organisms of concern (*i.e.* a high signal to noise ratio), and simple and cheap to enumerate.

The most widely used indicator organisms of microbial pollution are the enteric coliform bacteria, which are gram-negative bacilli that belong to the family *Enterobacteriaceae* (*e.g. Klebsiella* spp., *Enterobacter* spp. *Citrobacter* spp., *Escherichia coli*). Specific coliform measurements include total coliforms, faecal coliforms, and in particular the specific organism *E. coli* (Baudisova, 1997). The latter two are the most common since they are abundant in the faeces of humans and other warm blooded animals, and are hence thought to be a reliable indicator of faecal pollution. Total coliforms are used less frequently since they include organisms from soil and cold-blooded animals. Except for certain strains of pathogenic *E. coli* (*e.g.* O157), coliform bacteria are not a threat to human health, but their high abundance means that they are easy to detect, thereby alerting regulatory authorities to pollution events that may contain other organisms of concern. Other routinely used indicator bacteria include the gram-positive cocci, including Enterococci and faecal streptococci. However, it is now apparent that these bacterial indicators are not suitable for assessing the risk posed by protozoan pathogens and some enteric viruses (Ashbolt *et al*., 2001). Several outbreaks of cryptosporidiosis have now been documented where the water quality met microbiological standards based on bacterial indicators (MacKenzie *et al*., 1994; Lisle and Rose, 1995).

Various bacteriophages are used as index organisms for enteric viruses (Havelaar *et al*., 1993; Armon and Kott 1995; Tartera *et al*., 1989; Cornax and Morinigo, 1991). The single-stranded F-specific RNA (F^+ RNA) bacteriophages (*e.g.* strains *MS-2*, *F2* and *Q beta*) and the double-stranded somatic coliphages (*e.g.* strains T_2, T_7 and $\phi X174$) are routinely measured in fresh and coastal waters. However, faecal bacteriophages are not always suitable index organisms since they are present in a range of animal as well as human faeces, whereas human enteric viruses only originate from human faeces. There have also been reports of human enteric viruses being detected in waters in the absence of bacteriophages (Grabow *et al*., 2001). The rationale for their use as model organisms is based on their similar size and morphology, along with the low cost, ease and speed of detection compared to human enteric virus assays. The ideal host bacteria would be of human faecal origin only, consistently present in sewage in sufficient numbers for detection, and only lysed by phages that do not replicate in another host or the environment. While bacteriophages to *Bacteroides fragilis* strain HSB40 appear to be human specific and do not replicate in the environment (Tartera *et al*., 1989), their phage numbers are too low for general use. Due to their high abundance, studies have focused on the coliphage systems, including the double and single-stranded DNA and RNA-containing phages listed above, and for a range of bacterial hosts. The F^+ RNA coliphages attach to the sides of the bacterial pili that only occur on exponentially growing specific (F^+) strains of *E. coli* or an engineered *Salmonella typhimurium* (strain WG49), and are therefore the current models of choice (Havelaar *et al*., 1993; Grabow, 2001).

The use of spores of the gram-positive bacilli *Clostridium perfringens* has been suggested as a good indicator of human faecal contamination and may correlate with human parasitic protozoa and enteric viruses (Payment and Franco, 1993; Ferguson *et al*., 1996). However, two confounding factors must be considered; first, *C. perfringens* spores are very persistent (Davies *et al*., 1995) and second, they may be excreted by various animals (Leeming *et al*., 1998). Hence, they may show little relationship with

parasitic protozoa in animal-impacted raw waters, and could be misleading about the likely presence of infective human viruses.

Particle counting and turbidity levels have also been identified as potential surrogates of microbial pollution and weak epidemiological evidence exists that suggests waterborne illness from drinking water may be associated with the raw water turbidity (Juranek and Mackenzie, 1998). The use of turbidity alone to predict pathogen presence is difficult because turbidity is dependent on a range of processes that are independent of pathogen presence. For example, it is well established that many young calves are infected with *Cryptosporidium* (Ongerth and Stibbs, 1989), however, calving is timed to coincide with the period when feed is abundant and cows are on a rising plane of nutrition. Consequently, calving and high oocyst numbers occur when catchments are well vegetated, yet this is typically when turbidity is low. Additionally, surrogates such as turbidity are influenced by catchment specific factors such as soil-type distribution and non-grazing land-use such as horticulture that do not correlate with pathogen input. In the ocean, turbidity may be caused through resuspension of sediment during high wind events or strong currents, and therefore may exist unrelated to any catchment or wastewater discharges. Nonetheless, turbidity is a readily measurable parameter that warrants investigation as a potential early warning mechanism.

While no single water quality indicator can reliably assess the bacterial, protozoan and viral contamination of aquatic environments in all circumstances, it is feasible that a suite of surrogates may be identified that will estimate levels of microbial contamination within defined circumstances, such as within a storage reservoir with well characterized inputs. There is therefore a need for a process-based understanding of surrogate organisms in order to develop a model of their behaviour and assess their dynamics relative to their pathogenic counterparts.

Factors Controlling the Fate and Distribution of Enteric Organisms in Surface Waters

Despite numerous decades of research into the fate and distribution of pathogens and microbial indicators, information about the fate of pathogens once they enter a receiving environment remains fairly scattered. Even though some organisms are well studied within the biological and medical literature, studies of their response to the numerous biotic and abiotic pressures that they face within the environment are still ongoing.

Pathogen distribution and transport in rivers, reservoirs, estuaries and the coastal ocean is a function of the pathogen load in the source water (*e.g.* agricultural runoff or direct wastewater discharge), the settling or entrainment characteristics of the particles that they may attach to, and resuspension from sediment by turbulence at the benthic boundary layer. The distribution of organisms will also be impacted by predation by autochthonous organisms and degradation due to sunlight exposure or mortality due to undesirable physico-chemical conditions. For some organisms, growth may also need to be considered. Each of these will be expanded upon in detail throughout the thesis, however a brief overview is presented below.

Hydrodynamic controls on pathogen dynamics: The hydrodynamic distribution of pathogens in aquatic systems includes processes that determine the horizontal transport, dispersion and dilution, and vertical distribution. Horizontal transport is predominantly driven by basin-scale circulation patterns including wind-driven currents, inflows and basin-scale internal waves. Although wind-driven currents only influence the surface layer, inflows can occur at any depth in a stratified water column and internal waves can generate significant internal currents that may act in different directions at different depths. In stratified lakes and reservoirs, internal waves have been shown to be responsible for the vertical advection of pathogens past offtake structures resulting in periodic variations in water quality (Deen *et al*., 2000).

Dispersion describes both the turbulent dispersion (for example in the surface mixed layer) and shear dispersion due to the presence of a horizontal or vertical velocity shear, (*e.g.* rivers or tidally forced systems). Both processes are important in determining the distribution of pathogens and particles, however, since mixing processes occur at small-scale they are not resolved by numerical models of environmental flows and rely on 'closure' schemes.

Since the source of most pathogens is via catchment inflows or engineered outfalls, their behaviour as they enter the water column is of particular importance. Inflow dynamics are controlled by their density and momentum relative to that of the ambient water. For example, warm inflows will flow over the surface as a buoyant surface flow, and cold dense inflows will sink beneath the ambient water where they will flow along the bottom towards the deepest point. In either case, as it propagates the gravity current will entrain ambient water, increasing its volume, changing its density and diluting the concentration of pathogens and other properties. A further complication is introduced where the density difference is derived from particulate matter (turbidity current), in which case the settling of these particles will influence the density and propagation of the inflow. The speed at which the inflowing water travels, its entrainment of ambient water and resulting dilution of its properties, and its insertion depth are all of critical importance in determining the hydrodynamic distribution of pathogens. Prediction therefore requires a detailed numerical solution, often in three dimensions, which can resolve processes controlling momentum, mixing, and thermodynamics.

Kinetics: As particles are advected and mixed throughout a waterbody they are also subject to 'non-conservative' behaviour, *i.e.* growth or decay. Organisms become inactivated as they are exposed to the range of biotic and abiotic pressures that face them within the aquatic environment. In particular, organisms are known to be sensitive to temperature, salinity, pH, oxygen, turbidity, sunlight, and they are also subject to predation by autochthonous microorganisms. Some bacteria may also be able to support growth through assimilation of nutrients from the water (Evison, 1988; Lopez-Torres, 1988; Camper *et al*., 1991; Ashbolt *et al*., 1995; Solo-Gabrielle *et al*., 2000).

Sedimentation & association with particles: Except perhaps for the protozoan (oo)cysts, the settling rate of free-floating organisms is small. Association with inorganic and organic aquatic particles however can considerably increase the losses due to sedimentation, with particle settling being affected by their size and density according to Stoke's law (Reynolds, 1984). Pathogens may be associated with particles via adsorption at the surface, or they may be physically enmeshed within the organic matrix of faecal material. Differences in dynamic aggregation rates between different organism classes (*i.e.* protozoan, bacterial, viral) are thought to be an important determinant when deciding the applicability of surrogates.

Resuspension: Since pathogens may remain viable for significant periods in aquatic sediments (Gerba and McLeod, 1976; Davies *et al*., 1995; Howell *et al*., 1996), the resuspension and subsequent re-distribution of pathogens and indicator organisms can potentially be an important process. Sediment resuspension occurs when the shear stress due to currents and turbulent velocity fluctuations reaches a critical level. In rivers and estuaries, large currents are capable of generating significant critical bed-shear that exceeds the critical level regularly. In lakes and stratified environments such high velocities are reached less frequently, but can be caused by large underflow events and by basin-scale internal waves motions. Turbulent motions within the benthic boundary layer driven by currents and internal wave breaking (Lemckert and Imberger, 1998) are also known to result in the resuspension of particulate material (Michallet and Ivey, 1999). In environments with an active surface wave field such as the coastal ocean and estuarine environments, then oscillatory currents due to wind-wave action will also be important (Beach and Sternberg, 1992).

Pathogen Risk Management

A fundamental principle of drinking water supply is to use high quality, protected source waters as a means of reducing the potential load of drinking water contaminants and thus reducing treatment costs and subsequent health risks to consumers. A study by Edzwald and Kelley (1998) of the mean concentration of *Cryptosporidium* oocysts in protected reservoirs (0.52/100L) and pristine lakes (0.3 – 9.3/100L) compared with polluted rivers (43 – 60/100L) and polluted lakes (58/100L) highlights the merit of this strategy. With increasing pressures on catchments and coastal zones, aquatic systems are not always sufficiently protected and pathogen risks must therefore be appropriately managed. In developing countries this is further confounded since both drinking and recreational waters may be subject to direct and unregulated effluent discharges.

The presence or absence of pathogens within the aquatic environment does not always provide a satisfactory indication of risk to human health. For example, *Cryptosporidium* and *Giardia* (oo)cysts have been identified at levels that may present a health hazard within Lake Kinneret, which supplies approximately two-thirds of Israel's water, however no major outbreaks have been reported in Israel (Zuckerman *et al*., 1997). Conversely, several outbreaks of cryptosporidiosis have now been documented where the water quality met microbiological standards based on bacterial indicators (MacKenzie *et al*., 1994; Lisle and Rose, 1995). It is commonly recognized that pathogen data needs to be considered within a wider management framework that encompasses the entire system, from release to exposure. To obtain a more realistic assessment of the overall pathogen risk it is necessary to understand the critical variables controlling pathogen fate and distribution once they enter the aquatic environment.

Successful risk management of water supply reservoirs and fresh or coastal recreational waters requires a systematic approach to pathogen monitoring and prediction in order to reduce the risk of exposure to the public. This is best achieved through a quantitative understanding of the critical processes involved in pathogen distribution and transport, such as dilution rates and time scales for inactivation. Such information would enable water managers to quantify the risk to water quality associated with a pathogen threat in source water, revise monitoring protocols to detect pathogens, and to manage water treatment or beach closures proactively based upon detected or, ideally, modelled (anticipated) risk. Due to their flexibility, such 'adaptive' management strategies are more effective than their rigid counterparts, yet they are rarely adopted due to numerous uncertainties in our understanding and due to poor numerical predictions.

Allen *et al*. (2000) recently went further, and described pathogen monitoring as being of little value and highlighted several cases where monitoring had misled regulatory authorities as to the actual risk, including both false positives and false negatives. They highlight several technical and administrative barriers why this is the case, and instead suggest that the human and financial resources would be better invested in enhancing treatment processes and gaining a better understanding of the system (such as the major pathogen sources and sinks, and inactivation processes). Within a drinking water system this is fairly clear since there are many points at which the quality of the source water can be controlled before the public is ultimately exposed, but for other environmental waters there is only limited ability for intervention. However, aquatic systems have an inherent natural assimilative capacity and, through time, can act to attenuate pathogen concentrations (Kay and McDonald, 1980). The question then becomes whether or not it is possible to optimise the performance of aquatic storages as barriers to pathogen transmission. Again, this requires a more detailed quantitative understanding of organism fate and distribution.

Role of Numerical Models

Although the processes influencing enteric organism fate and distribution are fairly well established, there is still much uncertainty as to the relative importance of each process on a system-wide scale,

particularly the spatial and temporal variability. Furthermore, a detailed understanding of how pathogen dynamics vary between systems, which may differ in their loading, salinity, temperature and trophic status, remains elusive. As a result, *ad hoc* monitoring routines are often employed that rarely give an indication of the true risk. Numerical models are attractive since they offer to integrate the myriad of interacting and non-linear processes and place them within a system-wide context.

The use of numerical models to augment existing monitoring and risk-management activities is becoming increasingly widespread since they are able to highlight dominant processes controlling organism dynamics, and can be used to fill knowledge gaps and test catchment management scenarios or examine engineering interventions. Such models have also been used to support real-time decision-making by forecasting pathogen concentrations (Romero *et al*., 2006b). There have been several models used to simulate different components of microbial pollution reported in the literature that range in sophistication and that are relevant for different surface water environments, including freshwater lakes and reservoirs (Auer and Niehaus, 1993; Jin *et al*., 2003; Hipsey *et al*., 2005), streams and rivers (Wilkinson *et al*., 1995), and estuaries and coastal lagoons (Salomon and Pommepuy, 1990; Steets and Holden, 2003; McCorquodale *et al*., 2004). However, it remains difficult for practitioners within the water and environmental industries to confidently implement these models, since they tend to be system or organism specific.

Considering the effort placed in monitoring and risk management of enteric organisms in fresh, brackish and coastal waters, the reported models are fairly rudimentary and have not evolved considerably in the past two decades. This is particularly surprising in light of the substantial advances in microbiological techniques and physiological understanding of the organisms, and the considerable computational power that has become available.

Aims and Scope of Work

In light of the above discussion, it is clear that there is a need for an improved quantitative description of pathogen and microbial indicator organism dynamics within the aquatic environment. The aim of this thesis is to develop, test and verify models and techniques that will provide an improved process-based understanding of pathogen and indicator organism dynamics in aquatic systems. This will help scientists, the water industry and environmental regulators, understand, monitor and predict the dynamic and non-uniform distribution of pathogens in rivers, lakes, estuaries and the coastal ocean. Ultimately it is envisaged that such numerical tools will form an integral component of pathogen risk management systems.

To satisfy this aim, this thesis explores through literature review, field experimentation and numerical simulations, the key physical, chemical and biological processes that control the behaviour of enteric organisms once they enter the aquatic environment. In doing so, a new model of enteric organism behaviour is presented that is generic for protozoa, bacteria and viruses in fresh, estuarine and marine environments. With little to no calibration of the coefficients (pre-determined from experiments and review), the model is ultimately validated against data from three different freshwater systems. The model and field results presented herein will ultimately provide for improved decision making and pathogen risk management.

CHAPTER 2

HYDRODYNAMIC MODELLING

Overview

To have confidence in the model's ability to predict pathogen transport within an aquatic system, one must first be confident that the hydrodynamic model successfully captures the dominant hydrodynamic processes observed in field data since these predictions underpin much of the subsequent analysis. This particularly relates to the ability of the model to capture inflow dynamics and evolution through the basin, as well as other processes such as surface thermodynamics and internal wave generation and dissipation. It is the aim of this chapter to present a validation of the Estuary Lake and Coastal Ocean Model (ELCOM) against available historical data for three field sites within Australia: Myponga Reservoir, Sugarloaf Reservoir and Lake Burragorang. These sites were those proposed for the field campaigns and so this analysis also served as a virtual environmental laboratory enabling the exploration of logistical and scientific concerns prior to entering the field. There is no further presentation of Lake Burragorang in the subsequent chapters since this campaign yielded no useful pathogen data, however, the hydrodynamic validation remains here since it is still a useful test of the model.

ELCOM is a three-dimensional (3D) hydrodynamic code used to simulate spatial and temporal variation of temperature and salinity in lake, reservoir, estuarine and oceanic environments. Velocities are resolved through solution of the Reynolds-averaged Navier-Stokes equations (RANS), which uses a mixed-layer turbulence closure scheme and a unique mixing-model to directly compute vertical turbulent transport (Hodges *et al*., 2000). Heat exchange at the atmosphere-lake interface is separated into penetrative (solar radiation) and non-penetrative components (long wave radiation and sensible and latent heat fluxes). Solar radiation penetrates deep into the water following an exponential decay as described by Beer's Law. Sensible and evaporative heat losses are described by standard bulk-transfer equations (Imberger and Patterson, 1990). The user is required to supply meteorological information (solar and net radiation, wind-speed and direction, humidity and air temperature) and inflow and outflow volume fluxes.

In freshwater environments, validation of ELCOM is achieved by comparing simulation data with thermistor chain and profile data at various locations within the basin, and, where available, velocity data as collected by an Acoustic Doppler Velocity Probe (ADVP). For the validation of Lake Burragorang, simulated temperatures are compared with profile data, and for Myponga and Sugarloaf Reservoirs validation is through comparison with thermistor chain data. The validation focuses on the two factors that are of particular importance when modelling pathogen fate and transport in reservoirs: 1) inflow dynamics within the reservoir, and 2) surface thermodynamics.

Inflows are important since they are the vectors that transport pathogens and indicator organisms introduced from the surrounding catchment to the waterbody. In addition, they are the most important hydrodynamic process that controls pathogen transport once within a waterbody. Capturing the dynamics of these intrusions is often a challenge for hydrodynamic models because of insufficient grid-resolution, and an artificial 'stair-step' roughness scale that causes 'numerical convective entrainment' (Dallimore *et al*., 2003; 2004). This occurs because the base of the model domain is discretized into a number of steps as opposed to a continuous slope as might be expected in reality. The simulated inflow must therefore travel down a stepped structure and as it progresses down it will artificially entrain more water than would be realistically expected. The effects of numerical entrainment reduce as the height of the underflow increases relative to the vertical grid resolution, and so is less of an issue for large, cool inflows. It is these inflows that are of particular concern, as they have the greatest potential to introduce pathogens from the catchment.

An accurate representation of the surface thermodynamics is important in predicting the vertical temperature structure and evolution of the reservoir. Typically, the rate of inactivation of pathogens such

as *Cryptosporidium* spp. is temperature dependent, and so an inaccurate temperature prediction may cause erroneous pathogen viability estimates. Additionally, processes such as differential heating and cooling can generate density currents and therefore contribute to pathogen transport and distribution.

Hydrodynamic Modelling of Myponga Reservoir

Myponga Reservoir is located on the Fleurieu Peninsula, near Adelaide in South Australia (S 35°21'14", E 138°25'49"). It is fed by a 124 km^2 catchment that receives an average annual rainfall of approximately 750 mm. The catchment is drained by Myponga Creek, which feeds the 'long-arm' of the reservoir on the eastern side (Figure 2.1).

Myponga Reservoir is a drinking water supply and has a maximum storage of 26,800 ML, and a maximum depth of 36 m at the dam wall. To help manage water quality problems, the reservoir is artificially de-stratified during the summer period from September to March by an aerator near the dam wall and two surface mixers located in the main basin. As a result, release of nutrients from sediments is minimized (Brookes *et al*., 2000), and the nutrient loading is therefore dominated by catchment sources.

The dominant pathogen source is from the catchment via Myponga Creek. Typically, this river inflow is cooler than the ambient reservoir temperature, and so the inflow becomes a dense intrusion that flows towards the centre of the reservoir, potentially reaching the dam wall. When modelling Myponga, the focus is on accurately capturing the riverine intrusion, and accurately modelling the surface thermodynamics, as it is these processes that govern the fate and transport of pathogens throughout the reservoir. Here the model is validated against two separate events: the first is between 16 – 31 May 2001 and represents the first 'flushing' rains of the season, and 1 – 22 September 2001, which represents a typical winter inflow late in the season and is followed by the onset of stratification. For both of these events, a significant historical dataset exists which can be used to drive and validate the ELCOM simulations.

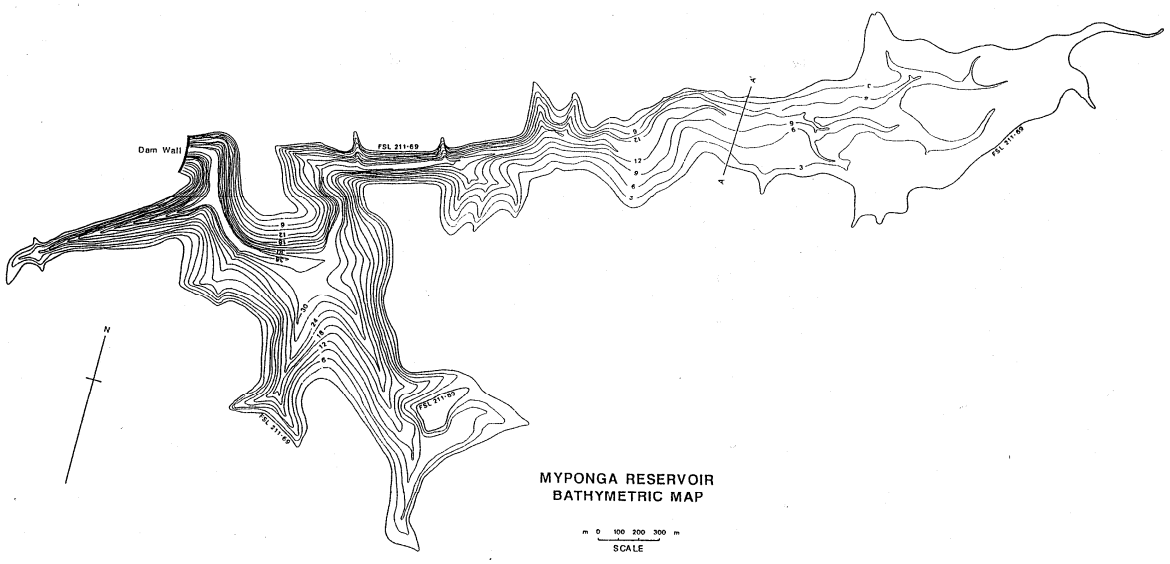

Figure 2.1: Myponga Reservoir bathymetry (contour units in metres below Full Service Level).

Field Monitoring and Data

Myponga Reservoir has two complete weather stations, Met1 and Met2, located on the 'main basin' and 'long-arm' sections, respectively. Met1 measures solar and net radiation, air temperature and relative

humidity, and wind-speed and direction, all at 2 metres above the water surface. Met2 measures only wind-speed and direction (also at 2 m). Inflow volumes are monitored at Myponga Creek using a V-notch weir approximately 1 km upstream from the where the creek meets the reservoir. Water temperature at the weir is also monitored. Evaporation is measured using a standard class-A pan on the western side near the dam wall, and is converted to lake evaporation estimates using an arbitrary pan-to-lake conversion factor of 0.8. Outflow volumes from the dam off-take (located at a height of 18 m from the base) are logged. Rainfall data is collected from a manual gauge adjacent to the evaporation pan about 20 m from the edge of Myponga reservoir. Groundwater inflow and outflow is not considered in these simulations since it is not though to make a significant contribution during the simulated periods.

The two meteorological stations support thermistor chains that log data every 10 minutes. The thermistors are variably spaced with fine resolution in the surface layer and increased spacing with depth. Analysis of the thermistor chain data for both the May and September data indicated that several of the thermistors were in error and so were not used in the validation.

May 2001

The May data extends from 16 – 31 May (Ordinal Date, OD: 136 – 152). This period represents the first significant river inflow for the season, following a 5-month drought. The meteorological, inflow and outflow data used to drive the May ELCOM simulations is shown in Figure 2.2 and 2.3 respectively. Due to a sensor malfunction however, wind-speed and direction data was not collected at Met1 during this time. Thermistor chain data is plotted in Figure 2.4.

The inflow hydrograph shows a major peak during days 137 – 138, followed by a recession and a second smaller peak at days 147 – 148. The first hydrograph peaks slightly below 3 m^3s^{-1}, which is considered a small-moderate inflow event for this system. The temperature of the peak inflow water (~10°C) is low compared to the minimum reservoir water temperature (~15°C).

As shown in the solar radiation, wind-speed and rainfall data (Figure 2.2), much of this period was characterized by thunderstorm activity. Comparison of the air and surface water temperatures indicates that for almost the entire May simulation period, the water surface is warmer than the air temperature (as measured at 2m above the water surface). This temperature gradient creates unstable atmospheric conditions over the water, and in particular results in enhanced evaporative (and sensible heat) losses as the turbulent eddies become more effective in removing moisture (and heat) from the water surface. This phenomenon is well described by the bulk Richardson number:

$$Ri = \frac{g}{T}\frac{\Delta T/\Delta z}{\left(\Delta u/\Delta z\right)^2} = \frac{gz\left(T_{air} - T_{surface}\right)}{Tu_z^2} \qquad (2.1)$$

where g is the acceleration due to gravity (ms^{-2}), T is temperature (°C), z is the height above the water surface (m) and u is the wind-speed (ms^{-1}). A high Richardson number reflects low wind-speed and high thermal stratification of the air over the water, and the sign reflects the nature of the stratification: positive for stable conditions and negative for unstable conditions. As seen for most of the simulation period, large negative Ri values reflect a dominance of convective instability over the water surface (*i.e.* unstable stratification and low wind-speed), and hence enhanced heat fluxes. Evaporation pan data however, does not reflect these conditions, as the water in the pan will remain much closer to air temperature. Additionally, the evaporation pan is not in the internal boundary layer that develops as the wind moves along the water, and so will be experiencing different meteorological conditions than the

waterbody. As a result, the pan-data is only used in a qualitative sense as an indicator of daily evaporation volumes.

The period experienced two rain events. Although the first rain event was significantly larger (60 mm over 4 days relative to 20 mm over 3 days), it is not reflected in the hydrograph peaks because the initial storm fell on a dry catchment, and therefore a significant component of water was consumed in wetting the catchment. For the second event, more runoff resulted as the catchment antecedent condition was closer to saturation following the previous rains.

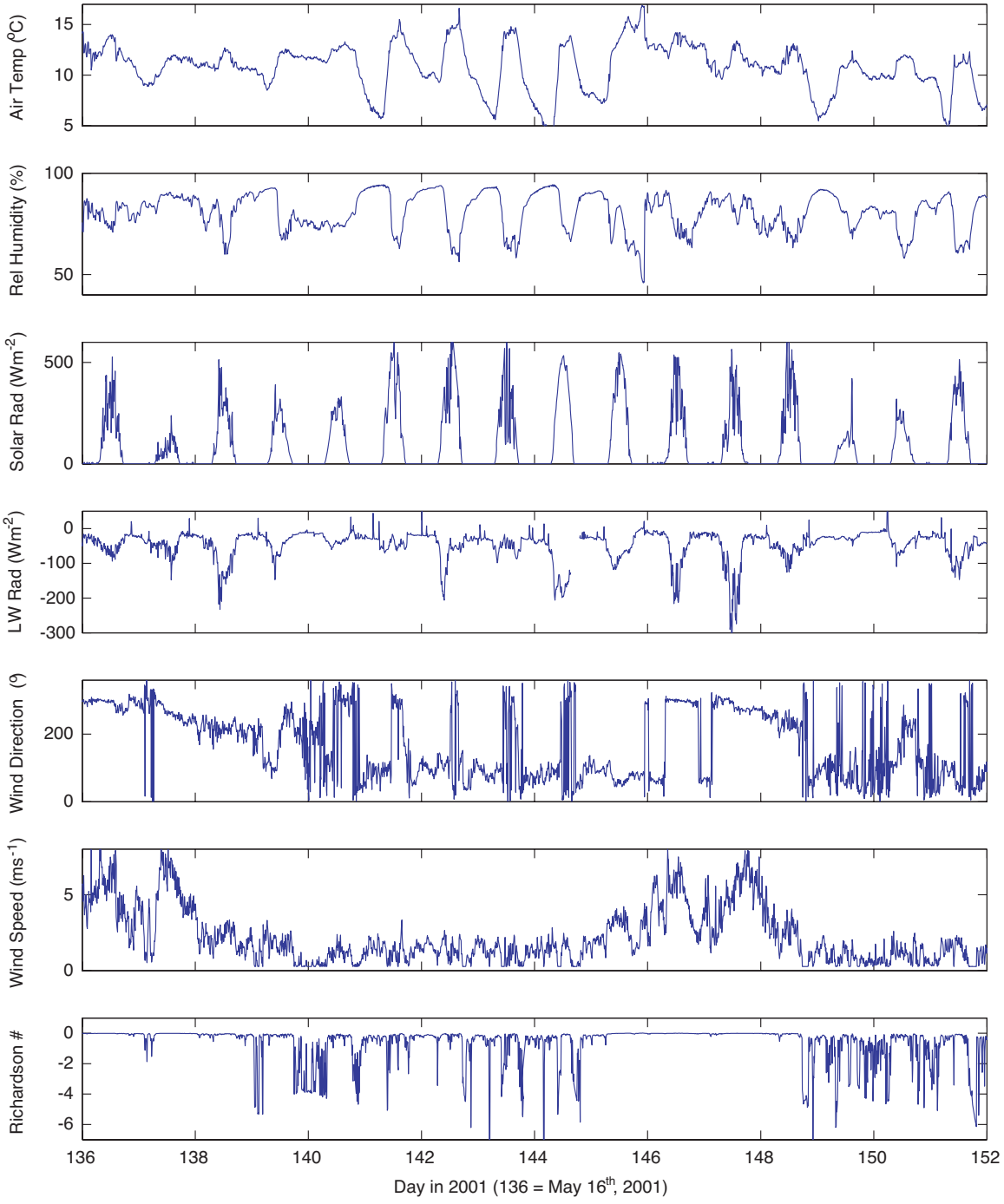

Figure 2.2: Meteorological data measured 2 m above the water surface for the May 2001 storm event.

The thermistor chain data (Figure 2.4) shows that the waterbody is initially well mixed. The inflow is seen as a subsequent pulse of cool water passing the Met2 thermistor chain, beginning day 138, with a height of approximately 5 m. The typical diurnal signal of surface heating (stratifying the water during midday and surface cooling mixing the water column at night) is seen for most of the measurement period, but is particularly evident from day 141 – 144. The thermistor data at Met1 (in the 'main basin' of the reservoir) shows that the cool inflow water gradually fills up the main portion of the basin, and although it is diluted with entrained reservoir water, the intrusion penetrates up to 10 m from the bottom.

September 2001

The September data extends from 1 – 22 September (Ordinal Date 244 – 265). Throughout this period there was a significant river inflow component, as is typical of winter and spring conditions. The meteorological, inflow and outflow data used to drive the September ELCOM simulations is shown in Figure 2.5 and 2.6. Both meteorological stations were fully operational. Thermistor chain data is plotted in Figure 2.7.

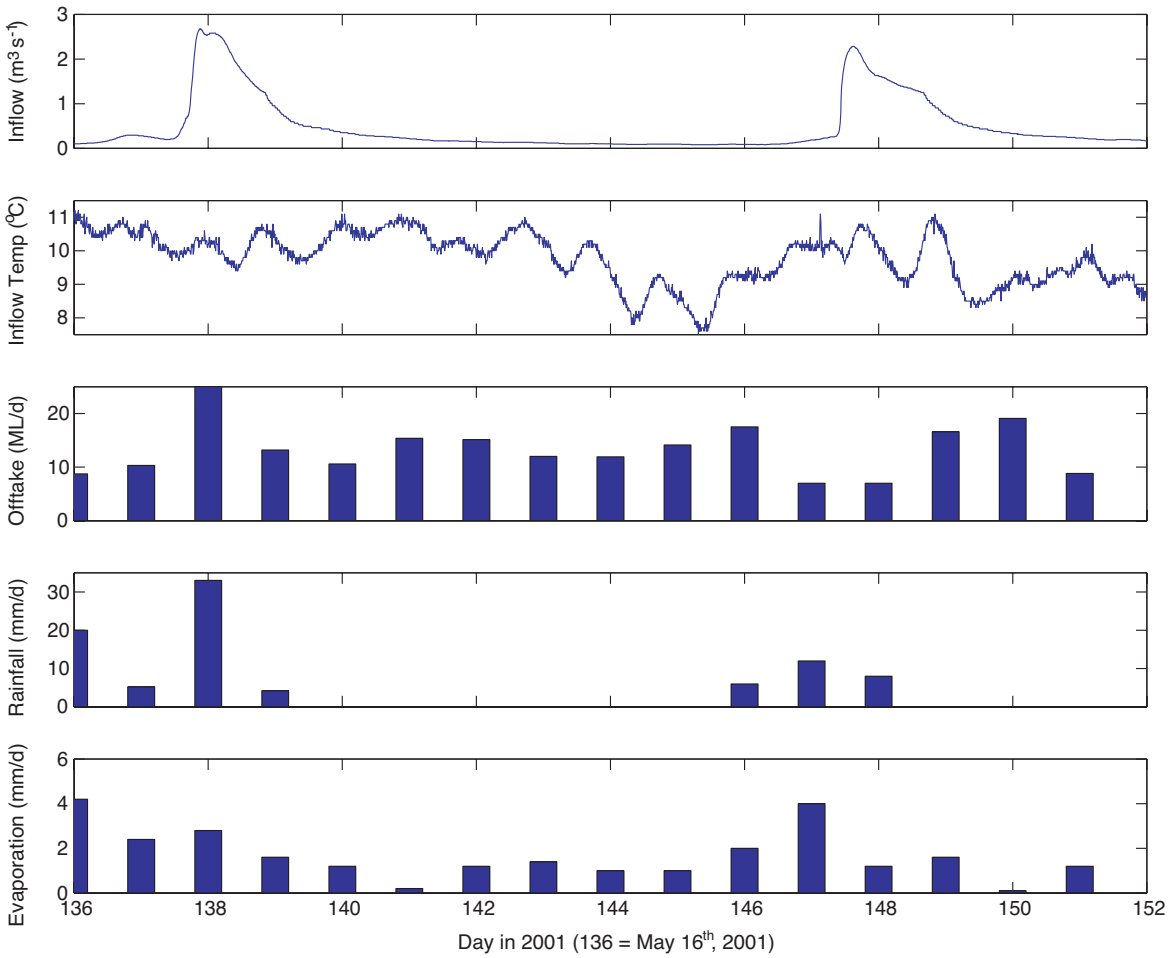

Figure 2.3: Inflow and outflow data for the May 2001 storm event. Evaporation rates are plotted as 0.8x the pan evaporation rate.

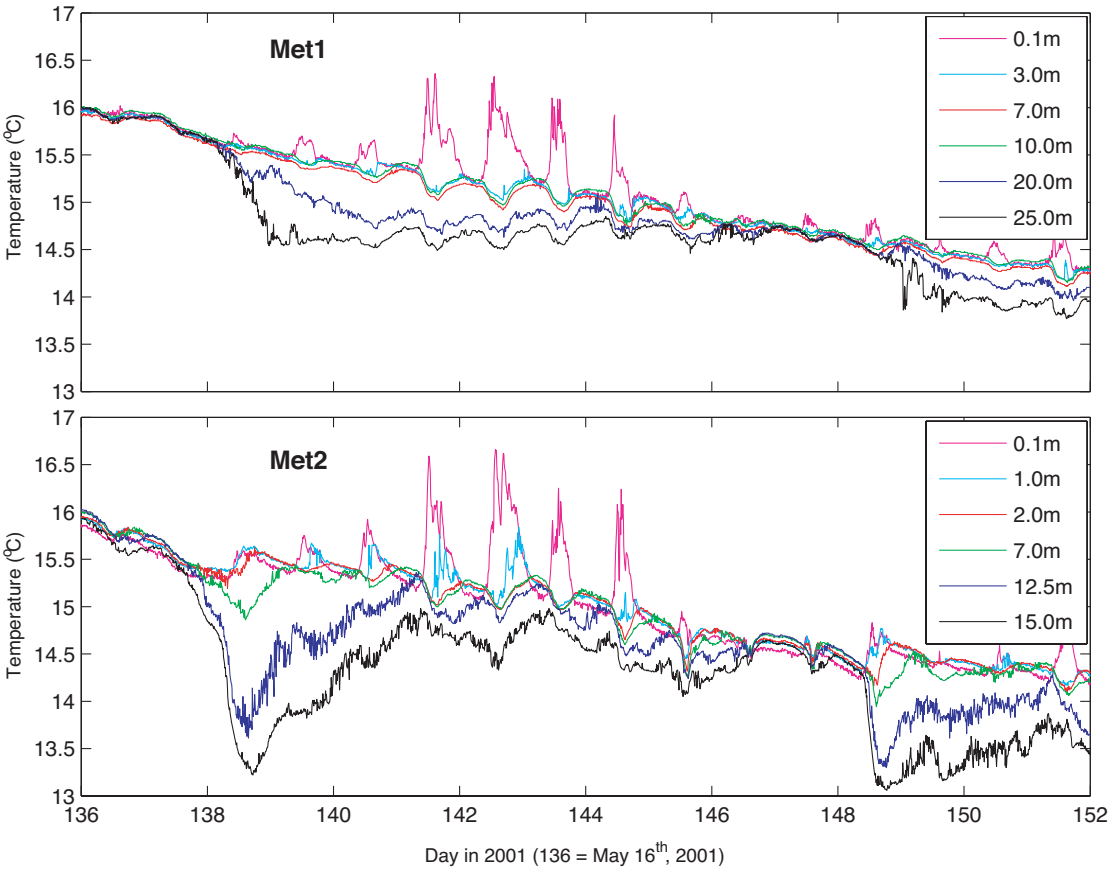

Figure 2.4: Myponga thermistor chain data for the May 2001 storm event.

At the beginning of the month, the reservoir is only weakly stratified (~0.5°C) and becomes fully mixed in response to the storm activity from days 250 – 252 (Figure 2.7). After the storm activity ceases on day 252, the surface layer begins a warming trend that extends beyond day 265. The stratification induced by the heating extends down approximately 7 m. Despite prolonged periods of unstable atmospheric conditions over the waterbody, particularly during the low-wind periods (large, negative Richardson numbers), nighttime surface cooling caused insufficient convective mixing of the surface layer to devolve the stratification.

The effects of the inflows on the reservoir thermal structure are not as pronounced as the May inflows despite their larger size, because the inflow temperatures are closer to the respective ambient reservoir temperatures. Indeed, there is little evidence of the inflows at the thermistor chain located in the main basin (Figure 2.7).

ELCOM Setup

A bathymetric map was digitized using ArcView and interpolated onto a regular 50×50 m grid. This created an ELCOM dataset of approximately 60,000 cells (for 0.5 m vertical resolution). This resolution was deemed too fine with respect to computational times for future ELCOM-CAEDYM runs, and the horizontal grid spacing was increased to 100 m, creating a final ELCOM wet-point dataset of 27,000 cells. Vertical grid spacing was originally tested at 1 m, but preliminary simulations showed insufficient accuracy. Much greater accuracy was achieved using a vertical grid depth of 0.5 and 0.4 m, but since there was no appreciable difference between the two, 0.5 m was chosen to reduce computational times.

The bathymetry along the 'long-arm' was straightened to reduce artificial momentum loss associated with grid discretization. The discretization of the bathymetry has the potential to alter the height-storage relationship, so the ELCOM bathymetry was incrementally adjusted until the real and discretized storage-height curves closely matched (Figure 2.8).

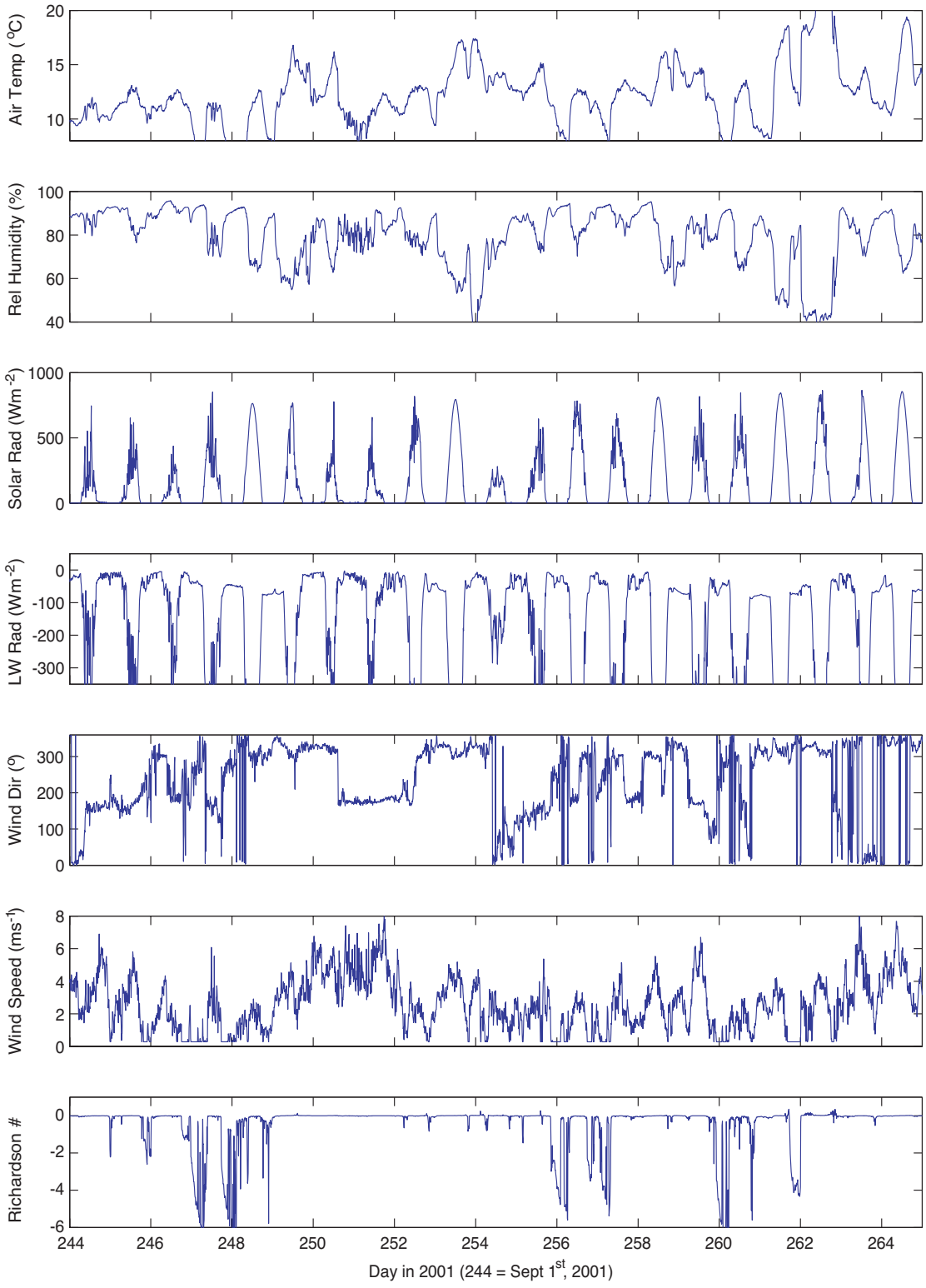

Figure 2.5: Meteorological data measured 2 m above the water surface for September 2001.

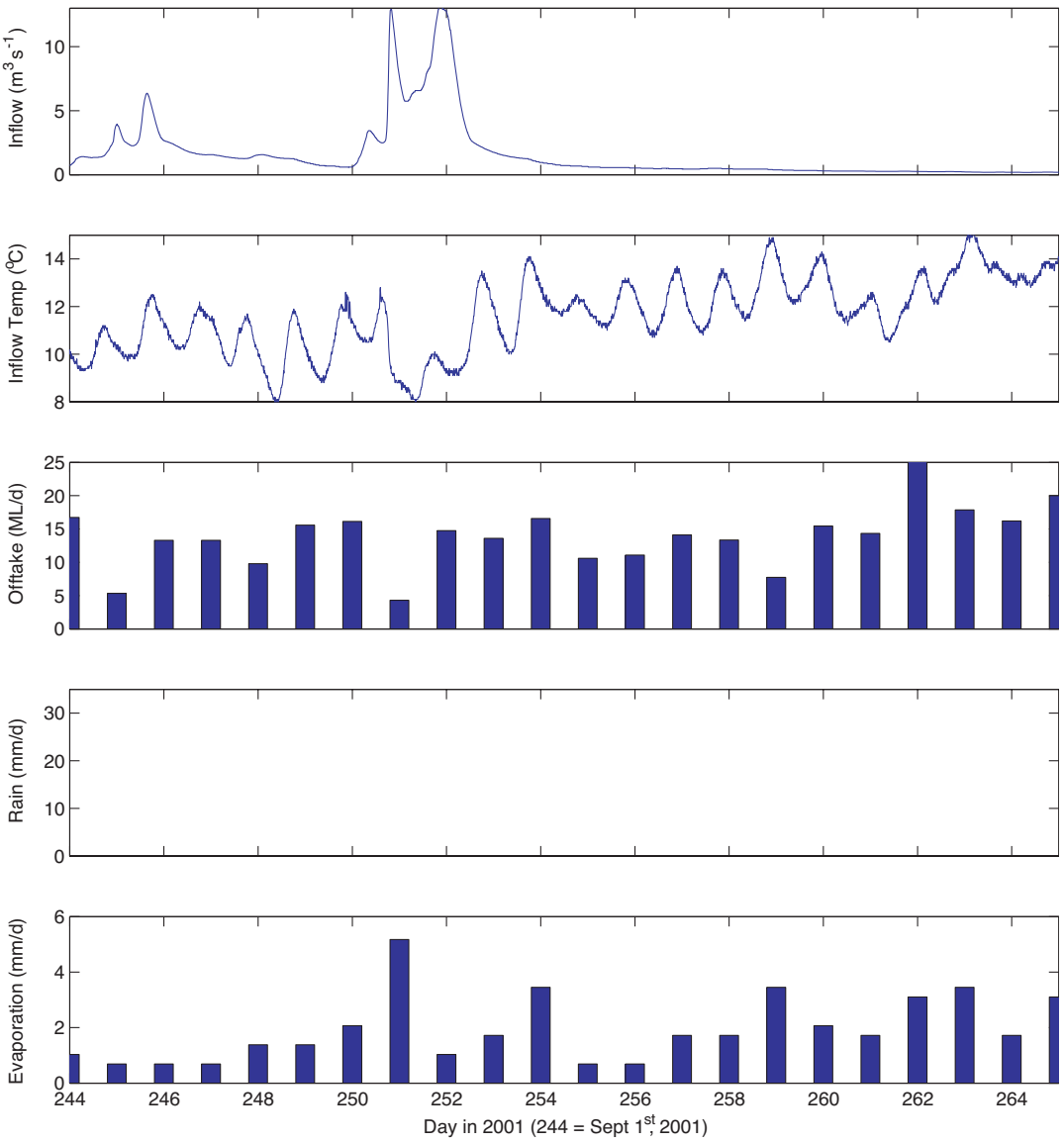

Figure 2.6: Inflow and outflow data for the September 2001 storm event.

A plan view of the ELCOM grid is shown in Figure 2.9, showing the location of the Myponga Creek inflow, the two meteorological stations, and the output points of the curtains and profiles. The two different surface forcing regions for wind-speed and direction are also illustrated. In addition, extensions were made to the code to allow longwave radiation data to be input directly, and correction for atmospheric stability was also included to minimize errors arising from the cloudy and cool nature of the simulation period (see Richardson number plots above).

The simulations were forced with the raw 10-minute meteorological data presented above. The inflow and outflow boundary forcing regions were set to be one grid cell, as indicated on Figure 2.9. For each of the simulations the water level data was compared with available field data to ensure accurate mass balance representation.

The simulations were run with a time-step of 240 secs, and, as suggested by thermistor chain data (see Figures 2.4 and 2.7), the entire basin was given a constant initial temperature. Based on field measure-

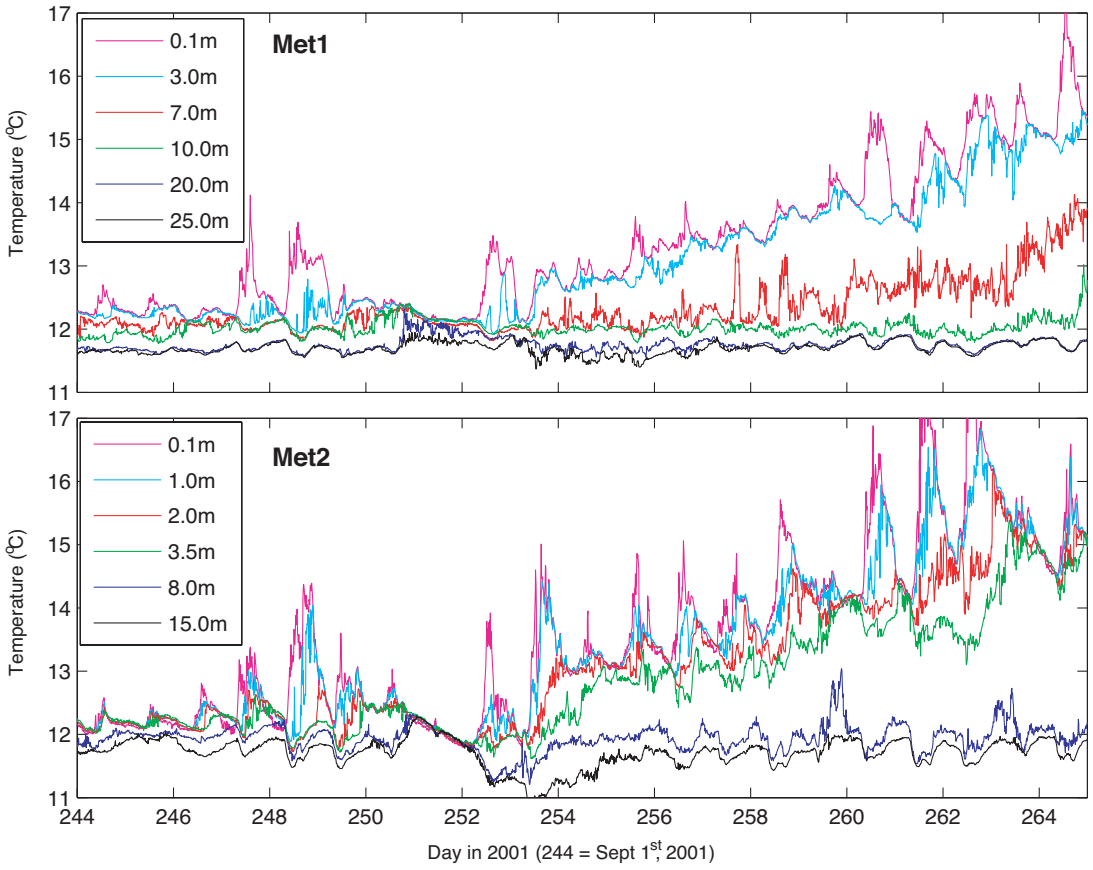

Figure 2.7: Myponga thermistor chain data for the September 2001 storm event (top:Met1, bottom:Met2).

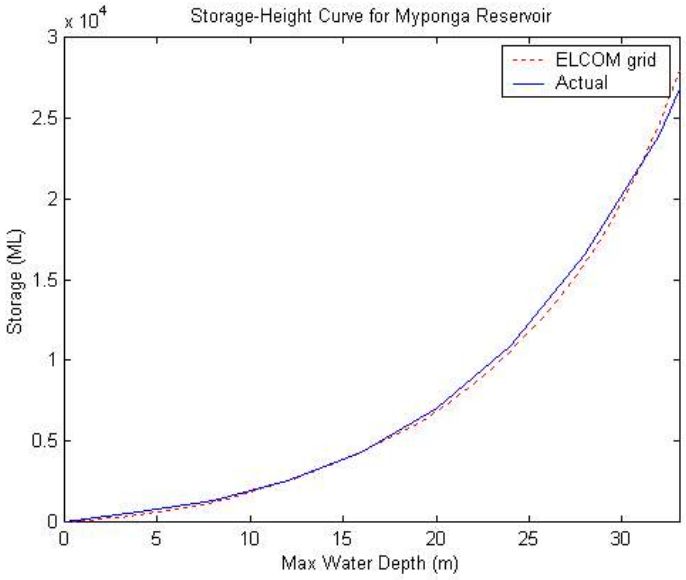

Figure 2.8: Comparison between the storage-height curves for the ELCOM grid and that based on field data.

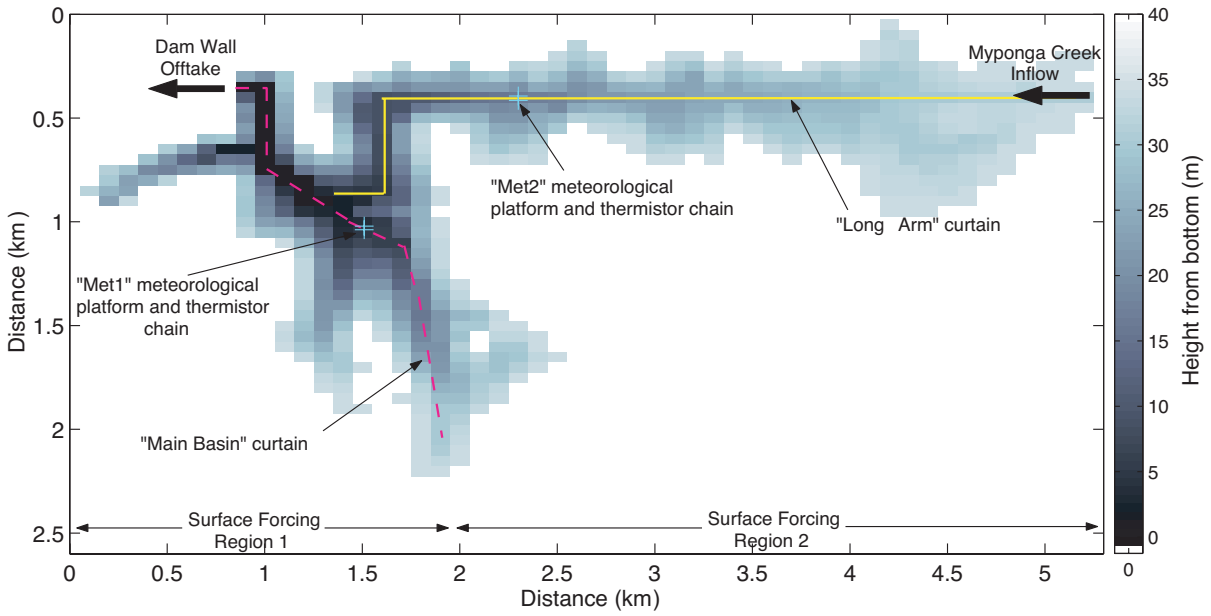

Figure 2.9: Plan view of ELCOM grid used for Myponga Reservoir, showing the bathymetry the two surface forcing regions, inflow and outflow locations, and the location of the meteorological stations and thermistor chains.

-ments, an extinction coefficient of 1.2 was used. Additionally, both the reservoir and inflow water were assumed to be fresh, so that only temperature was responsible for creating density gradients.

ELCOM Performance

May 2001

Comparison of the ELCOM simulations with the field data is presented in Figure 2.10 for the May simulations. The cool river inflow is first seen midway through day 138 in Met2 as it descends down the 'long-arm'. This shows a lag of approximately half a day from its entry at the mouth of Myponga Creek, implying a mean underflow velocity of ~0.07 ms^{-1} in this region.

ELCOM accurately captures the timing and height of the underflow (Figure 2.10a), although the temperature of the main underflow pulse was over-predicted by 0.5 – 1.0 degree, suggesting over-estimation of entrainment. However, this calculation is complicated because of the inflow itself being masked with cool water that originated from the shallow reaches near the mouth of Myponga Creek. Accurate modelling of the underflow pulse was consequently highly dependent on accurate modelling of the cooling experienced by the water being entrained. The temperature of the second underflow that occurred during days 148 – 149 was more accurately simulated, although it arrived approximately 6 hours early. This is potentially a result of over-estimation of the horizontal dispersion of the front, although again it seems that this underflow is coincident with cool water resulting from surface cooling in the shallow reaches near the mouth of Myponga Creek.

As the underflow progresses into the main basin, it remains cooler than the reservoir water, and begins to displace water within the hypolimnion. As captured at the Met1 thermistor chain, the intrusion takes a further 1/2 day to progress through into the main basin. A reduction in underflow speed (0.03 ms^{-1}

compared to 0.07 ms^{-1}) results from the lower bed gradients in addition to the right angle turn made as it exits the 'long-arm'. In addition, the underflow volume and momentum is gradually entrained as the water progresses down the slope. Although ELCOM accurately modelled this progression, it over-predicted its height of influence (as measured by the 14.5°C isotherm displacement) by approximately 7 m. Despite this, it is emphasized that ELCOM reproduced the thermistor chain data to within 0.5°C, as indicated by the difference plots.

During initial simulations poor predictions of the temperature structure motivated the development of a new module to correct the bulk transfer equations for the effect of non-neutral atmospheric conditions (Appendix A1). The implementation of this correction scheme in ELCOM significantly improved the surface thermodynamics due to the persistent non-neutral conditions as indicated in the Richardson number plots (Figure 2.2). Scatter plots highlight the improvement between ELCOM simulations conducted with and without atmospheric stability module (Figure 2.11). Ignoring the influence of atmospheric stability over the water resulted in the surface waters significantly over-heating as indicated by the tendency for the points to deviate above the 1:1 line. This is particularly evident for the Met1 thermistor data, which shows an improvement in the R^2 value from 0.692 to 0.936 upon inclusion of the atmospheric stability correction. Similarly, Met2 showed an increase from 0.727 to 0.892. It is also interesting to note that the improvement is not confined to the surface layer predictions, but also to the underflow. As discussed above, this is a result of the superposition of differential surface cooling and the inflow to create the underflow seen in Figure 2.10a. There is therefore a shift of the entire set of points above the 1:1 line, as opposed to skewing of only the upper section (*i.e.* surface waters).

Overall the errors were small, and based on the results from both thermistor chains, ELCOM consistently predicted the temperature structure to within $\pm$0.5°C, with an average error of <0.2°C. This is considered to be an excellent validation of the ability of the model to simulate the hydrodynamics in Myponga Reservoir under both inflow and meteorological forcing during a storm event.

<u>September 2001</u>

The September simulation period runs over a longer period, and so provides an important test to determine whether errors accumulate or are controlled and sustainable. This period varies from the May simulation period primarily because, a) the river inflow is of a closer temperature to the ambient reservoir temperature, and b) the inflows are considerably larger and have a larger capacity to displace the reservoir water. Additionally, after the major storm event in the first 10 days of the month, a prolonged heating period tests the ability of the ELCOM in capturing the developing temperature stratification.

The initial 5 m^3s^{-1} inflow, (*i.e.* twice the magnitude of the May inflows) had little influence on the reservoir temperature structure because the inflowing water was of a similar temperature as the already well-mixed reservoir water (Figure 1.12). The larger inflow that occurred during days 251 – 252 (12 m^3s^{-1}) was 3 – 4°C cooler than the reservoir water and so had a more pronounced effect on the temperature structure. Prior to the inflow, the ambient reservoir water was completely mixed as a result of the high wind-speeds that occurred during the storm event that created the inflow. The cooler inflowing water created a mild stratification that was eroded away within 1.5 days. This is most likely a result of the tail end of the inflow hydrograph having a temperature similar to that of the reservoir, thus acting to mix the cooler water that had entered previously. This is supported by Met1 thermistor chain data, which indicates that negligible cool water entered the main basin. The difference plots (Figure 2.12) indicate ELCOM accurately predicts the timing, height and the temperature (to within 0.5°C) of the underflow.

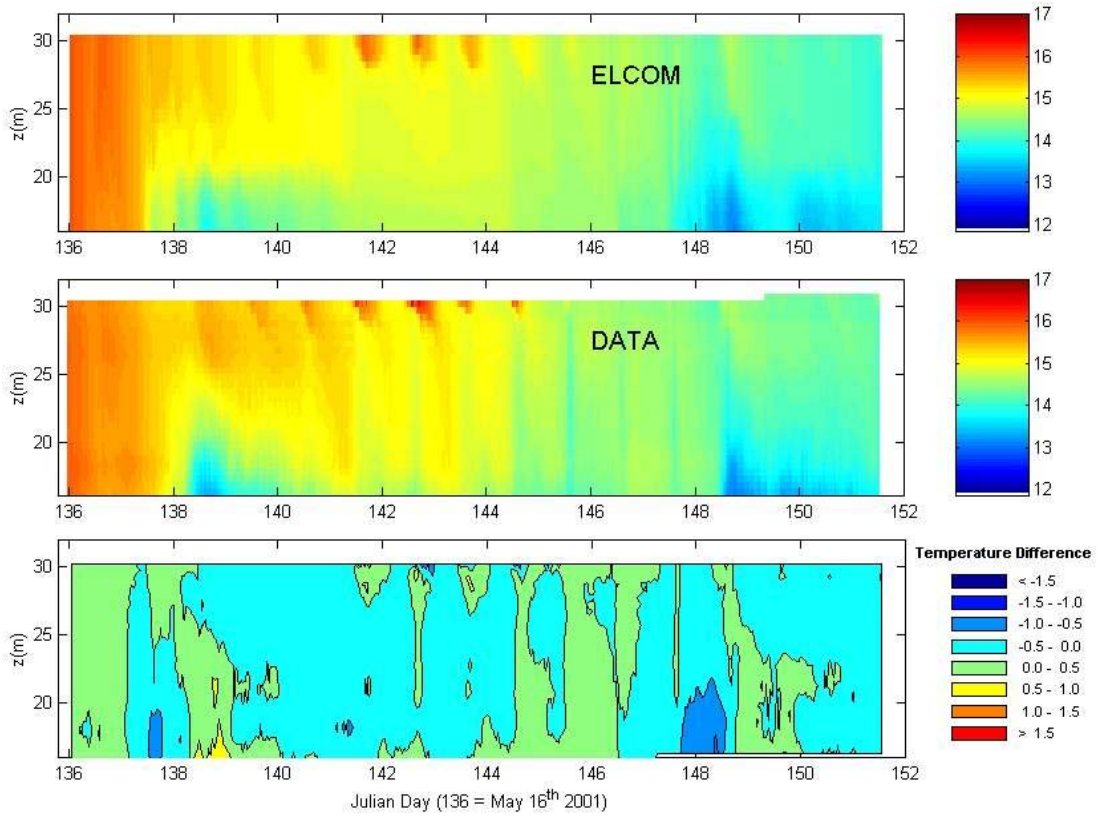

Figure 2.10a: Comparison of thermistor chain data and ELCOM simulation at station Met2 ('long-arm') for May 2001 flood event. The bottom panel shows the error with 0.5°C contour resolution.

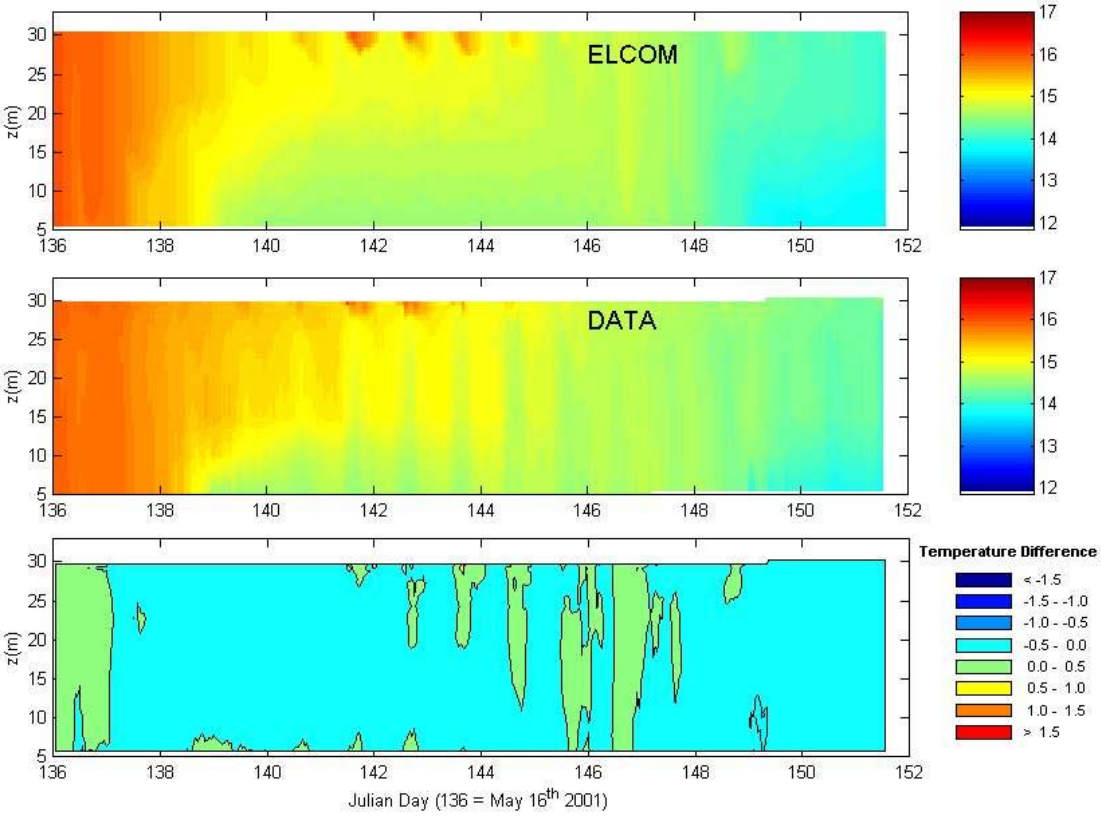

Figure 2.10b: Comparison of thermistor chain data and ELCOM simulation at station Met1 ('main basin') for May 2001 flood event. The bottom panel shows the error with 0.5°C contour resolution.

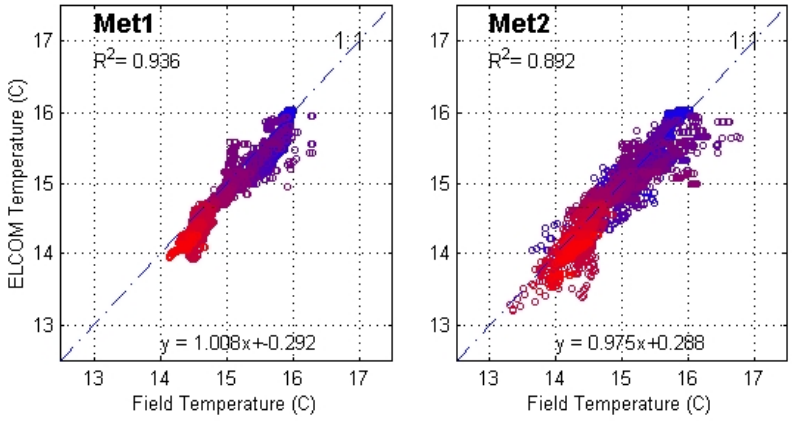

a) with atmospheric stability.

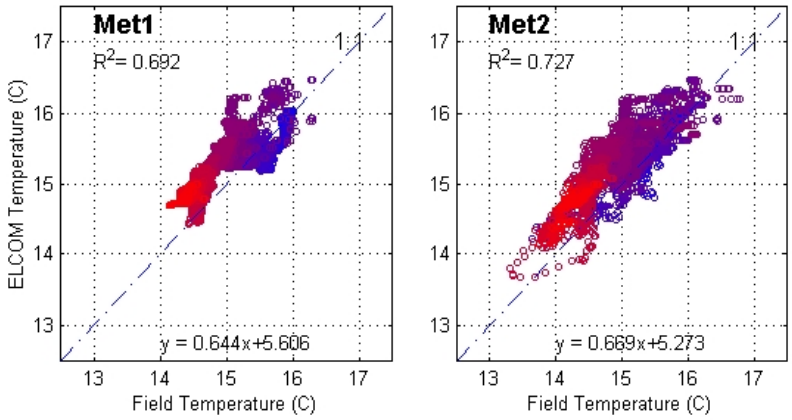

b) without atmospheric stability.

Figure 2.11: Scatter plots comparing thermistor chain data with equivalent ELCOM data for the May 2001 Myponga simulations. The colour scale reflects the time of measurement: blue at the beginning of the period (Day 136) through to red at the end (Day 151).

As with the May event, the September simulation period was largely forced by unstable atmospheric conditions, and so the atmospheric stability module within ELCOM was used to approximate the surface heat fluxes. During the initial storm period (Days 244 – 256), ELCOM accurately models the surface thermodynamics to within 0.5°C, including the period of high wind-speed that mixed the warm surface water throughout the water column. After the storm event passed, strong surface heating and mild wind-speeds promoted the development of a highly stratified water column. This stratification continued to evolve to day 265, where the thermocline was located approximately 8 m below the surface. In the main basin and long-arm, ELCOM performs well in simulating the degree of stratification and the depth to the thermocline.

The simulated profile captures the diurnal cycle of thermocline deepening. However, during days 261 and 262, the simulated profile at the long-arm station (Met2) fails to predict the strong diurnal thermocline that formed after a period of strong heating. As the equivalent period in the main basin (where temperature, insolation and humidity is measured) is accurately predicted, it suggests that this error is an artifact of basin-wide application of surface forcing parameters.

Comparison of the variance between the simulated and observed data for the September event again indicates the benefits in including atmospheric stability for periods when the Richardson number departs

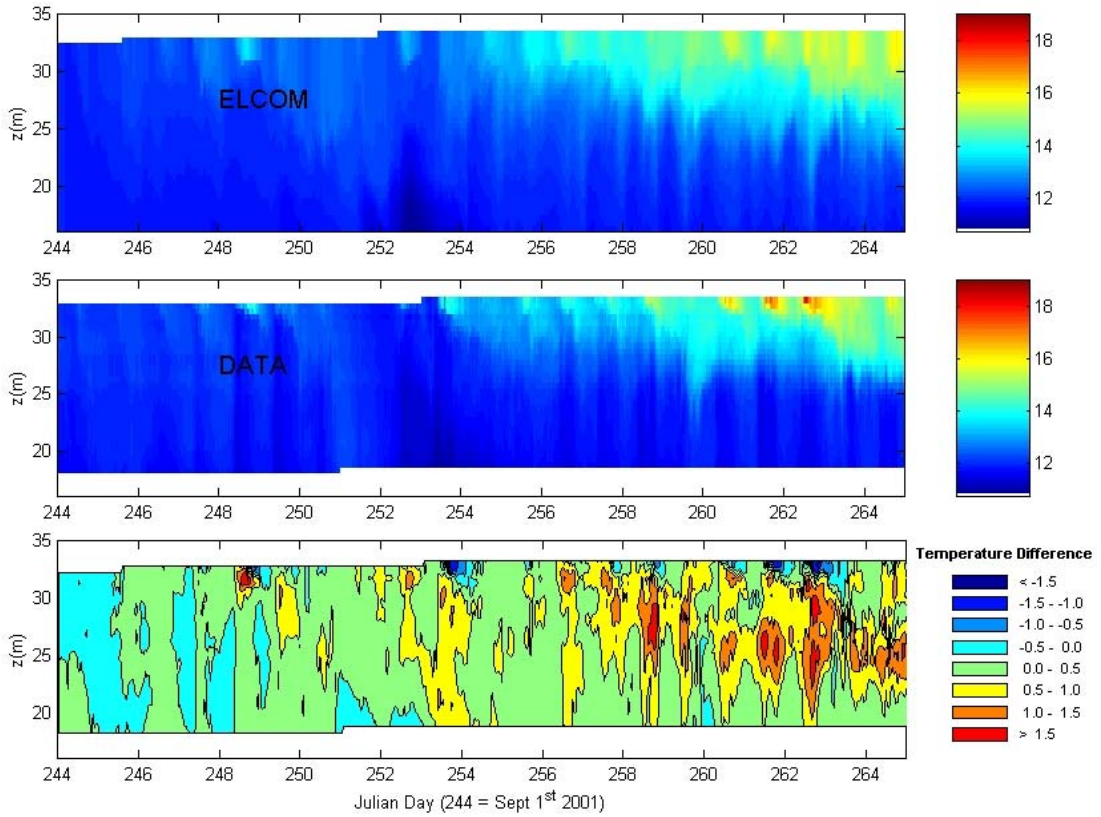

Figure 2.12a: Comparison of thermistor chain data and ELCOM simulation at station Met2 ('long-arm') for Sept 2001 flood event. The bottom panel shows the error with 0.5°C contour resolution.

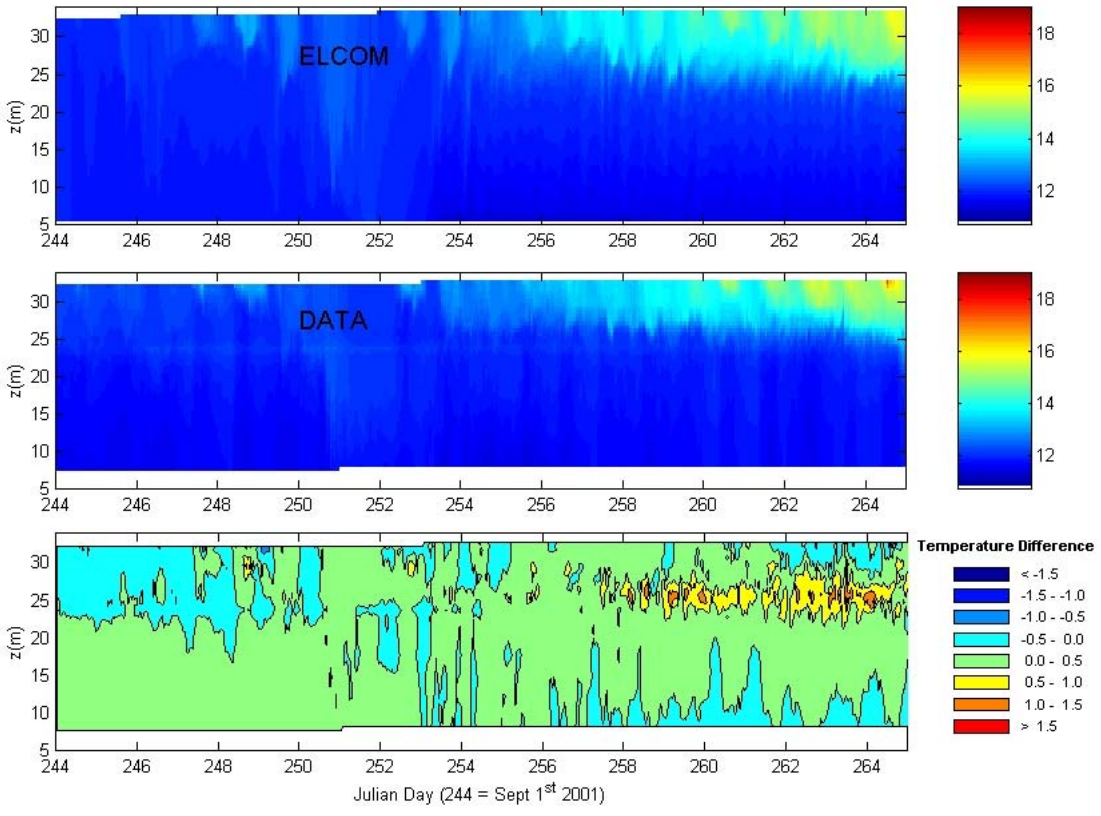

Figure 2.12b: Comparison of thermistor chain data and ELCOM simulation at station Met1 ('main basin') for Sept 2001 flood event. The bottom panel shows the error with 0.5°C contour resolution.

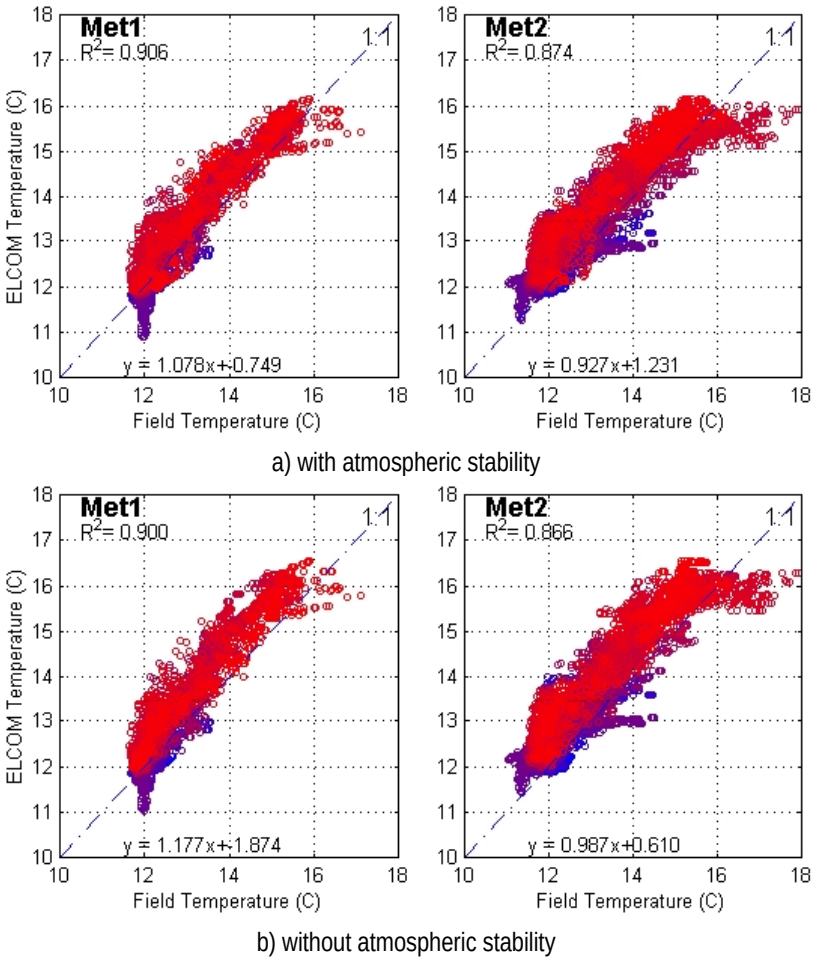

Figure 2.13: Scatter plots comparing thermistor chain data with equivalent ELCOM data for the September 2001 Myponga Reservoir simulations. The colour scale reflects the time of measurement: blue at the beginning of the period (Day 244) through to red at the end of the period (Day 265).

from zero (Figure 2.13). The overall improvement is less significant than the May simulations for both Met1 and Met2 because the September simulation period has a greater proportion with near-neutral stabilities. An interesting feature seen in these plots, particularly Met2, is the 'flattening' of the top section. This is indicative of over-predicting the depth to which the surface layer mixes, and consequently ELCOM surface layers peak at approximately 16°C, whereas the thermistor chain data indicates a gradient between 15 and 17°C. Conversely, the underflow signal is constant at 12°C as seen at station Met1, whereas ELCOM predicts a pulse between 11 and 12°C. Nonetheless, these are relatively subtle features, and overall ELCOM accurately captures the surface and inflow dynamics

Hydrodynamic Modelling of Sugarloaf Reservoir

It is the intention of this section to outline the predictive hydrodynamic modelling conducted for Sugarloaf Reservoir prior to the field experiment conducted on the 24 – 31 August 2003. Sugarloaf Reservoir is operated quite differently from Myponga Reservoir. Whereas Myponga fills based on rainfall falling in the surrounding catchment, Sugarloaf receives little from its supporting catchment and is filled by pumping water from surrounding rivers. Therefore, pathogen seeding of Sugarloaf can occur consistently over a period of months while the inflow pumps are activated in comparison to the Myponga experience where pathogen seeding is event based.

Site Description

Sugarloaf Reservoir is a 96,000 ML storage located in the Yarra Valley, near Melbourne in Victoria, with a maximum depth of approximately 75 m. Water is pumped into the reservoir from the upper reaches of the Yarra River and from a nearby aqueduct. Figure 2.14 shows a plot of Sugarloaf bathymetry showing the inflow and outflow locations. A meteorological station and high resolution thermistor chain is located in the deepest section, approximately 500 m out from the dam wall.

The period being investigated is the two months preceding the field experiment: 1 July – 24 August 2003. This period was characterized by zero inflow concentrations until OD 205 and then a roughly constant value of 8 m^3s^{-1} (Figure 2.15). The outflow over the entire period was constant. The meteorological data from this period is shown in Figure 2.16.

The reservoir began a cooling trend at the beginning of the study period, which occurred mostly as a result of cool air temperatures (5 – 12°C relative to the reservoir 11°C) and prolonged periods with wind speeds in excess of 5 ms^{-1}. As seen later the inflowing water was also cooler than the reservoir water, and owing to the magnitude of the inflow, this also significantly cooled the entire reservoir.

ELCOM Application

The Sugarloaf bathymetry was discretized onto a 60×60×1.0 m (x-y-z) mesh (Figure 2.17) with some small modifications to the grid to allow for correct configuration of inflow and outflow regions. The ELCOM storage-height curve compared well to that of the data (Figure 2.18).

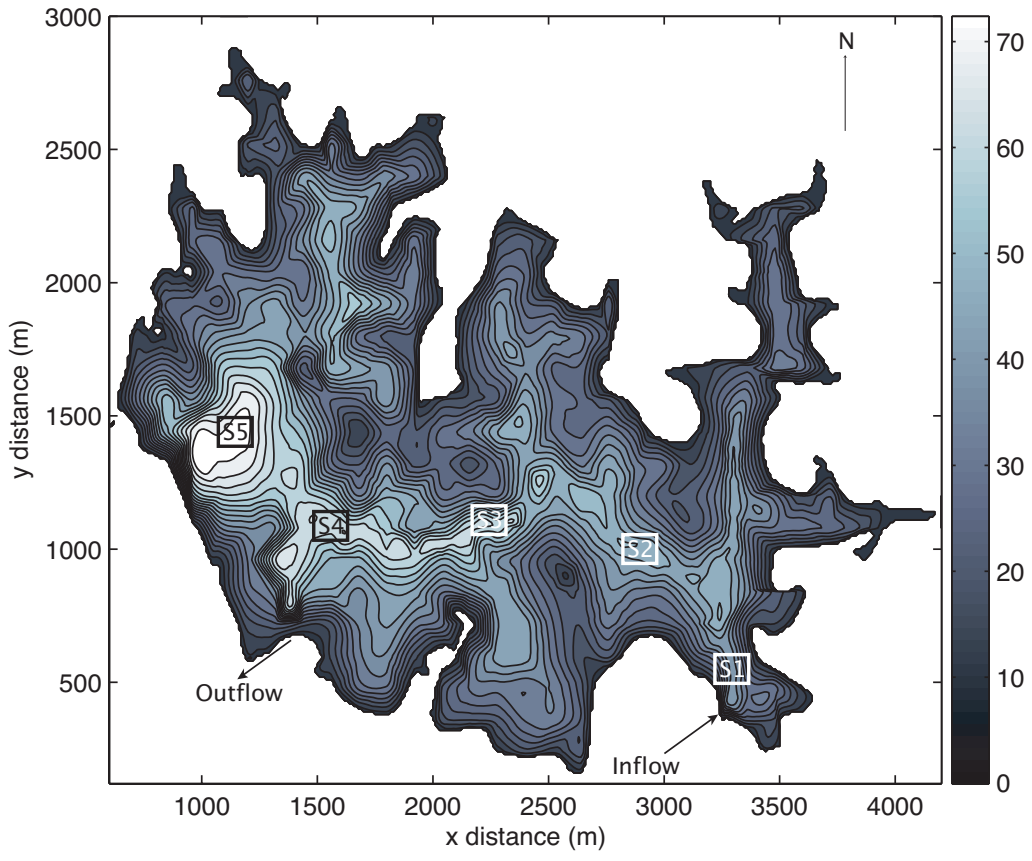

Figure 2.14: Plot of Sugarloaf Reservoir bathymetry (m below FSL), indicating the inflow, outflow and proposed sample locations.

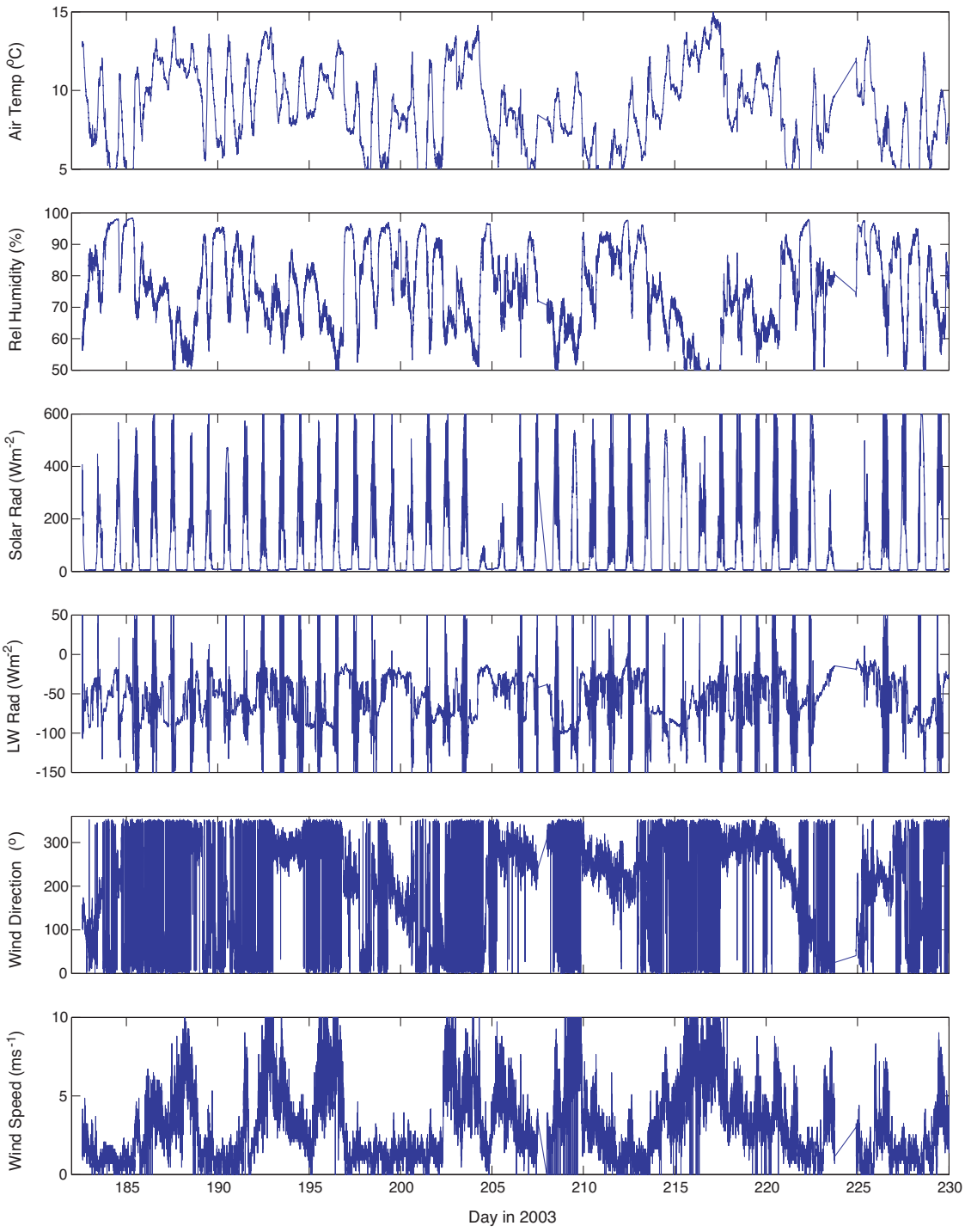

Figure 2.16: Meteorological conditions measured above Sugarloaf Reservoir during the simulation period, Days 182 – 230 in 2003.

The model was run with uniform surface forcing using the meteorology data collected at a two-minute timestep from the meteorological station located near the dam wall. The atmospheric stability correction used in Myponga (Appendix A1) was also enabled. Only daily inflow and outflow data were available, and these were input at the relevant locations illustrated in Figure 2.14. Note the inflow location is not near the surface, but 30 m below Full Service Level (FSL); 17 m below the initial height of 165 m.

ELCOM was also run into the future to predict the likely conditions during the field experiment. This was done by extrapolating the inflow and outflow volumes and temperatures (a fair assumption since they were relatively constant), and by using the previous fortnights meteorological data.

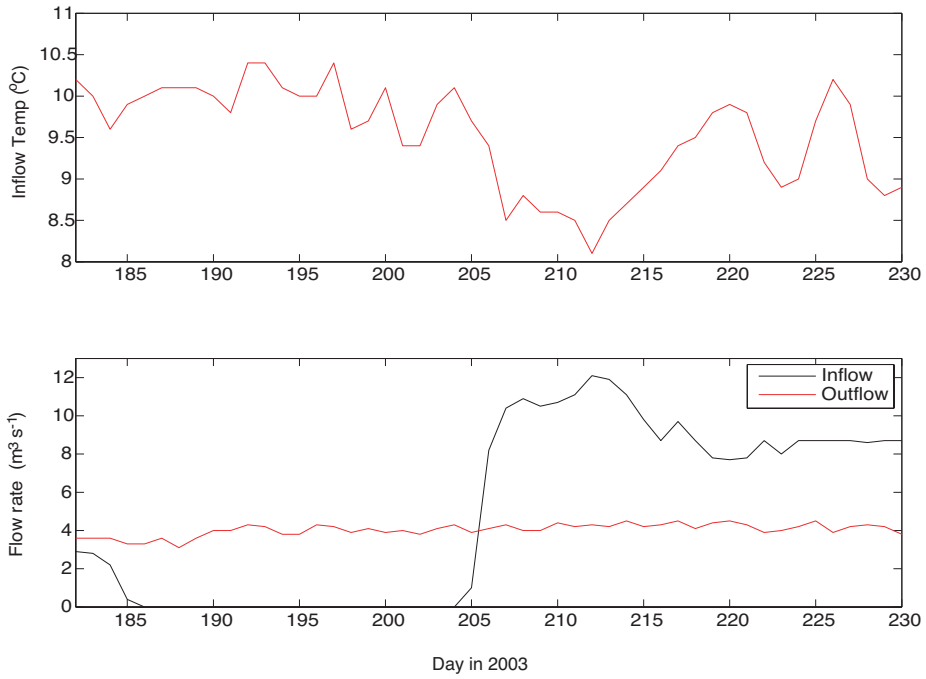

Figure 2.15: Inflow temperature and inflow/outflow volume fluxes for Sugarloaf Reservoir during the simulation period, Days 182 – 230 in 2003.

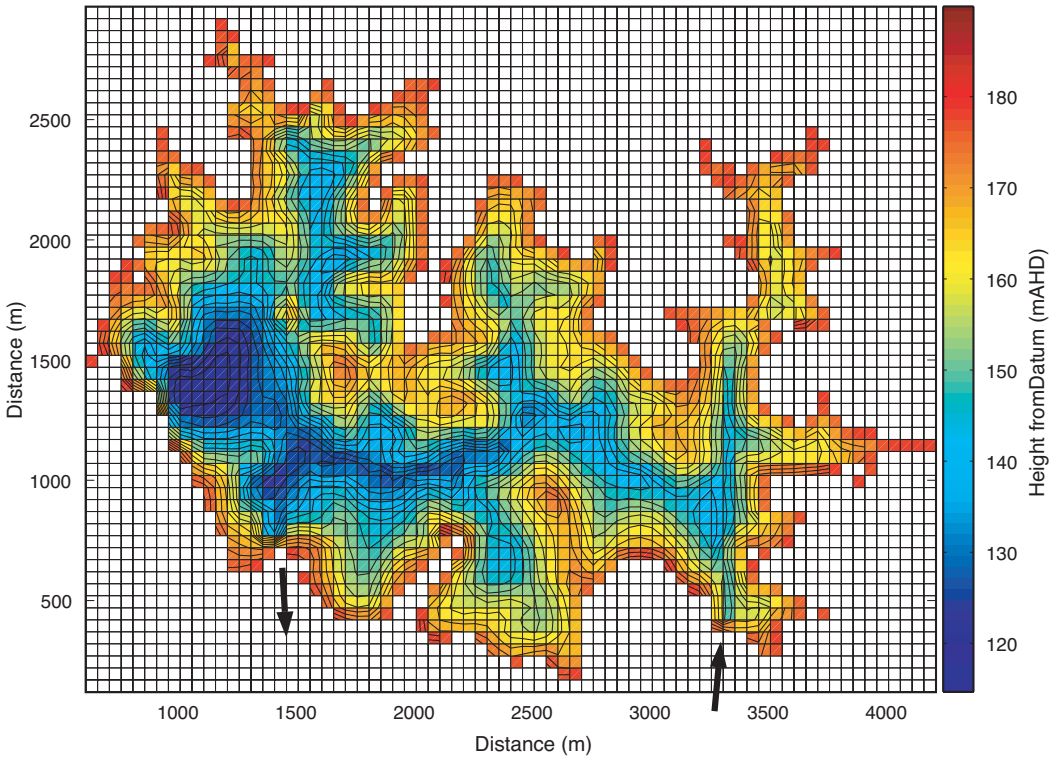

Figure 2.17: Discretized 60×60 m Sugarloaf Reservoir grid used for ELCOM. Colour scale is in units of metres above Australian Height Datum.

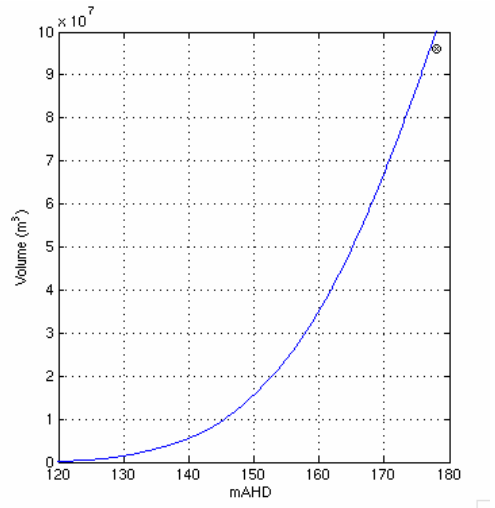

Figure 2.18: Storage-height curve for the ELCOM and raw data bathymetries (indistinguishable because of overlap). The circle is the actual volume estimate at FSL.

Results and Discussion

A comparison of the ELCOM prediction and the thermistor chain data is shown in Figure 2.19. Inflow (blue) and outflow (green) flow rates are shown in the top panel. The ELCOM simulation continues on past the available data as a forecast prediction of conditions during the field experiment.

Initially, the domain is fairly well mixed with little sign of stratification. Over the first 30 days, a period of cooling is evident with temperatures falling from 12 to 10°C over this time. This cooling trend causes much mixing through convective cooling at the surface, and so over this time only mild stratification is evident. The ELCOM prediction for the first 30 days is excellent, to within 0.1°C. This suggests that the surface thermodynamics are accurately simulated since the observed trend is caused through cooling at the surface. The magnitude and depth of the diurnal thermoclines are also similar to the observed values.

The underflow signal from the cool inflow is seen at the dam wall approximately 5 days from the commencement of pumping (day 205). The magnitude of the underflow is almost 30 m high and causes rapid cooling throughout. During the inflow the ELCOM results indicate the underflow to be overly cool (by ~0.4°C) suggesting either insufficient entrainment or prescription of the upstream boundary condition too close to the main waterbody; in reality inflow water would entrain more between the measurement point and the ELCOM boundary condition point. If it was the former however, then the timing and height of the underflow would also be poorly predicted, so it is likely that that the overly cool prediction is a result of prescribing the boundary condition too close to the actual reservoir domain. Nonetheless, the magnitude of the error is relatively small and the height and timing of the hydrodynamic features are modelled accurately.

Sampling Program

The system as simulated prior to the inflow, and the forecast prediction during the period of the campaign suggests the inflow water is most likely to move along the bottom of the reservoir (underflow), but since the temperature difference may not be that marked, periods where the inflow inserts at mid locations (as an interflow) or even comes to the surface (overflow) may be experienced. The sampling

program therefore involves more intensive sampling in the vertical compared to the Myponga campaign (Figure 2.20). Additionally, since it is less of an event based system, and the inflow will be held on for a long period, the experimental period should be performed over a longer period of time, such as 5 – 7 days.

Some preliminary sampling of reservoir water by Melbourne Water between 18/06/03 and 16/07/03 found very low levels of *Cryptosporidium* (<0.05 oocysts L^{-1}), Total *Giardia* (max recorded 0.1 cysts L^{-1}); Enterococci (max recorded 190 $(100mL)^{-1}$), and some *Campylobacter* detected by PCR and Enteroviruses (<1 $(20L)^{-1}$). Total coliforms and *E. coli* appear to be the best organism to focus on, due to the relative high signal to noise ratio of these organisms (Table 2.1).

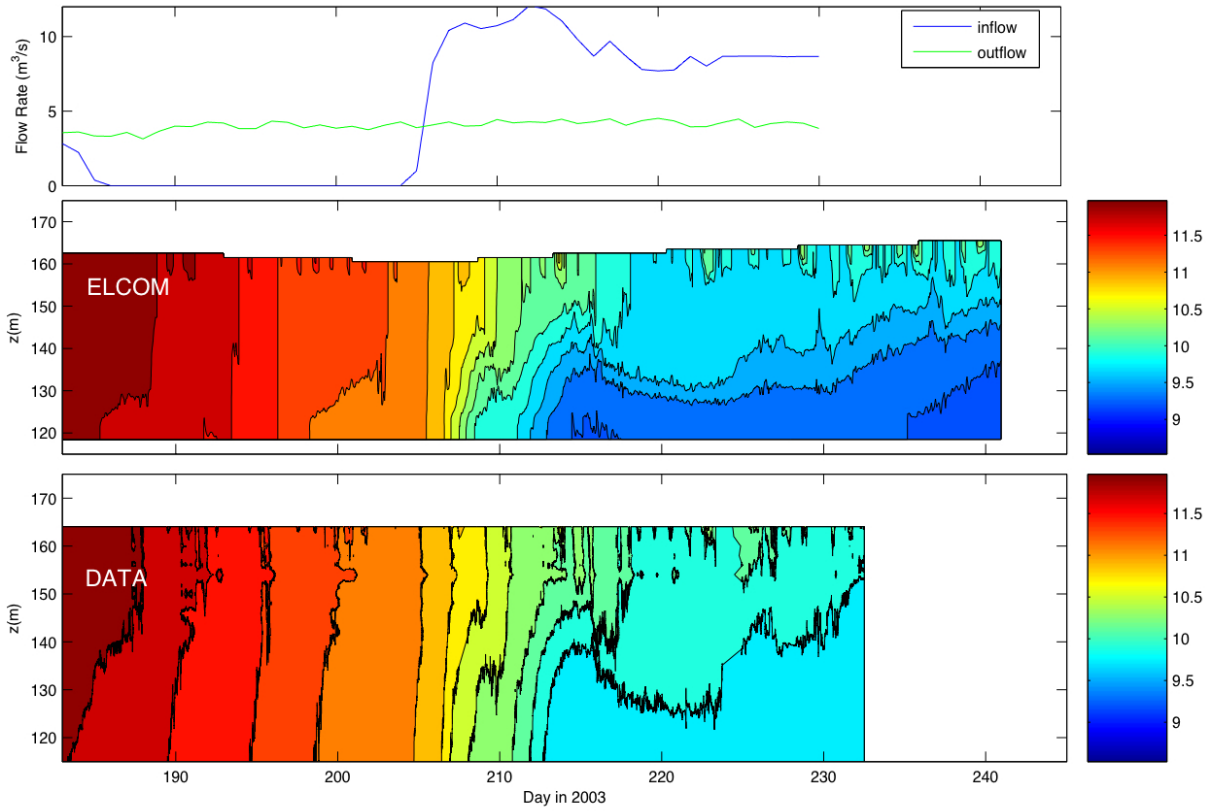

Figure 2.19: Comparison of thermistor chain data (bottom, °C) and ELCOM temperature prediction (middle). The top panel shows the inflow (periodic) and outflow (constant) volume fluxes for the simulation period.

Table 2.1: Results of preliminary monitoring of pathogens near the Sugarloaf river inflow.

Date	Coliforms (per 100mL)	*E. coli* (per 100mL)
18/06/03	1000	230
08/07/03	730	210
10/07/03	1400	290
11/07/03	1200	260
14/07/03	2000	220
16/07/03	1300	330

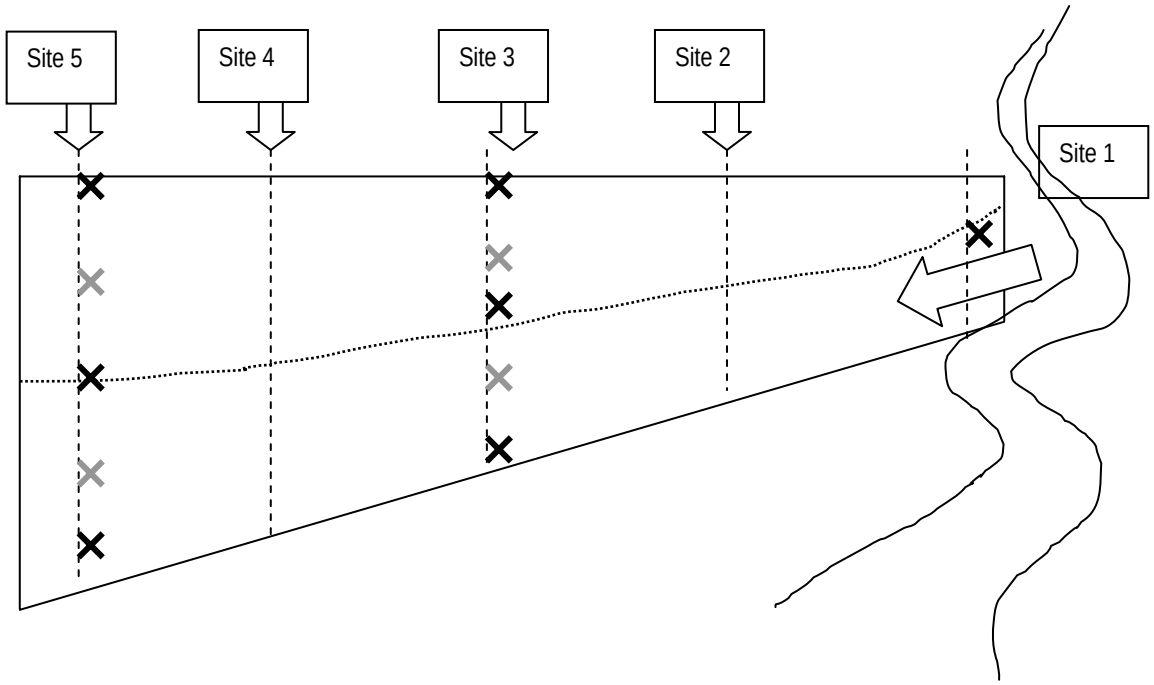

Figure 2.20: Proposed sampling strategy for Sugarloaf Reservoir field experiment. The dashed lines indicate the locations where detailed profiling will be conducted using the CTD and LISST profilers. The crosses indicate the locations where microbiological samples will be collected (black = 2 per day; grey = 1 per day).

Hydrodynamic Modelling of Lake Burragorang

Lake Burragorang is a large (2,000,000 ML, z_{max} = 93 m), dendritic lake formed by construction of the Warragamba Dam in New South Wales, Australia (Figure 2.21). It is made up of a main canyon section to the northeast, which is supplied by the Wollondilly River arm to the southwest, and the Cox and Kowmung River arm to the northwest.

Lake Burragorang is the major water supply for Sydney, Australia's largest city. It is characterized by large inflow events that threaten to introduce pathogens from the surrounding catchment and therefore have the potential to create significant public health risks. It has been observed that inflows take approximately seven days to reach the dam wall, however, cool inflows are likely to plunge deep enough to avoid UV levels capable of pathogen inactivation almost immediately upon entry. As a result, the threat of pathogens remaining viable all the way to the dam wall and off-take structures cannot be ignored.

Validation of ELCOM for Lake Burragorang is therefore conducted during a moderately sized flood event that occurred in June – July 1997, for which a significant validation dataset exists.

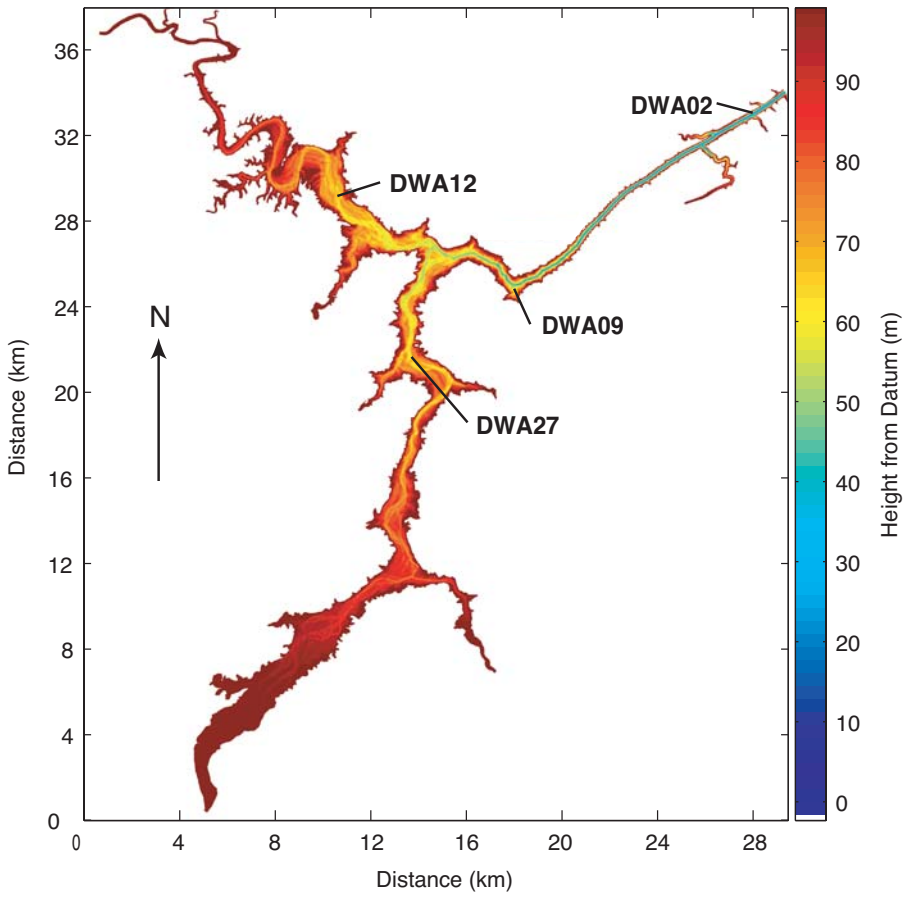

Figure 2.21: Lake Burragorang bathymetry (colour scale indicates depth from deepest point; Full Service Level, FSL = 116.72 mAHD). Also shown are the four sampling locations: DWA02, DWA09, DWA12 and DWA27.

Field Monitoring and Data

Meteorological Information:

Meteorological data for the 1997 flood event is presented in Figure 2.22. The forcing data is of a 15-minute resolution, with the exception of the 3-hourly cloud cover and relative humidity data. Wind-speeds are typically low (<5 ms^{-1}), except for an extreme period during days 190 – 191 where values in excess of 10 ms^{-1} are reached. It is important to note that much of the data was sourced from Richmond Airport, approximately, 40 km to the northeast, and so is likely to depart significantly from that experienced at the lake surface. For this reason, the focus for this event is on the flood inflow and less emphasis is placed on the surface thermodynamics predictions.

Reservoir Data:

A network of five thermistor chains was installed in Lake Burragorang, but unfortunately, during the period of interest (June – July 1997), the most data is unusable. The understanding of the inflow event, and the validation of ELCOM, is based on available profile data collected at the four stations: DWA02, DWA09, DWA12 and DWA27 (see Figure 2.21). The first profile was taken on 30 June 1997 (Day 181), the second on 1 July (Day 182) and then approximately every second day until July 15 (Day 196). Generally the profiles had a high vertical sampling resolution (1 m) and covered the entire depth of the water column.

A comparison of the inflow hydrographs for the major rivers indicated that >90% of the total inflow volume originated from the Wollondilly River Arm. This flow peaked at 680 m^3s^{-1} during day 179

(Figure 2.22). The water temperature (~10°C) of this inflow was low relative to the ambient reservoir water (~14°C), and so the inflow became a dense underflow. The flow reached station DWA27 on the Wollondilly River arm by day 182, implying an average velocity of approximately 0.01 ms^{-1}. As little inflow came down the Cox/Kowmung River arm, the cool Wollondilly underflow intruded back up this arm and reached station DWA12 by day 184. As the inflow progressed to the main canyon section upstream of the dam wall, the narrowing and deepening of the bathymetry amplified the thickness of the underflow to a maximum of 40 m.

ELCOM Setup

Application of a Cartesian grid model to such a narrow reservoir is somewhat of a challenge due to insufficient grid resolution in the cross-channel dimension and around the many tight bends. This results from the averaging process not being able to preserve the actual bathymetric detail when the computational domain is constructed from the available survey data, as sub-grid scale information is lost. Of course, a finer (*i.e.* more resolved) grid would alleviate this problem, but instead would create a computational demand that was not practical at the time of this analysis. To overcome this difficulty, an idealized bathymetry was developed to allow exploitation of a relatively coarse grid resolution, and hence attractive run times, yet allowing resolution of the dominant 3D hydrodynamic processes. To this end, a straightened bathymetry was generated that maintained the storage-height relationship of the actual reservoir, but removed all but the most significant bends and kinks. The straightening methodology has been described previously for 3D modelling of Lake Burragorang (Romero and Imberger, 2003).

Straightened bathymetry is generated by identifying the centre of the main channel and transforming this onto a straight line. In this analysis two straightened grids were tested: (1) a 'semi-straightened' grid where sections of the reservoir were straightened but major bends left intact (Figure 2.23-top), and (2) a 'fully-straightened' grid that transformed the Burragorang bathymetry onto two main lines representing the Wollondilly and Cox reaches (Figure 2.23-bottom).

To exploit lower run-times for future ELCOM-CAEDYM simulations the performance of various coarsened grid resolutions were also explored. The 'optimum' solution was considered to be the 200×200 m domain, and subsequently coarsened grids were explored by altering the along-stream grid thickness to 400×200 and 800×200 m (Figure 2.24). This comparison serves as a test for grid convergence and is useful in assessing the relative importance of fast run times versus high accuracy. Figure 2.24 additionally shows how the storage-height relationship of the computational domain compares to that observed in the field for the different domains. The ELCOM domain represents the observed data well, and importantly there is no loss in accuracy as the grid is coarsened. It should be noted that along the main canyon-section of the reservoir, it was necessary to manually adjust some of the bathymetry values generated by the averaging process to ensure that the depth-structure was maintained. This was achieved by ensuring there was a monotonic increase in depth from the Wollondilly-Coxs confluence to the dam wall. Preliminary simulations showed that this was important in correctly modelling the timing and mixing characteristics of the dense underflows in this region, primarily because the averaging process created an artificial surface roughness in the narrow reaches.

The vertical grid resolution was held uniform at 1 m for the various grids, except for a version of the 800×200 grid where a uniform 2 m vertical resolution was specified. Due to insufficient meteorological data, surface meteorological forcing was specified as constant across the domain. Similarly, uniform initial conditions in the x and y dimensions were applied, but an initial vertical stratification based on an average of available field data was used. Although the field data did indicate some horizontal variation of epilimnion temperatures, presumably due to differential surface heating/cooling across the domain, application of the average value was found to have little effect on the evolution of the front. A timestep

of 6 minutes was applied to each grid. The 200×200 and 800×200 fully-straightened grids were also run with a timestep of 3 mins.

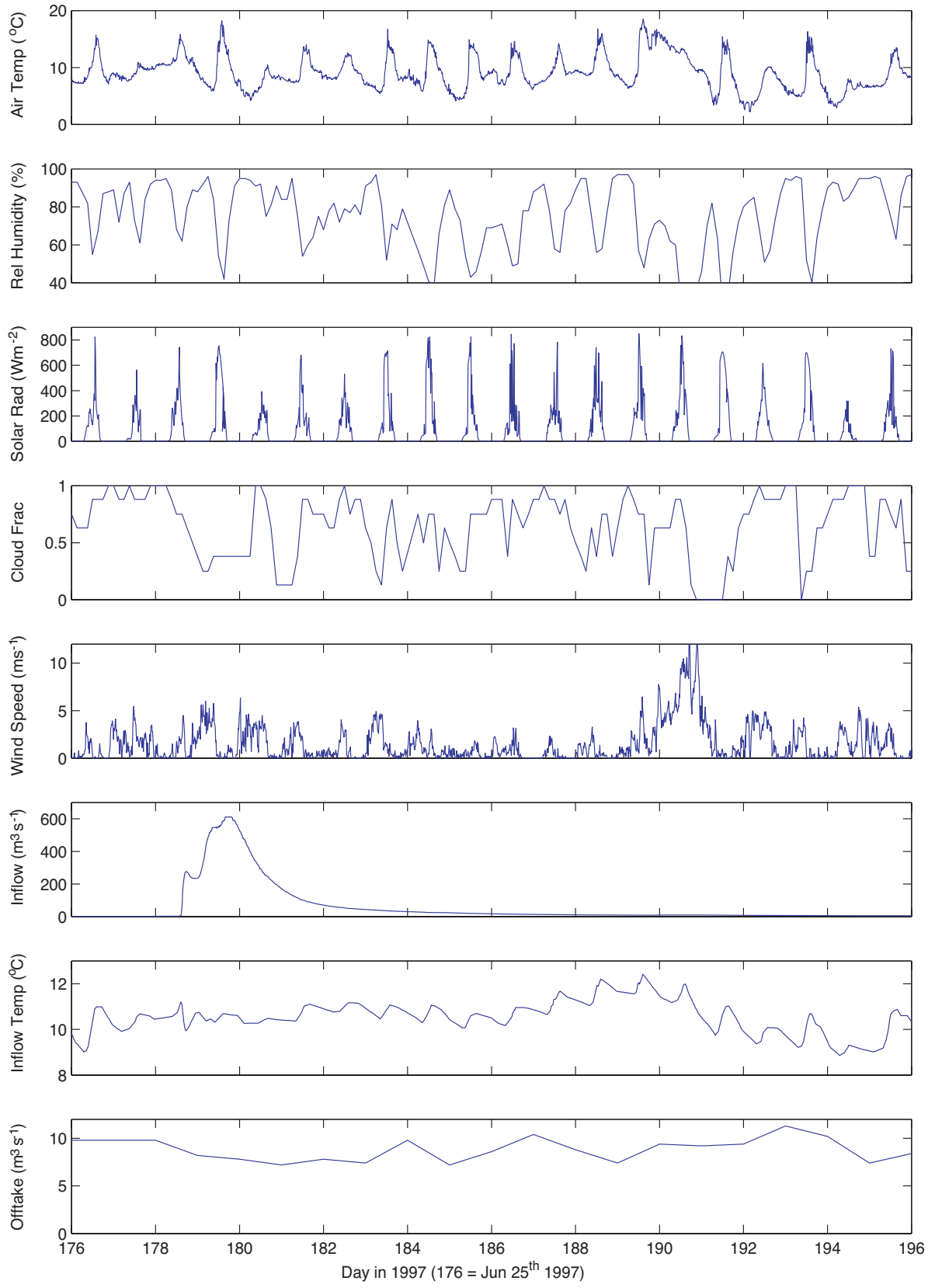

Figure 2.22: Meteorological and inflow/outflow data for Lake Burragorang during the June-July 1997 flood event.

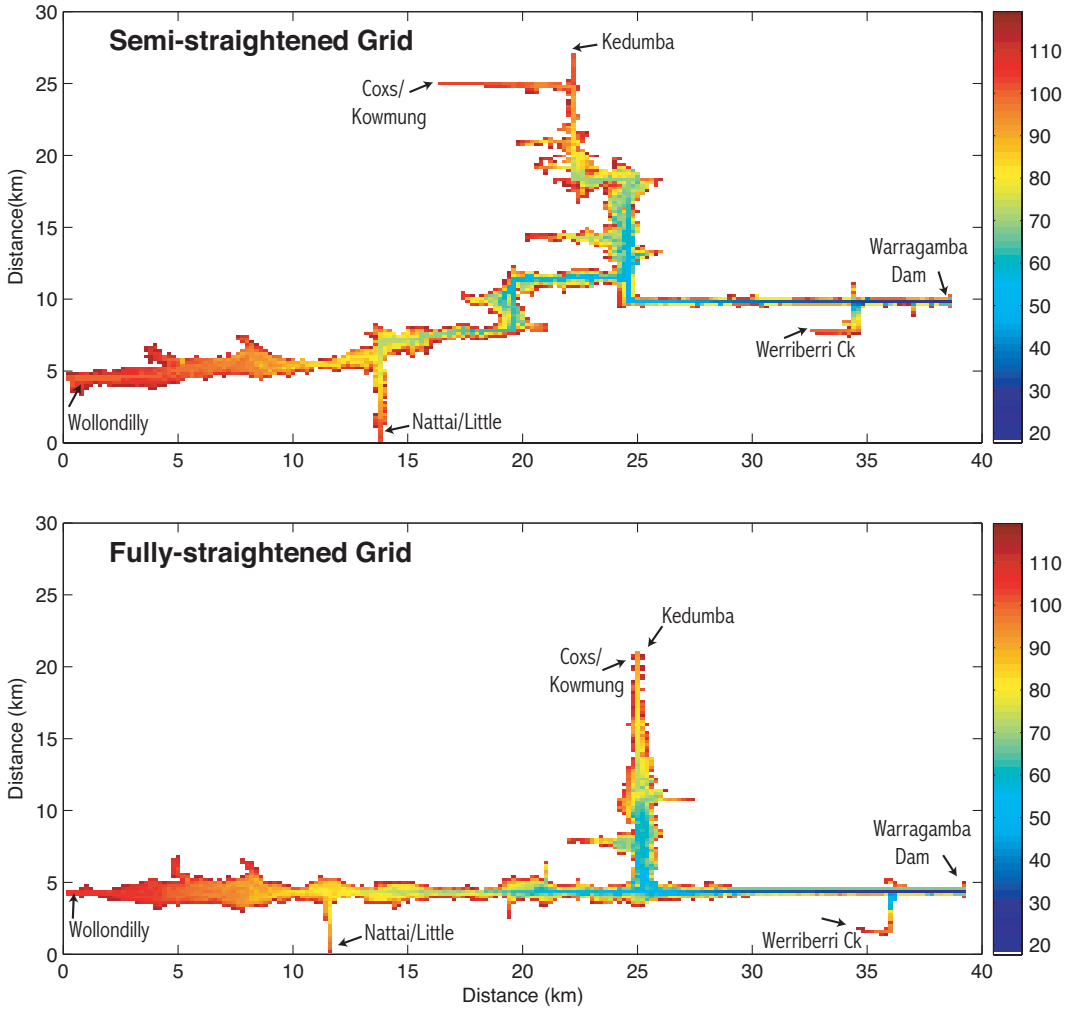

Figure 2.23: Plan view of the idealized ELCOM grids (200×200 m): semi-straightened (top) and fully-straightened (bottom). Colour scale reflects height in mAHD.

During the 1997 flood event, >90% of the total inflow volume came down the Wollondilly River arm, and so within ELCOM the other stream inflows were ignored. Outflows were specified from the HEPS off-take (45 m) and the 40 m and 24 m off-takes. As the main focus was the underflow dynamics, and since the meteorological data was poor, influence of rain and atmospheric stability was ignored. Longwave radiation was estimated from cloud cover using the ELCOM longwave model, and not directly provided as an input.

ELCOM Performance

Figure 2.25 compares the results of the 200×200 m fully-straightened (Δt = 3 mins) simulation with the field profile data taken from stations DWA02, DWA09, DWA12 and DWA27. To facilitate a quantitative comparison between the various grid configurations a summary of the salient features of the inflow event (underflow height, onset, temperature) are presented in tabular form (Table 2.2). The semi-straightened grid performed poorly for the majority of the criteria, particularly in regard to the timing of the front, and so the focus below is on the results of the fully-straightened grid.

For all stations ELCOM accurately predicted the onset, height and temperature of the inflow front. Due to the low temporal resolution of the profile data, interpolation of results to produce the contour plots introduced some artificial front 'smearing'. In reality, one would expect to see a sharp leading edge as is predicted by ELCOM. Similarly, the profile data is unable to resolve sub-daily characteristics of the underflow.

On day 191, in response to a high wind event (Figure 2.22), ELCOM simulates a large tilt in the thermocline (raised at DWA27 and lowered at DWA09 and DWA02), which creates a vertical excursion of approximately 20 m and lasts of the order of 24 hrs. This is not seen in the profile data for two possible reasons: (1) the profile data was taken at an interval of two days during this period, which is insufficient to resolve an event of the order of a day, or (2) ELCOM is responding to erroneous wind forcing data. If the latter is true, then it stands that more accurate (and spatially variable) forcing data would resolve the problem. Recent experimental work on the lake has found large spatial differences in wind forcing (Romero *et al.*, 2002), and so this is likely to be the case. Nonetheless, it is concluded that ELCOM accurately predicts the characteristics of the underflow with respect to its height, temporal variability (at a single point and in space), and the temperature structure (and hence entrainment volume).

The surface layer however was less accurately modelled. This is not surprising given the poor forcing meteorological information in addition to basin-wide application of a single vertical temperature structure during initialization. Hence, at stations DWA09, DWA12 and DWA27, the simulated surface layer profile data is ~0.5°C cooler than that seen in the field, but near the dam wall (DWA02), the simulated surface layer is too warm. Because of the poor meteorological information available for this period, the focus of the analysis during this event is the underflow, and the results from Myponga and Sugarloaf Reservoir's are relied upon for a comprehensive assessment of the surface thermodynamics.

A more general comparison of ELCOM performance is achieved by plotting the equivalent ELCOM temperature at every point in time and space where a field measurement was made (*i.e.* the crosses indicating the profile measurement points on Figure 2.25). Figure 2.26 is an example of such a plot for the 200×200 m fully-straightened grid (the equivalent plots for the other grid configurations are similar and so are not all presented here, although the results of the regressions are summarized in Table 2.2). In stratified systems, points at the top of the plot typically refer to the surface layer and points towards the lower end refer to the underflow. With respect to the underflow temperatures, the plot indicates that ELCOM replicates the observed data to within ±0.2 °C.

This comparison provides additional information (correlation coefficient, R^2, and regression parameters) that assists in determining the accuracy of the simulation, but also it allows us to compare the relative performance of the various grid configurations in a quantitative manner (Table 2.2). The results of this analysis for the various ELCOM simulations were not as expected. They indicate that sacrifices in accuracy with coarsening grid resolution and time-step refinement are small. Indeed, the coarsest grid (800×200×2 m) provided the best overall correlation coefficient (R^2=0.873, based on all available profile data) of all those tested. It appears the only disadvantage of the coarsened grids (400×200 and 800×200) is their under-prediction of underflow entrainment. In particular, the underflow temperature at sites DWA02 and DWA09 is 0.5°C cooler than the observed data. It is unclear whether the more accurate results for the underflow temperature of the 200×200 ELCOM simulations stem from better resolution of the front and the mixing that occurs at the top of the underflow, or whether the larger number of grid cells (and hence computations) resulted in more significant numerical diffusion mimicking that seen in the data (see Laval *et al.*, 2003a). Nonetheless, predictions to within 0.5°C are considered an excellent result for the coarsest grid, particularly considering the order of magnitude decrease in run time.

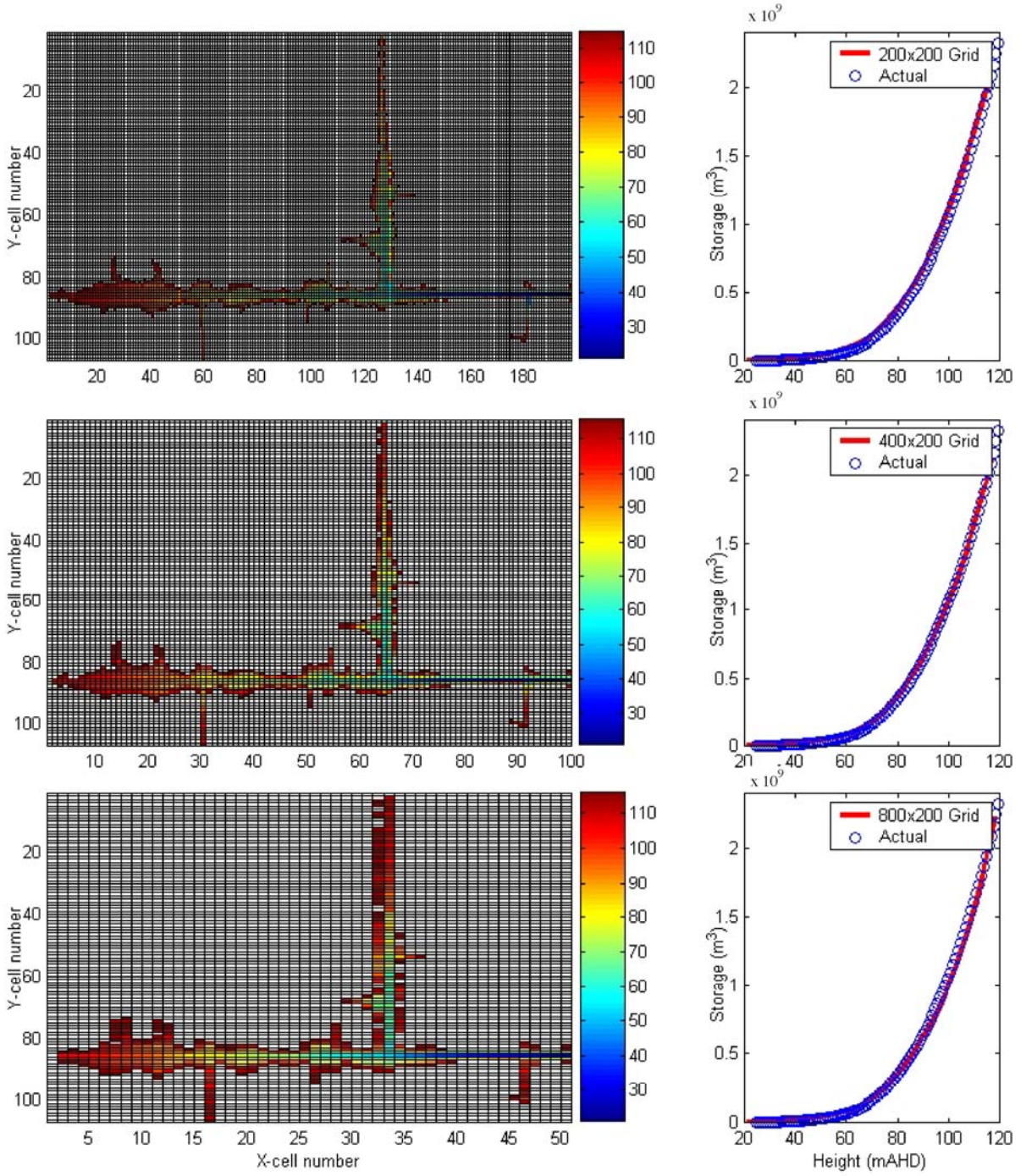

Figure 2.24: Comparison of three variations of the fully-straightened ELCOM grid (colour indicates ground height in meters AHD) for Lake Burragorang: 200×200 (top), 400×200 (middle) and 800×200 (bottom). The storage-height curve is shown next to each against the actual relationship.

Summary

The aim of this chapter was to present the validation of ELCOM as applied to Lake Burragorang and Myponga and Sugarloaf Reservoirs. This work was conducted prior to performing the intensive field experiments using available historical data and the analysis therefore provided important information about the dominant process controlling the hydrodynamic behaviour of the study sites, which was exploited during design of the experimental sampling regimes.

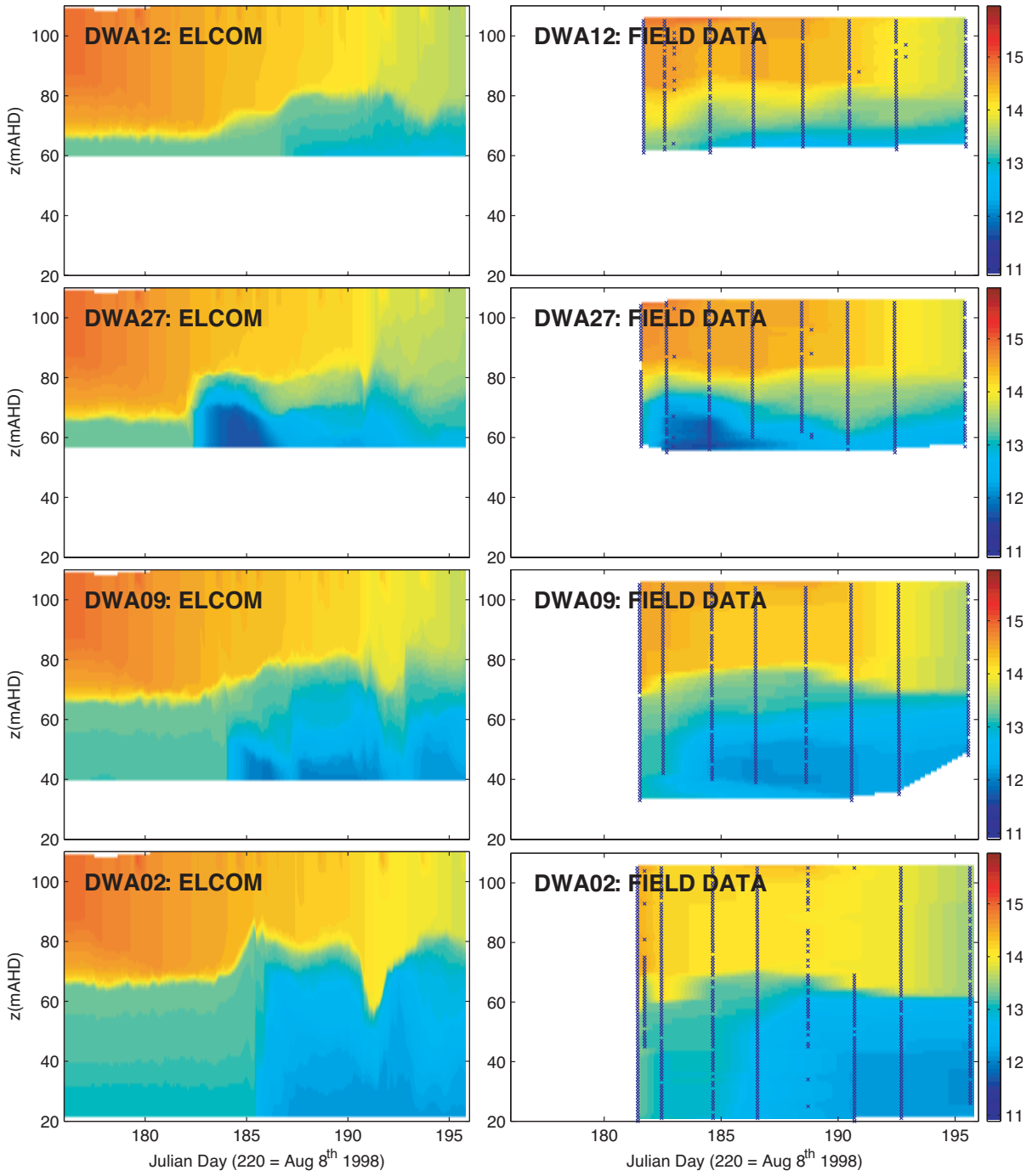

Figure 2.25: ELCOM simulations of the temperature (°C) structure during the 1997 flood event compared against profile data for the four stations: DWA02, DWA09, DWA12 and DWA 27. Crosses on the field data plots indicate points of measurement. The ELCOM results are from the 200×200 m fully-straightened grid.

Myponga Reservoir was validated against two storm events that occurred in May and September of 2001. The focus was on the inflow hydrodynamics, but in addition, high quality meteorological forcing data provided an excellent dataset to validate the surface thermodynamics module of ELCOM. However, the meteorological data for both the May and September simulation periods indicated persistent periods of atmospheric instability, which motivated the development and trial of a new atmospheric stability module within ELCOM's surface thermodynamics routines (see Appendix A1 for

detail). The improvement resulting from the atmospheric stability module was significant for both the May and September periods, particularly during low wind conditions, where ELCOM would have otherwise underestimated the effects of convective instability on the heat fluxes from the water's surface. Overall, the ELCOM simulations captured the inflow dynamics and surface thermodynamics to within 0.5°C for two locations within the reservoir for both the May and September study periods.

Sugarloaf Reservoir was validated for a two-month long simulation that compared ELCOM results against thermistor chain data. The simulated period initially experienced significant cooling and was then followed by a large inflow volume that progressed as a steady state underflow.

Lake Burragorang was validated against data from a moderately sized storm event that occurred in June – July 1997. For this event, poor meteorological data existed, and so the focus was on modelling the evolution of the dense underflow and not on the surface thermodynamics. To this end, several different grid configurations were compared against profile data taken from four locations throughout the reservoir. It was concluded that it was necessary to develop a fully straightened idealized bathymetry for Lake Burragorang to accurately reproduce the observed data because of its narrow and tortuous nature. Additionally, various coarsened grid resolutions were explored, but little difference was seen between the 200×200×1 grid and the 800×200×2 grid (the finest and coarsest grids respectively), except for a relatively small difference in the entrainment of the underflow. Based on the comparisons with the profile data, it was concluded that ELCOM accurately captured the evolution of the underflow in time and space (to within 0.5°C), and so could be confidently applied as the hydrodynamic driver for modelling pathogen transport in this system.

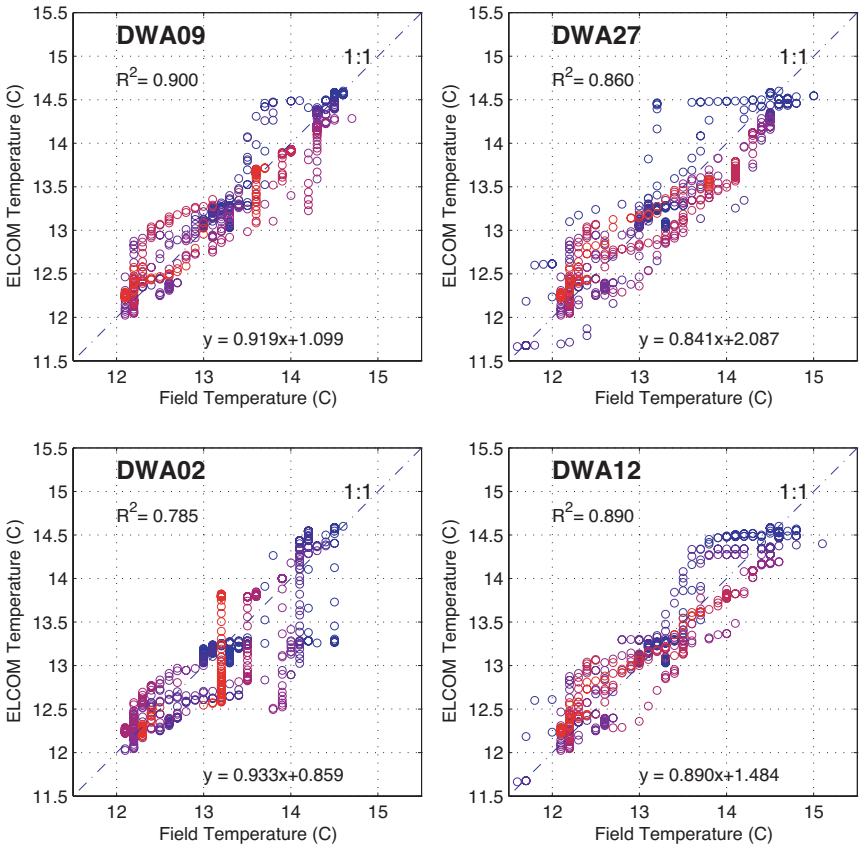

Figure 2.26: Comparison between all measured temperatures and the equivalent ELCOM prediction for the 1997 flood event for all four stations. The ELCOM results are from the 200×200 m fully-straightened grid (Δt = 3 mins). The colour scale reflects the time the sample was taken: blue at the beginning of the period (Day 181) through to red at the end of the period (Day 196).

Table 2.2: Comparison of ELCOM simulation results for the various grid configurations, presenting the underflow characteristics, and the results of the regressions against the profile data. Figures in bold indicate the results closest to the observed data.

Station	Parameter	Units		Observed Data	200x200x1-Fully-straightened dt=3min	200x200x1-Fully-straightened dt=6min	200x200x1-Semi-straightened dt=6min	400x200x1-Fully-straightened dt=6min	800x200x1-Fully-straightened dt=6min	800x200x2-Fully-straightened dt=6min	800x200x2-Fully-straightened dt=3min
DWA02											
Underflow	Height[1]	(mAHD)	62	60-70	60-70	60	60-70	60-70	60-75	60-70
	Onset	OD in 97	186	185.5	184.5	186.5	184.1	184.2	184.5	185.4
	Temperature	(ºC)	12.5	12.5	12.5	12.2	12	12	12	12
Regression	R^2		N/A	0.769	0.737	0.779	0.771	0.800	0.788	0.781
	Slope, m		N/A	0.935	0.874	0.890	1.030	0.989	1.007	1.025
	Offset, c		N/A	0.829	1.634	1.419	-0.564	-0.003	-0.266	-0.502
DWA09											
Underflow	Height	(mAHD)	60	50-60	55-60	45-65	50-60	58	50-60	50-60
	Onset[2]	OD in 97	182.5-184	184	183.5	186	183	183	183.5	184
	Temperature	(ºC)	12	12	12	11.7	11.5	11.5	11.5	11.5
Regression	R^2		N/A	0.917	0.909	0.860	0.896	0.894	0.918	0.911
	Slope, m		N/A	0.926	0.889	0.842	1.006	0.988	1.009	1.011
	Offset, c		N/A	0.986	1.465	2.279	-0.201	0.035	0.283	-0.281
DWA27											
Underflow	Height	(mAHD)	75	75	75	62	75	75	75	75
	Onset	OD in 97	182	182	182	184.5	182	182	182	182.2
	Temperature	(ºC)	11.5	11.5	11.5	11.5	11.3	11.3	11.3	11.3
Regression	R^2		N/A	0.880	0.902	0.673	0.848	0.854	0.892	0.886
	Slope, m		N/A	0.843	0.822	0.679	0.924	0.899	0.921	0.930
	Offset, c		N/A	2.034	2.307	4.307	0.874	1.197	0.868	0.766
DWA12											
Underflow	Height	(mAHD)	80	80	80		80	80	80	80
	Onset	OD in 97	186	186	186		185.5	186	186	186
	Temperature	(ºC)	12.8	13	13		13	13	13	13
Regression	R^2		N/A	0.907	0.903		0.880	0.882	0.910	0.905
	Slope, m		N/A	0.894	0.862		0.982	0.957	0.970	0.980
	Offset, c		N/A	1.407	1.818		0.134	0.461	0.247	0.147
GENERAL[3]	R^2		N/A	0.8664	0.8604	0.7312	0.8519	0.8664	0.8731	0.8683
	Slope, m		N/A	0.8889	0.8594	0.7617	0.9743	0.9519	0.9629	0.9652
	Offset, c		N/A	1.4714	1.8456	3.1500	0.2098	0.5035	0.3436	0.3373
	Runtime Ratio[4]		1:1	1:9	1:16	1:16	1:34	1:70	1:128	1:69

[1] Height to 13ºC isotherm

[2] Some uncertainty due to low resolution sampling

[3] Statistics based on all available data (DWA02,09,12,27)

[4] Runtimes based on simulations run using a G4 Mac Dual 733MHz Processor with 900Mb RAM (run in 2002)

CHAPTER 3

A THREE-DIMENSIONAL MODEL OF *CRYPTOSPORIDIUM* DYNAMICS IN LAKES AND RESERVOIRS – A NEW TOOL FOR RISK MANAGEMENT

Hipsey, M.R.[1,2], Antenucci, J.P.[2], Brookes, J.D.[1,3], Burch, M.D.[3,4], Regel, R.H.[3], Linden, L.[1,3]

[1] School of Earth and Environmental Sciences,
The University of Adelaide, Adelaide, South Australia, 5005.

[2] Centre for Water Research,
The University of Western Australia, 35 Stirling Hwy, Crawley, Western Australia, 6009.

[3] CRC for Water Quality and Treatment,
PMB 3 Salisbury, South Australia, 5108.

[4] The Australian Water Quality Centre,
PMB 3 Salisbury, South Australia, 5108.

International Journal of River Basin Management – 2004; 2(3): 181-197.

Hipsey, M.R., Antenucci, J.P., Brookes, J.D., Burch, M.D., Regel, R.H. and Linden, L. (2004) A three-dimensional model of Cryptosporidium dynamics in lakes and reservoirs – a new tool for risk management.
International Journal of River Basin Management, v. 2 (3), pp. 181-197

CHAPTER 4

THE RELATIVE VALUE OF SURROGATE INDICATORS FOR DETECTING PATHOGENS IN LAKES AND RESERVOIRS

Brookes, J.D. [1,2], Hipsey, M.R. [1,3], Burch, M.D. [2,4], Regel, R.H. [2], Linden, L. [1,2], Ferguson, C.M. [2,5], Antenucci, J.P. [3]

[1] School of Earth and Environmental Sciences,
The University of Adelaide, Adelaide, South Australia, 5005.

[2] CRC for Water Quality and Treatment,
PMB 3 Salisbury, South Australia, 5108.

[3] Centre for Water Research,
The University of Western Australia, 35 Stirling Hwy, Crawley, Western Australia, 6009.

[4] The Australian Water Quality Centre,
PMB 3 Salisbury, South Australia, 5108.

[5] Ecowise Environmental,
PO Box 1834, Fyshwick, Australian Capital Territory, 2069.

Environmental Science and Technology – 2005; 39(22): 8614-8621.

NOTE: Statements of authorship appear in the print copy of the thesis held in the University of Adelaide Library.

NOTE:
Although I was not listed as the first author on the final published manuscript, after discussion with the authors, the chapter has been included as part of the main thesis body for three main reasons:

- I conducted a significant amount of the work done for the paper, including a substantial percentage of the original written manuscript;
- I have included extra figures in this chapter (Figure 4.4a,b) which were not in the original published paper;
- This chapter serves as an important link between the experimental campaign in Myponga and the subsequent campaign in Sugarloaf Reservoir, since it was this analysis that found the large differences between the protozoan (oo)cysts and the indicator bacteria and phages. This difference motivated the Sugarloaf experimental campaign (outlined in Chapter 5) to focus on sedimentation behaviour of the coliform bacteria.

In light of these points, this paper is included as a 'supporting' chapter at this point within the chronology of the thesis, and I wish to acknowledge the contribution of the above named co-authors.

Brookes, J.D., Hipsey, M.R., Burch, M.D., Regel, R.H., Linden, L.G., Ferguson, C.M. and Antenucci, J.P. (2005) Relative Value of Surrogate Indicators for Detecting Pathogens in Lakes and Reservoirs.
Environmental Science and Technology, v.39 (22) pp. 8614-8621

CHAPTER 5

IN SITU EVIDENCE FOR THE ASSOCIATION OF TOTAL COLIFORMS AND *ESCHERICHIA COLI* WITH SUSPENDED INORGANIC PARTICLES IN AN AUSTRALIAN RESERVOIR

Hipsey, M.R.[1,2], Brookes, J.D.[1,3], Regel, R.H.[3], Antenucci, J.P.[2], Burch, M.D.[3,4].

[1] School of Earth and Environmental Sciences,
The University of Adelaide, Adelaide, South Australia, 5005.

[2] Centre for Water Research,
The University of Western Australia, 35 Stirling Hwy, Crawley, Western Australia, 6009.

[3] CRC for Water Quality and Treatment,
PMB 3 Salisbury, South Australia, 5108.

[4] The Australian Water Quality Centre,
PMB 3 Salisbury, South Australia, 5108.

Journal of Water, Air and Soil Pollution – 2006; 170(1-4): 191-209.

Hipsey, M.R., Brookes, J.D., Regel, R.H., Antenucci, J.P., Burch, M.D. (2006) In situ evidence for the association of total coliforms and Escherichia coli with suspended inorganic particles in an Australian reservoir.
Journal of Water, Air and Soil Pollution [i.e. Water, Air and Soil Pollution], v. 170 (1-4), pp. 191-209

CHAPTER 6

A GENERIC, PROCESS-BASED MODEL OF MICROBIAL POLLUTION IN AQUATIC SYSTEMS

Hipsey, M.R.[1,2], Antenucci, J.P.[2], Brookes, J.D.[1,3]

[1] School of Earth and Environmental Sciences,
The University of Adelaide, Adelaide, South Australia, 5005.

[2] Centre for Water Research,
The University of Western Australia, 35 Stirling Hwy, Crawley, Western Australia, 6009.

[3] CRC for Water Quality and Treatment,
PMB 3 Salisbury, South Australia, 5108.

Manuscript to be submitted.

Hipsey, M.R., Antenucci, J.P. and Brookes, J.D. A generic, process-based model of microbial pollution in aquatic systems.
Manuscript to be submitted.

CHAPTER 7

DECISION SUPPORT TOOLS FOR MANAGING MICROBIAL POLLUTION IN LAKES AND RESERVOIRS

Hipsey, M.R.[1,2], Antenucci, J.P.[2], Brookes, J.D.[1,3]

[1] School of Earth and Environmental Sciences,
The University of Adelaide, Adelaide, South Australia, 5005.

[2] Centre for Water Research,
The University of Western Australia, 35 Stirling Hwy, Crawley, Western Australia, 6009.

[3] CRC for Water Quality and Treatment,
PMB 3 Salisbury, South Australia, 5108.

LakeLine – 2004; 24(4): 25-28.

Hipsey, M.R., Antenucci, J.P. and Brookes, J.D. (2004) Decision support tools for managing microbial pollution in lakes and reservoirs.
LakeLine, v. 24 (4), pp. 25-28

CHAPTER 8

SYNTHESIS AND CONCLUSIONS

Microbial pollution of surface waters and coastal zones is one of the foremost challenges facing the water industry and regulatory authorities charged with reducing public health risks. Yet despite the concern and increasing pressures on water resources in both developed and developing countries, our understanding of microbial pollutants in the aquatic environment is fairly scattered. As a result, numerical prediction of enteric organisms in aquatic systems is fairly rudimentary and has not advanced significantly over the past two decades. This is particularly surprising when consideration is given to the significant advances in laboratory microbiology and increases in computational power that have also occurred over the same period. There is a need for an improved ability to quantify the processes that control the fate and distribution enteric organisms to support decision-making and risk-management activities.

It has been the aim of this thesis to advance our understanding of the dynamics of microbial pollution in surface waters and the coastal ocean through a program of review, field experimentation and numerical modelling. In particular, the study focused on the protozoan pathogen *Cryptosporidium parvum*, and several key bacterial and viral microorganisms that are indicators of pathogenic contamination. The outcomes of the thesis are an improved understanding of pathogen and indicator organism behaviour in surface waters, and the development of new and sophisticated predictive tools for improving pathogen risk management.

Prior to field experimentation, a detailed hydrodynamic modelling exercise of the proposed study sites was undertaken, since the transport and mixing of enteric organisms is heavily dependent on accurate hydrodynamic predictions. Hydrodynamic modelling was conducted using the three-dimensional (3D) Estuary Lake and Coastal Ocean Model (ELCOM), which is a based on the hydrostatic, Reynold's Averaged Navier-Stokes equations. ELCOM is able to resolve velocity, temperature and salinity distributions and how they respond to atmospheric and inflow forcing, and where applicable, oceanic exchange. Initial assessments of the model focused on accurate capture of the inflow dynamics, and the surface thermodynamics, since long-term predictions of temperature are important for calculating enteric organisms inactivation. When validating the model against a historical dataset from Myponga Reservoir (South Australia), it was found that the model accurately captured the inflow dynamics into the reservoir, but the surface thermodynamics were poorly captured. The surface thermodynamic module of ELCOM was therefore extended to account for non-neutral atmospheric stability effects (see Appendix A1), which significantly improved the predictions. ELCOM was also applied to Sugarloaf Reservoir (Victoria, Australia) and Lake Burragorang (New South Wales, Australia) and validated against available historical data.

Using the results of the hydrodynamic modelling investigation, the experimental program for Myponga Reservoir, South Australia, was devised. The aim of the experiment was to follow a riverine intrusion carrying significant concentrations of pathogens and other microbes, as it progressed throughout the waterbody. The model was used to determine the likely inflow behaviour, transport time and dilution rate, and thereby guide the appropriate sampling locations and frequency. A large flood event occurred in June of 2003 that seeded the reservoir with numerous microbial pollutants. The flood formed a dense intrusion that moved quickly through the reservoir and reached the dam wall within two days. Constant physico-chemical and particle (LISST) profiling and grab sampling at numerous locations within the reservoir provided a complete and unprecedented dataset. The dataset was firstly used to validate the physical predictions of ELCOM and the suspended sediment module of the Computational Aquatic Ecosystem Dynamics Model (CAEDYM), which dynamically couples with ELCOM.

Based on a detailed review of *Cryptosporidium* dynamics within the literature, a new pathogen module was developed and implemented within CAEDYM that accounted for natural mortality, sunlight inactivation, sedimentation and resuspension. The new pathogen module was validated against the Myponga dataset, and without calibration, performed to a high degree of accuracy.

Following the data analysis and numerical simulation of *Cryptosporidium* oocyst behaviour in Myponga Reservoir, the investigation sought to examine the differences between the pathogenic protozoa, and other microbial contaminants that are routinely used as indicators of pathogen risk. This analysis involved comparing through a Spearman rank correlation the attenuation of the various microbial contaminates. The results clearly highlighted the significant difference between *Crytposporidium* and the bacterial and viral indicators.

The findings of these first two studies suggested that microbial contaminants did not all behave similarly once introduced into a waterbody despite being subject to the same advective and mixing processes that were previously considered to be the dominant control. Over the short timescales typical of intrusion transport, it was thought that this variability between organisms would have insufficient time to manifest into any noticable differences. The key factors known to vary between organisms were natural mortality, susceptibility to inactivation by incident shortwave radiation and association with suspended particles. During the experiment, Myponga Reservoir was characterized by high UV light attenuation (DOC >10mgL^{-1}) and low mortality rates (T~10°C), suggesting the major factor creating the observed difference between organisms was primarily sedimentation.

To examine the role of bacterial association with particles in more detail, a second experimental campaign was carried out in Sugarloaf Reservoir, Victoria. Specifically it was the aim of this campaign to gain insights into the *in situ* association of coliform bacteria with suspended sediment and to quantify their sedimentation dynamics. This campaign again used the intensive physico-chemical and particle (LISST) profiling to track the passage of the inflow water through the reservoir. As in Myponga Reservoir, numerous grab samples were taken from multiple locations and at multiple depths, but this time only total coliforms and *E. coli* were measured. Using an inverse technique, the detailed particle profile data was used to create a simple Lagrangian model, which was used to back-calculate the sedimentation rates of the coliform bacteria. The results indicated that 80-100% were associated with a relatively small-sized clay fraction. This was in contrast with the *Cryptosporidium* dynamics studied in Myponga Reservoir, where it was concluded that oocysts did not settle with the inorganic particles.

By this stage it became clear that the current models and knowledge available for simulating the array of organisms of interest to water utilities and regulatory authorities were inadequate to resolve the level of detail necessary for useful predictions and risk management. Large differences between the protozoa and the bacteria and phages were being observed due to a) different particle association rates and therefore sedimentation dynamics, b) order of magnitude differences in natural mortality rates, and c) different sensitivity to different sunlight bandwidths. The original *Cryptosporidium* model implemented within CAEDYM was therefore rewritten to be more complete and generic for all microbial pollutants and different types of aquatic systems. The model was built using a generic set of parameterizations that describe the dynamics of most protozoan, bacterial and viral organisms of interest. The parameterizations dynamically account for the effects of environmental conditions such as temperature, salinity, pH, dissolved oxygen, sunlight, nutrients and turbidity on the growth and mortality of enteric organisms. Parameters for a range of organisms were also estimated based on a synthesis of literature data.

The new model significantly advances previous studies in several areas. First, inclusion of the growth term allows for simulation of organisms in warm, nutrient rich environments, where typical die-off models tend to over-predict loss rates. The growth term allows for simulation of potential regrowth effects and includes nutrient and temperature limitation functions. Second, the natural mortality term has been extended to independently account for the effects of salinity and pH, in addition to temperature. The salinity–mediated mortality has also been adapted to account for the nutrient status of the medium to simulate the importance of nutrient starvation on the ability of an organism to survive under osmotic stress. Third, a new model for sunlight-mediated mortality is presented that dynamically accounts for

mortality induced by visible, UV-A and UV-B bandwidths. This additionally has capacity to simulate the photo-oxidative and photo-biological mechanisms of inactivation through included sensitivities to dissolved oxygen and pH. Fourth, the model allows for organisms to be split between free and attached pools, and sedimented organisms may become resuspended in response to high shear stress events at the water-sediment interface caused by high velocities or wind-wave action. Fifth, the enteric organism module has been implemented within the bio-geochemical model CAEDYM, which gives it dynamic access to concentrations of dissolved oxygen, organic carbon, and suspended solids, in addition to pH, shear stress and light climate information.

Without adjustment of the literature derived parameter values, the new model was implemented within the 3D model ELCOM-CAEDYM, and was validated against data from three aquatic systems that differed in their climatic zone, trophic status and operation. The model was able to accurately capture the observed trends in each system, lending confidence to the parameter set since calibration was not relied upon. This analysis highlighted the significant spatial and temporal variabilites that exist in the processes that control enteric organism fate, not only within a particular system, but also between different aquatic systems. For example, *E. coli* was found to be mainly controlled by sedimentation in Myponga Reservoir, natural mortality in Sugarloaf Reservoir and growth and predation in Billings Reservoir. Since the new model is capable of resolving these processes dynamically, it is a significant advance for scientists and managers relative to the commonly used die-off models.

The analysis has highlighted the large differences between species that originate from variable rates of growth, mortality and sedimentation. It is emphasized that the use of surrogates for quantifying risk is problematic and that care must be taken when inferring risk of exposure to pathogens from microbial indicator data. Indeed the study has highlighted that the commonly used coliform organisms are a very poor indicator of protozoan pathogens since they have higher sedimentation rates, natural mortality rates, sunlight-induced mortality rates, and in some case they can multiply within the environment. They therefore have the potential to provide false negatives (since they die and settle faster) and false positives (since they may bloom in the absence of faecal contamination).

The model developed under this study is already being used in a range of organizations for a variety of applications:

- *as a scientific tool for exploring the dominant processes within a given system* – for scientists interested in understanding the spatial and temporal variabilities in the dynamics that control enteric organism behaviour, and conducting pathogen budgets and exploring sensitivities;

- *to guide the design targeted monitoring programs* – the model can be run to provide information about expected transport and kinetic controls to ensure that the sampling locations and frequency is focused on the areas that present the largest risk;

- *to quantify differences between species* – the model can be used to ‘correct’ the observed microbial indicator organism data so that the true risk by actual pathogenic organisms can be quantified;

- *to quantify the impact of proposed management scenarios* – scenarios such as catchment remediation, climate change and engineering interventions can be compared to the base case system as part of a cost-benefit analysis prior to any remedial action;

- *to support real-time decision-making* – the model can be used to provide now- and fore-casts of conditions within an aquatic system to enable managers to alter pumping regimes or issue recreational closures.

Finally, the analysis has also served to identify the areas where more experimentation is required. The areas that are in the most urgent need of attention are the parameters (and parameterizations) of both growth and predation. Evidence of growth of coliforms and Enterococci in environmental waters is substantial, however, only the Camper *et al*. (1991) study is sufficiently quantitative for estimation of the growth rate and nutrient and temperature sensitivities as required by the model. Similarly for predation, substantial evidence of grazing and/or predation of enteric organisms exists, but it is difficult to convert the results of these studies into a form relevant for use within a process-based model. There is also a clear need for more experimentation of actual pathogenic protozoan, bacteria and viruses within different aquatic environments, since these are the organisms that ultimately provide the risk to human health.

APPENDIX A1

ON THE IMPORTANCE OF ATMOSPHERIC STABILITY EFFECTS WHEN MODELLING THE SURFACE THERMODYNAMICS OF LAKES AND RESERVOIRS

Overview

Poor predictions of temperature response in a reservoir during prolonged periods of non-neutral atmospheric stability motivated the implementation of a simple scheme to correct for the effects of atmospheric stratification on the surface fluxes of momentum and sensible and latent heat.

Introduction

Of increasing importance in lake research and management is the application of coupled hydrodynamic and water quality/aquatic ecology models. In these applications, the hydrodynamic driver models the physics, and simulates spatial and temporal patterns of temperature, salinity and velocity. These predictions are used to drive water quality and aquatic ecology subroutines, which may have the capacity to alter physical attributes (*e.g.* light extinction) and consequently affect the hydrodynamic behaviour. Most water quality and ecological processes that occur in lakes and reservoirs are highly temperature dependent, and so poor predictions of temperature will result in poor representation of the water quality variables of interest.

The predominant process affecting the accuracy of temperature predictions for lakes and reservoirs is the heat exchange that occurs at the surface. In its simplest form, this exchange is a balance between incoming solar radiation and outgoing latent heat. Longwave radiation and sensible heat also play an important role, but their importance tends to be more site specific. Momentum input to the lake by the wind is also an important process that influences how the surface heat transfers manifest within the temperature structure of the water column.

It is well known that the momentum and sensible and latent heat transfers that occur at the air-water interface are highly dependent on the degree of atmospheric stratification experienced above the waterbody. Despite this, it is commonplace for modellers to assume neutral atmospheric stratification when modelling these transfers. This is particularly the case for inflow events that many water quality modellers are interested in because the meteorological conditions that create the inflow forcing are rarely neutral. In light of the importance of surface heat fluxes on the hydrodynamic behaviour of the water body, ignoring stability effects can potentially introduce a large source of error.

There is therefore a need for a simple scheme to account for the effect of atmospheric stability on the surface momentum and heat fluxes to be applied to hydrodynamic models. Such schemes are not new; Hicks (1975) was the first to present an iterative procedure that solved the stability corrected bulk-transfer coefficients using Monin-Obukhov similarity theory. More detailed analyses were later presented by Launiainen and Vihma (1990), Imberger and Patterson (1990) and Launiainen (1995). In the literature however, there has been few reports on the significance of atmospheric stability effects on the surface thermodynamics of lakes and reservoirs. Launiainen and Cheng (1998) used the iterative procedure to model the thermodynamics of ocean ice-cover under extremely stable conditions typical of relatively warm air over ice, but their results are not applicable to reservoirs or lakes in temperate climates.

The objective of this chapter is to present the results of a simple iterative scheme to correct for non-neutral atmospheric stabilities coupled to a three dimensional hydrodynamic model. The coupled model is applied to a moderate sized reservoir in South Australia during a period when the reservoir is subjected to inflow forcing and persistent non-neutral atmospheric conditions. The model results are compared against thermistor chain data and used to illustrate the importance of incorporating atmospheric stability effects in hydrodynamic models.

Study Site and Data Collection

Myponga Reservoir is a drinking water supply with a maximum storage of 26,800 ML and a maximum depth of 36 m at the dam wall, and is located on the Fleurieu Peninsula near Adelaide in South Australia (35°21'14''S, 138°25'49''E). It is fed by a 124 km^2 catchment that receives an average annual rainfall of approximately 750 mm. The catchment is drained by Myponga Creek, which feeds the 'side-arm' of the reservoir on the eastern side (Figure 3.1).

There are two floating weather stations installed on the water surface that also support thermistor chains. Station 'Met1' is located in the main basin and measures solar and net radiation, air temperature, and relative humidity at 2 m above the water surface. Station 'Met2' is located on the side-arm of the reservoir and measures only windspeed and direction. The thermistor chains were installed on each station such that there was fine thermistor spacing in the surface layer and increased spacing with depth.

Inflow volumes and water temperatures were monitored at Myponga Creek using a V-notch weir approximately 1 km upstream from the mouth of the creek at the reservoir. Outflow volumes from the dam off-take (located at the dam wall, 18 m above the reservoir floor) were also logged.

The study period extends from 16 – 31 May 2001 (Julian Day 136 – 152). This period was chosen as it was the first inflow event of the season, following a five month drought, and is therefore of particular interest to reservoir managers because of potential water quality ramifications. Additionally, the thunderstorm activity responsible for the river inflow was followed by a prolonged period of non-neutral atmospheric stratification over the waterbody. The forcing meteorological and inflow/outflow data for this period is shown in Figure A1.1.

Hydrodynamic Model

Background

The hydrodynamic model used in the investigation is the three dimensional (3D) Estuary, Lake and Coastal Ocean Model (ELCOM) presented in Hodges *et al.* (2000). This model solves the full unsteady Reynolds-averaged, hydrostatic, Boussinesq, Navier-Stokes and scalar transport equations, and is specifically adapted for stratified lakes and reservoirs as it uses a unique vertical mixing model for the vertical Reynolds stress terms in place of vertical eddy diffusivity. The mixed-layer model has been shown to more accurately predict the spatial and temporal evolution of the mixed-layer depth and basin-scale internal wave behaviour compared to typical geophysical models that parameterise the vertical eddy diffusivities using methodologies similar to those used to estimate their horizontal counterparts.

ELCOM makes use of a wind-momentum model that uniformly distributes the introduction of wind momentum throughout the surface mixed-layer (Imberger and Patterson, 1990). This is applied across the lake surface prior to solution of the Navier-Stokes equations to directly capture velocity increases in the surface layer caused by wind-induced stress. Heat transfer across the atmosphere-lake interface includes both penetrative (shortwave radiation) and non-penetrative (longwave radiation and sensible and latent heat transfer) components. The shortwave component is introduced to one or more water column grid cells following the exponential decay described by Beer's Law. Non-penetrative effects are only active in the surface grid cells. The surface heat fluxes in particular are the subject of the following section.

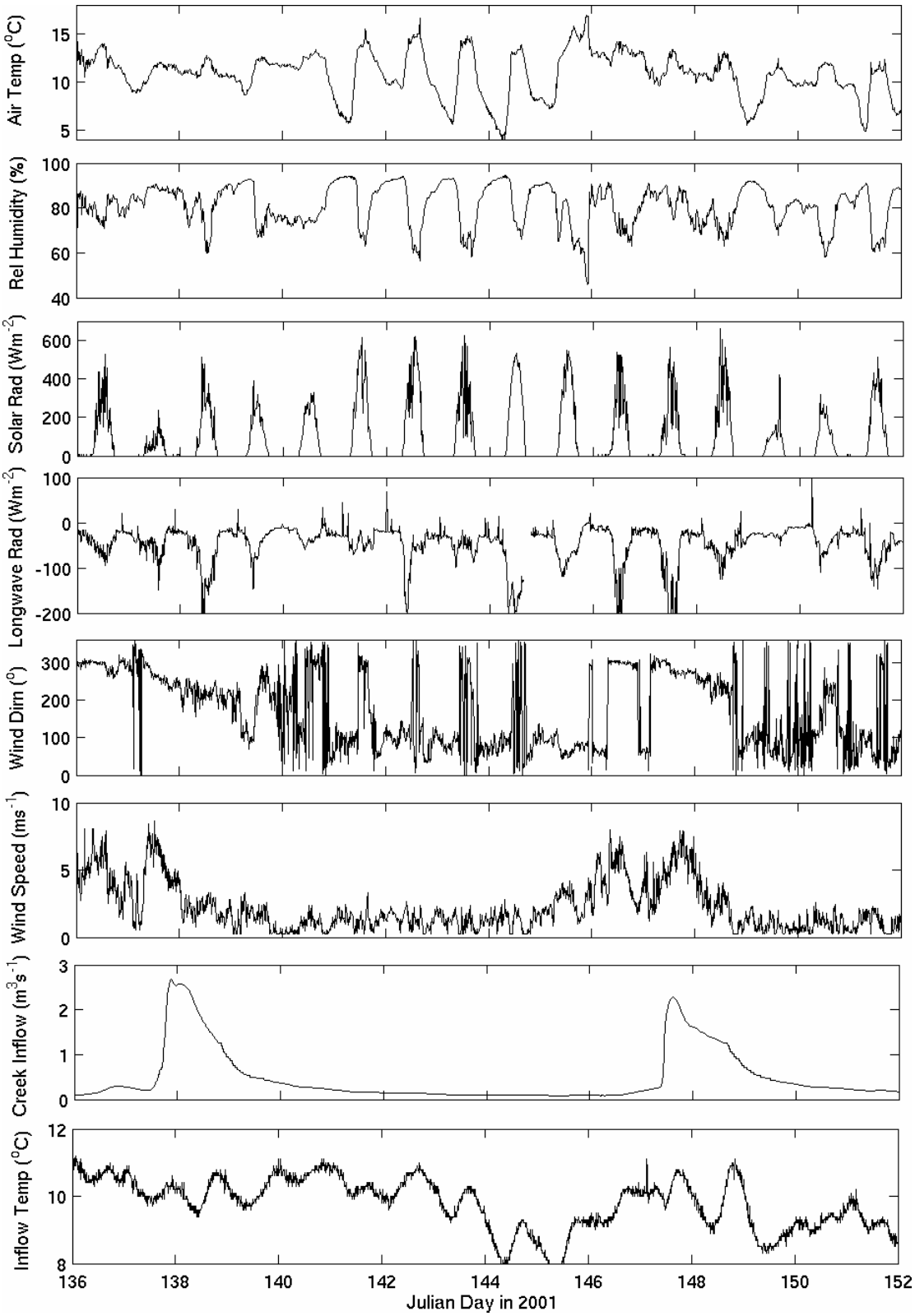

Figure A1.1: Meteorological and inflow forcing data for the study period. The meteorological parameters are taken from a height of 2.0 m above the water surface.

Surface Thermodynamics

ELCOM employs the familiar bulk aerodynamic formulae, which have been shown to competently capture the surface fluxes of momentum, and sensible and latent heat from a variety of waterbodies:

$$\tau = \rho\overline{u'w'} = \rho C_D U_z^2 \quad \text{(A1.1)}$$

$$H = \rho c_p \overline{\theta' w'} = -\rho c_p C_H U_z (\theta_z - \theta_s) \quad \text{(A1.2)}$$

$$E = \rho\lambda\overline{q'w'} = -\rho\lambda C_E U_z (q_z - q_s) \quad \text{(A1.3)}$$

where τ = surface stress [Nm^{-2}]
H = sensible heat flux [Wm^{-2}]
E = latent heat flux
ρ = air density [kgm^{-3}]
c_p = specific heat of air []
λ = latent heat of vaporization []
u', w' = turbulent velocity fluctuations in the horizontal and vertical directions respectively, and the overbar indicates a time average.
U_z = windspeed at height z [m] above the water [ms^{-1}]
θ_z = temperature at height z [m] above the water [ºK]
q_z = humidity at height z [m] above the water [kg/kg]
θ_s = temperature of water at the air-water interface [ºK]
q_s = saturated humidity at the air-water interface [kg/kg].

Over long time integrations (*i.e.* seasonal), the bulk-transfer coefficients for momentum, C_D, sensible heat, C_H, and latent heat, C_E, can be assumed approximately constant because of the negative feedback between surface forcing and the waterbody's temperature response (*e.g.* Strub and Powell, 1987), but at finer timescales (hours to weeks), the thermal inertia of the waterbody is too great and so the transfer coefficients must be specified as a function of the degree of atmospheric stratification experienced in the internal boundary layer that develops over the water. Monin and Obukhov (1954) parameterised the stratification seen in the air column using the now well-known stability parameter, z/L, where L is the Obukhov length defined as:

$$L = \frac{-\rho u_*^3 \theta_v}{kg\left[\frac{H}{c_p} + 0.61\frac{\theta E}{\lambda}\right]} \quad \text{(A1.4)}$$

where k = von Karman's constant
u_* = friction velocity [ms^{-1}]
θ_v = $\theta(1 + 0.61q)$ is the virtual temperature.

Paulson (1970) presented a solution for the vertical profiles of windspeed, temperature and moisture in the developing boundary layer as a function of the Monin-Obukhov stability parameter; the so-called flux-profile relationships:

$$U = \frac{u_*}{k}\left[\ln\left(\frac{z}{z_o}\right) - \psi_M\left(\frac{z}{L}\right)\right] \quad \text{(A1.5)}$$

$$\theta_z - \theta_s = \frac{\theta_*}{k}\left[\ln\left(\frac{z}{z_\theta}\right) - \psi_H\left(\frac{z}{L}\right)\right] \quad \text{(A1.6)}$$

$$q_z - q_s = \frac{q_*}{k}\left[\ln\left(\frac{z}{z_q}\right) - \psi_E\left(\frac{z}{L}\right)\right] \tag{A1.7}$$

where ψ_M, ψ_H and ψ_E are the similarity functions for momentum, heat and moisture respectively, and z_o, z_θ and z_q are their respective roughness lengths. For unstable conditions ($L<0$), the stability functions are defined as (Paulson 1970, Businger *et al.*, 1971, Dyer, 1974):

$$\psi_M = 2\ln\left(\frac{1+x}{2}\right) + \ln\left(\frac{1+x^2}{2}\right) - 2\tan^{-1}(x) + \frac{\pi}{2} \tag{A1.8}$$

$$\psi_H = \psi_E = 2\ln\left(\frac{1+x^2}{2}\right) \tag{A1.9}$$

where

$$x = \left[1 - 16\left(\frac{z}{L}\right)\right]^{1/4}$$

During stable stratification ($L>0$) they take the form:

$$\psi_M = \psi_H = \psi_E = \begin{cases} -5\left(\frac{z}{L}\right) & 0 < \frac{z}{L} < 0.5 \\ 0.5\left(\frac{z}{L}\right)^{-2} - 4.25\left(\frac{z}{L}\right)^{-1} - 7\ln\left(\frac{z}{L}\right) - 0.852 & 0.5 < \frac{z}{L} < 10.0 \\ \ln\left(\frac{z}{L}\right) - 0.76\left(\frac{z}{L}\right) - 12.093 & \frac{z}{L} > 10.0 \end{cases} \tag{A1.10}$$

Substituting Equations A1.1 – A1.3 into A1.5 – A1.7 and ignoring the similarity functions leaves us with neutral transfer coefficients as a function of the roughness lengths:

$$C_{XN} = k^2\left[\ln\left(\frac{z}{z_o}\right)\right]^{-1}\left[\ln\left(\frac{z}{z_X}\right)\right]^{-1} \tag{A1.11}$$

where N denotes the neutral value and X signifies either D, H or E for the transfer coefficient and o, θ or q for the roughness length scale. Inclusion of the stability functions into the substitution and some manipulation (Imberger and Patterson, 1990; Launianen and Vihma, 1990) yields the transfer coefficients relative to these neutral values:

$$\frac{C_X}{C_{XN}} = \left[1 + \frac{C_{XN}}{k^2}\left(\psi_M\psi_X - \frac{k\psi_X}{\sqrt{C_{DN}}} - \frac{k\psi_M\sqrt{C_{DN}}}{C_{XN}}\right)\right] \tag{A1.12}$$

Hicks (1975) and Launianen and Vihma (1990) suggested an iterative procedure to solve for the stability corrected transfer coefficient using A1.12 based on some initial estimate of the neutral value. The surface flux is subsequently estimated according to A1.1 – A1.3) and used to provide an initial estimate for L (Equation A1.4). The partially corrected transfer coefficient is then recalculated and so the cycle goes. Strub and Powell (1987) and Launiainen (1995), presented an alternative based on estimation of the bulk Richardson number, Ri_B, defined as:

$$Ri_B = \frac{gz}{\theta_v}\left(\frac{\Delta\theta + 0.61\theta_v\Delta q}{U^2}\right) \tag{A1.13}$$

and related as a function of the stability parameter, z/L, according to:

$$Ri_B = \frac{z}{L}\left(\frac{k\sqrt{C_{DN}}/C_{HWN} - \psi_{HW}}{\left(k/\sqrt{C_{DN}} - \psi_M\right)^2}\right) \tag{A1.14}$$

where it is specified that $C_{HN} = C_{WN} = C_{HWN}$. Figure A1.2 illustrates the relationship between the degree of atmospheric stratification (as described by both the bulk Richardson number and the Monin-Obukhov stability parameter) and the transfer coefficients scaled by their neutral value.

The iterative procedure used in this analysis is conceptually similar to the methodology discussed in detail in Launiainen and Vihma (1990). The first estimate for the neutral drag coefficient is specified as a function of windspeed (and hence the momentum roughness length) as it is has been commonly observed that C_{DN} increases with U_{10}. This is modelled according to:

$$C_{DN-10} = \begin{cases} 1.00\times10^{-3} & U_{10} < 5.0ms^{-1} \\ \left(1.00 + 0.07\left[U_{10} - 5.00\right]\right)\times10^{-3} & U_{10} \geq 5.0ms^{-1} \end{cases} \tag{A1.15}$$

which is empirically based on data from Hicks (1972), Francey and Garratt (1978) and Hicks (1975). The neutral humidity/temperature coefficient, C_{HWN-10}, is held constant at 1.25×10^{-3} (1.9×10^{-3} at $z = 2.0$ m). This is somewhat of a restrictive assumption as it inherently assumes the temperature and humidity roughness lengths are invariant with windspeed and therefore sea-state.

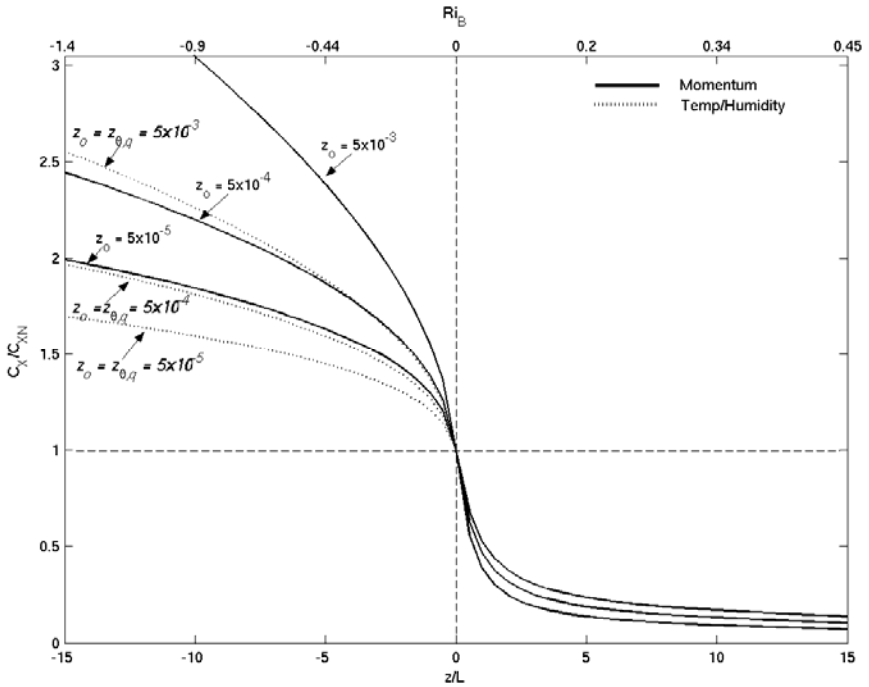

Figure A1.2: Relationship between atmospheric stability (bottom axis – **z/L**, top axis – $\mathbf{Ri_B}$) and the bulk-transfer coefficients relative to their neutral value ($\mathbf{C_X/C_{XN}}$ where **X** represents **D**, **H** or **W**) for several roughness values. The solid line indicates the momentum coefficient variation ($\mathbf{C_D/C_{DN}}$) and the broken line indicates humidity and temperature coefficient ($\mathbf{C_{HW}/C_{HWN}}$) variation.

ELCOM was applied to Myponga Reservoir for the May 2001 flood event with and without atmospheric stability correction of the bulk-transfer coefficients for momentum and sensible and latent heat. These two scenarios have been denoted ELCOM-AS and ELCOM respectively.

Computational Aspects

Myponga Reservoir bathymetry was discretized to a 50×50×0.5 m Cartesian grid based on some preliminary grid convergence testing. The bathymetry along the 'side-arm' was straightened to reduce artificial momentum loss associated with grid discretization. The ELCOM bathymetry was also incrementally adjusted until the real and discretized storage-height curves closely matched.

Windspeed and direction was held constant across the entire basin at the value measure at Met2. Similarly, air temperature and humidity were held constant at the Met1 value over the entire water surface. The ELCOM simulations were forced with 10-minute meteorological and inflow/outflow data as presented above. The simulations were run with a timestep of 240 secs, and, as suggested by thermistor chain data, the entire basin was given a constant initial temperature. Based on field measurements, an extinction coefficient of 1.2 m^{-1} was used. Additionally, both the reservoir and inflow water were assumed to be fresh, so that only temperature was responsible for creating density gradients.

Results and Discussion

Surface Heat Fluxes

The degree of atmospheric stratification during the study period and the model estimates of the stability-corrected bulk-transfer coefficients are shown in Figure A1.3. For the majority of the period the temperature of the water surface is considerably higher than the air temperature, as reflected by the predominantly negative values of the stability parameter (z/L). When the windspeed is high, advective forces dominate over the temperature instability (note the square of the momentum term in the denominator of Equations A1.13 and A1.14) and therefore $z/L \rightarrow 0$. Under these conditions, the assumption of constant bulk-transfer coefficients is valid, as the stability corrected estimates oscillate around the constant values. When the windspeed is low however (between days 140 – 145 and beyond day 149), the boundary-layer over the water becomes convectively unstable resulting in large, negative values of z/L. Following Equation A1.12, and as suggested in Figure A1.2, these high instabilities manifest in dramatic changes in the values of C_D and C_{HW}. Indeed, it is not uncommon for the stability-corrected bulk-transfer coefficients to vary twofold when compared to their neutral values. Under these unstable temperature conditions, the importance of the stability correction is most notable below windspeeds of 3 ms^{-1}.

The manifestation of the corrected bulk-transfer coefficients on the basin-wide surface heat and momentum budget is significant (Table A1.1). The average input of momentum over the 15 day study period was 11.8 and 14.3 TNs for the ELCOM and ELCOM-AS simulations respectively, a difference of approximately 21%. The total energy loss from the sensible heat flux increased approximately 30%, from 56.9 to 74.5 TJ through inclusion of the atmospheric stability correction. Similarly, the predicted total latent heat loss over the period increased greater than 26%, from 145.9 to 184.2 TJ, by accounting for the stability effects. The impact of the improved heat flux predictions is most notable on examination of the basin-wide, net change in surface heat input (the net change is defined as the sum of all surface heat fluxes: shortwave and longwave radiation and sensible and latent heat, with all specified as positive into the water). The net loss of heat increases from 61 TJ to 117.3 TJ, a 91% difference. Therefore, for this scenario, the assumption of neutral transfer coefficients results in a miscalculation of the net surface heat transfer, generally/arguably the most important factor affecting lake and reservoir hydrodynamics (Imboden and Wüest, 1995), by approximately a factor of two. It should also be noted

that most of the divergence between the two model predictions occurs during the 6 day period from JD 139 – 144. This has implications particularly for long hydrodynamic simulations, as even relatively short periods of non-neutral stabilities can significantly compromise model accuracy. As is shown in the following section, the error is likely to propogate as the simulation progresses even once the atmospheric forcing returns from its non-neutral state.

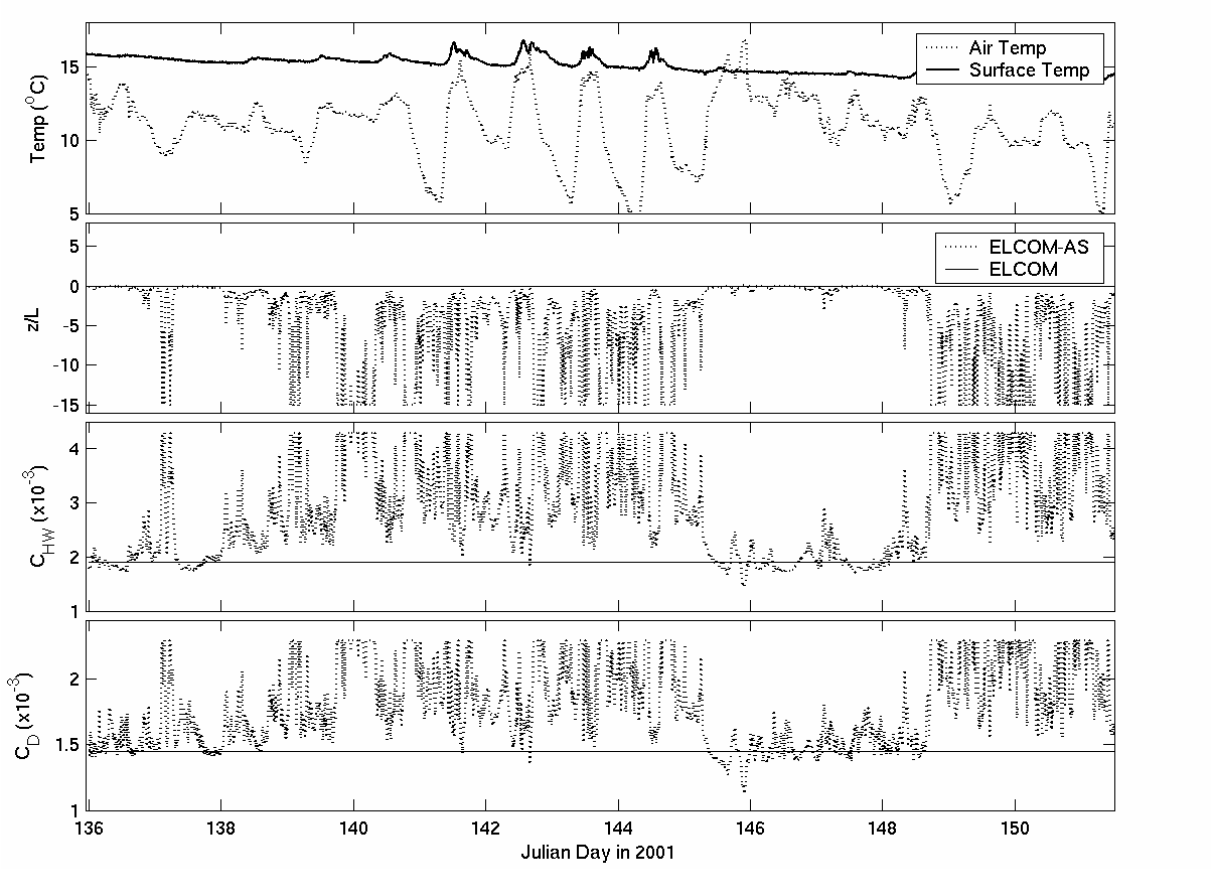

Figure A1.3: Variation of the Monin-Obukhov stability parameter (z/L) and the bulk-transfer coefficients (C_D and C_{HW} taken at 2.0 m above the water surface) during the study period. The ELCOM-AS predictions have been calculated using the simulated surface temperature at a location corresponding to station Met1 for the purpose of this plot.

Table A1.1: Comparison of the basin-wide net surface fluxes over the study period with and without the correction for atmospheric stability. All fluxes are positive into the waterbody.

		ELCOM	ELCOM-AS	% difference
Momentum	(510^{12} Ns)	11. 8	14.3	21.2
Sensible Heat	(510^{12} J)	-56.9	-74.5	30.9
Latent Heat	(510^{12} J)	-145.9	-184.2	26.2
Longwave	(510^{12} J)	-141.7	-141.7	N/A
Shortwave	(510^{12} J)	283.1	283.1	N/A
Net Change in Storage	(510^{12} J)	-61.4	-117.3	91.0

Hydrodynamics

It is the purpose of this section to illustrate how the heat and momentum flux estimates of the two models manifest in the hydrodynamic predictions of Myponga Reservoir. The application of the atmospheric stability correction was seen to influence not only the surface layer thermodynamics, but also the inflow dynamics.

Figure A1.4 indicates the importance of this on the thermal structure of the reservoir; both stations Met1 and Met2 illustrate that the (uncorrected) ELCOM surface layer predictions begin to diverge from the thermistor data on day 140 at the onset of the low wind period. This overheating continues to cumulate over the five days of high instability. In accordance with the field data, the ELCOM-AS results indicate less heating of the surface and an increased depth of the mixed layer as expected from the heightened values of the transfer coefficients. However, even the improved ELCOM-AS results appear to under predict the depth of the diurnal mixed layer, as indicated in the thermistor chain data that shows the 15ºC isotherm oscillating with an amplitude of approximately 10 m and a period of 1 day. This is a result of either 1) surface wind forcing, 2) inflow forcing, 3) convective cooling, or 4) differential surface cooling resulting in a dense underflow.

Nonetheless, the ELCOM-AS deficiency in this regard is small and the error is less than 0.5ºC. This is better illustrated in the temperature comparisons of Figure A1.4, which illustrate that ELCOM-AS performs significantly better in the surface layer, for both Met1 and Met2, following the period of instability. During the period of mild instability and high winds that accompanied the first inflow event, ELCOM captured the data most accurately because ELCOM-AS exhibited a high heat transfer coefficient during the higher windspeeds, which may be responsible for the over-estimation of sensible and latent heat loss. However, it is suspected that this error is not because of poor predictions of the transfer coefficients (although the assumption of a invariant temperature and humidity roughness lengths may contribute), but due to the inclusion of the rain in the model. The rain data is of daily resolution, and so, within ELCOM/ELCOM-AS, the rainstorm is spread across all the timesteps of that day. In reality, the rain would have fallen over the course of an hour or so and as the rain is input as being at air temperature, if the daily air temperature average was less than that at the time the storm occurred, it acts to overly cool the surface layer. An extra simulation conducted without the rain model improved the surface thermodynamics in the period but at the expense of poor mass-balance predictions.

The improved surface layer predictions also improved the simulated underflow dynamics. This occurred because the water entrained by the inflow as it entered and descended through the shallow reaches of the side-arm was cooler than that predicted by the uncorrected ELCOM simulation. This phenomenon is emphasized by the differential heating and cooling that occurs along the reservoir's side-arm – the shallow reaches near the creek inflow respond to surface exchange with more sensitivity, and because most of the inflows entered during the evening, the cool waters in this shallow region maintained the inflow water at its relatively cool temperature.

Regression plots of simulated and observed temperatures within the basin provide a more quantitative indicator of model performance (Figure A1.5). These plots were obtained by comparing hourly thermistor chain values with the equivalent ELCOM or ELCOM-AS estimates. The results from this analysis emphasize the trends described previously; the overheating of the surface layer in the ELCOM simulation causes the data to diverge from the 1:1 line increasingly as the simulation progresses. A second statistical indicator used to assess model performance was the average RMS (Table A1.2), obtained by averaging the RMS error for each point plotted on the above regression diagrams:

$$RMS = \frac{1}{N}\sum_{N}\sqrt{\left(T_{simulated} - T_{observed}\right)^2} \qquad \text{(A1.16)}$$

where *N* is the number of points used in the comparison. This analysis yielded an error of less than 0.15ºC for ELCOM-AS and greater than 0.3ºC for ELCOM. The poorer performance of ELCOM in these statistics is not surprising on comparison of the net effect of the atmospheric stability correction on the surface fluxes over the study period (Table A1.2). ELCOM-AS predicted a 21% increase in momentum input and a 31 and 26% increase in the sensible and latent heat loss respectively when compared to the ELCOM estimates. The significance of this on the net basin-wide surface heat budget for the study period is considerable. This analysis showed the atmospheric stability correction manifested in a 91% change of the net heat-transfer for the entire 12-day period.

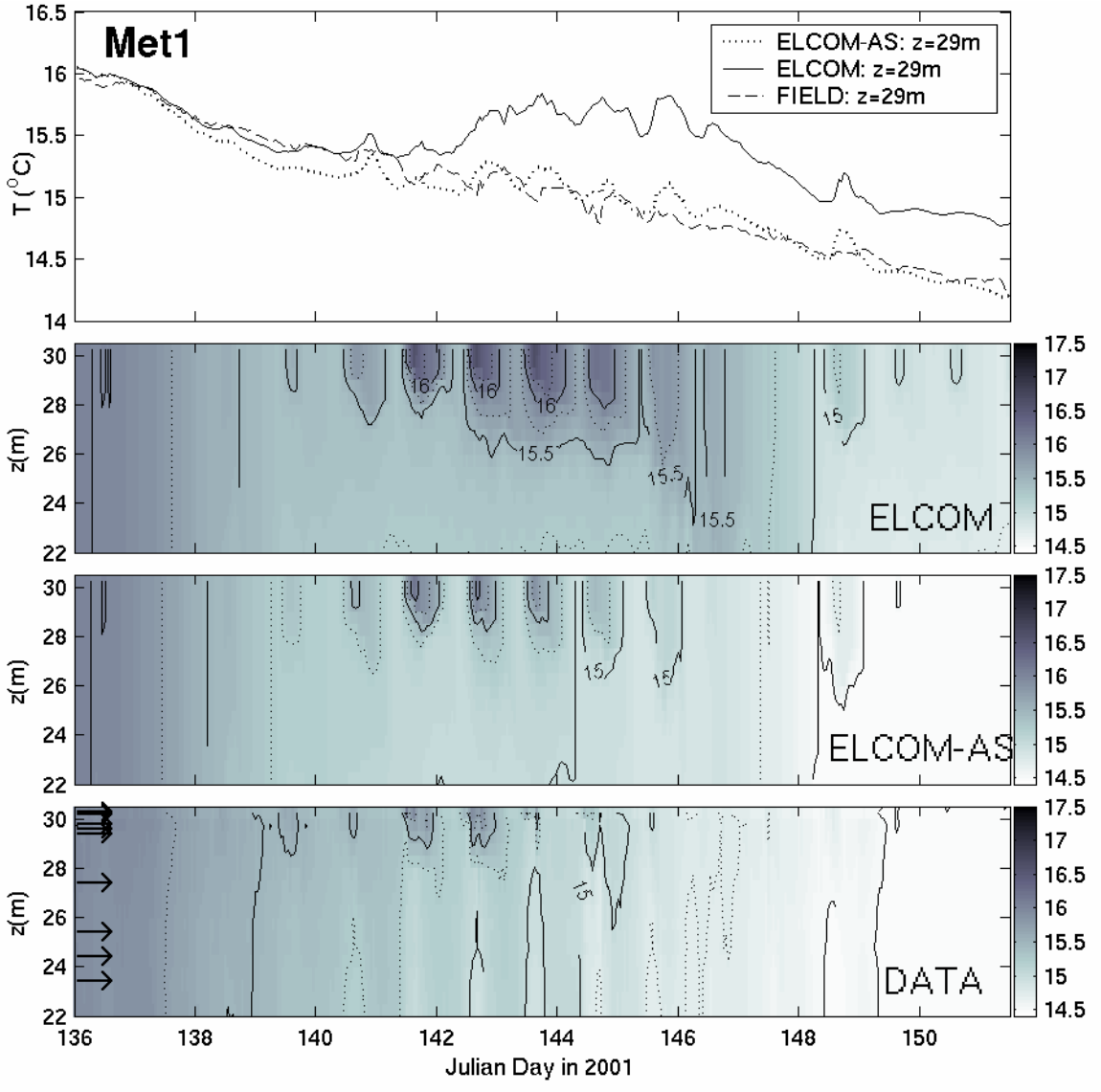

Figure A1.4a: Surface layer comparison of ELCOM and ELCOM-AS simulations and the thermistor chain data for station Met1. Shading indicates temperature (ºC). The contour interval is 0.5ºC for the solid contours and 0.25ºC for the broken contours. The arrows on the left of the data plots indicated the locations of the thermistors in the field.

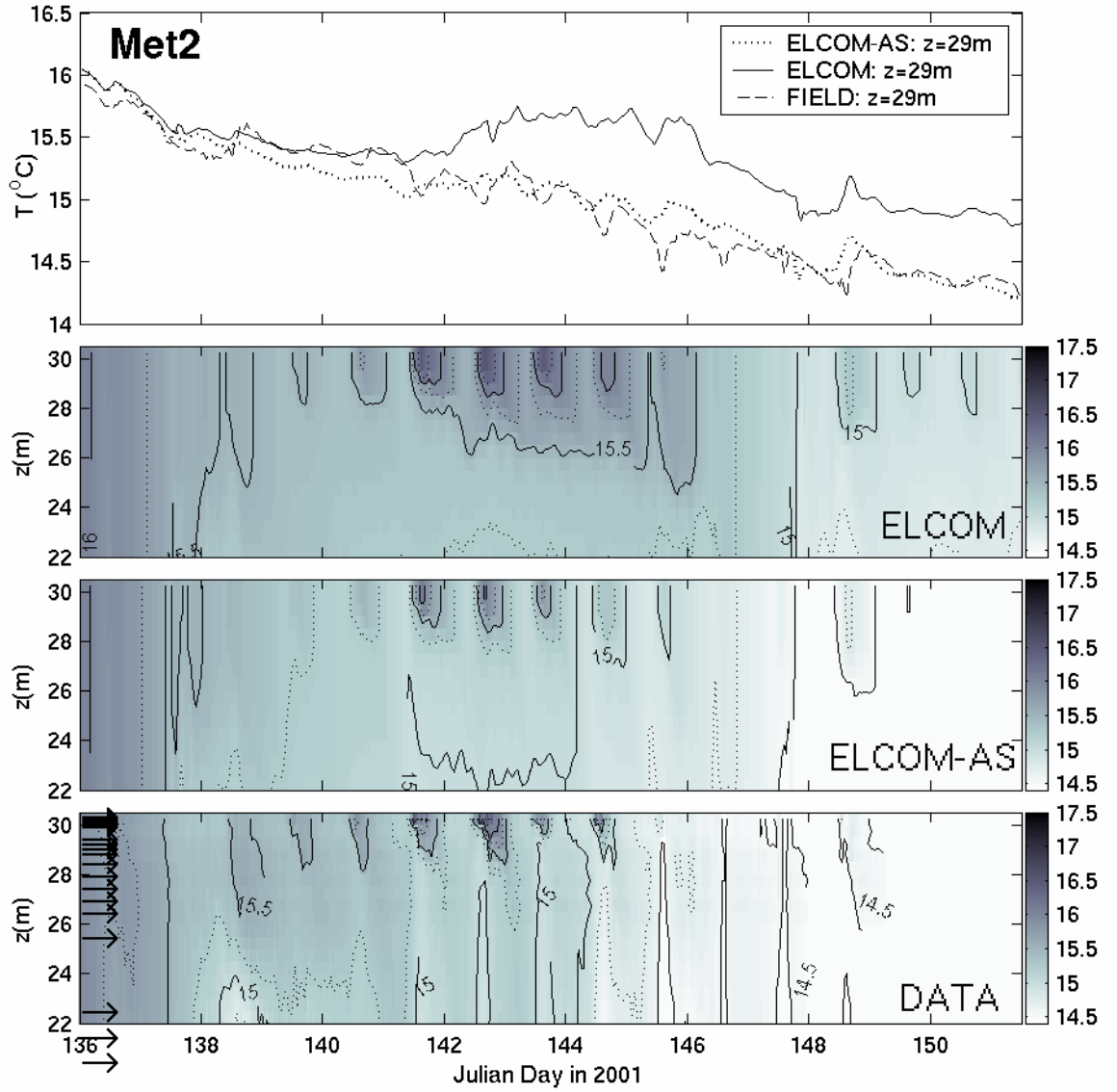

Figure A1.4b: Surface layer comparison of ELCOM and ELCOM-AS simulations and the thermistor chain data for station Met2. Shading indicates temperature (ºC). The contour interval is 0.5ºC for the solid contours and 0.25ºC for the broken contours. The arrows on the left of the data plots indicated the locations of the thermistors in the field.

Table A1.2: Statistical comparison of modelled and measured temperature data at thermistor chain locations Met1 and Met2 for simulations conducted with and without atmospheric stability correction.

Statistic:	*R^2*		*RMS (ºC)*	
Simulation:	*ELCOM*	*ELCOM-AS*	*ELCOM*	*ELCOM-AS*
Met1	0.620	0.917	0.319	0.129
Met2	0.696	0.881	0.405	0.142

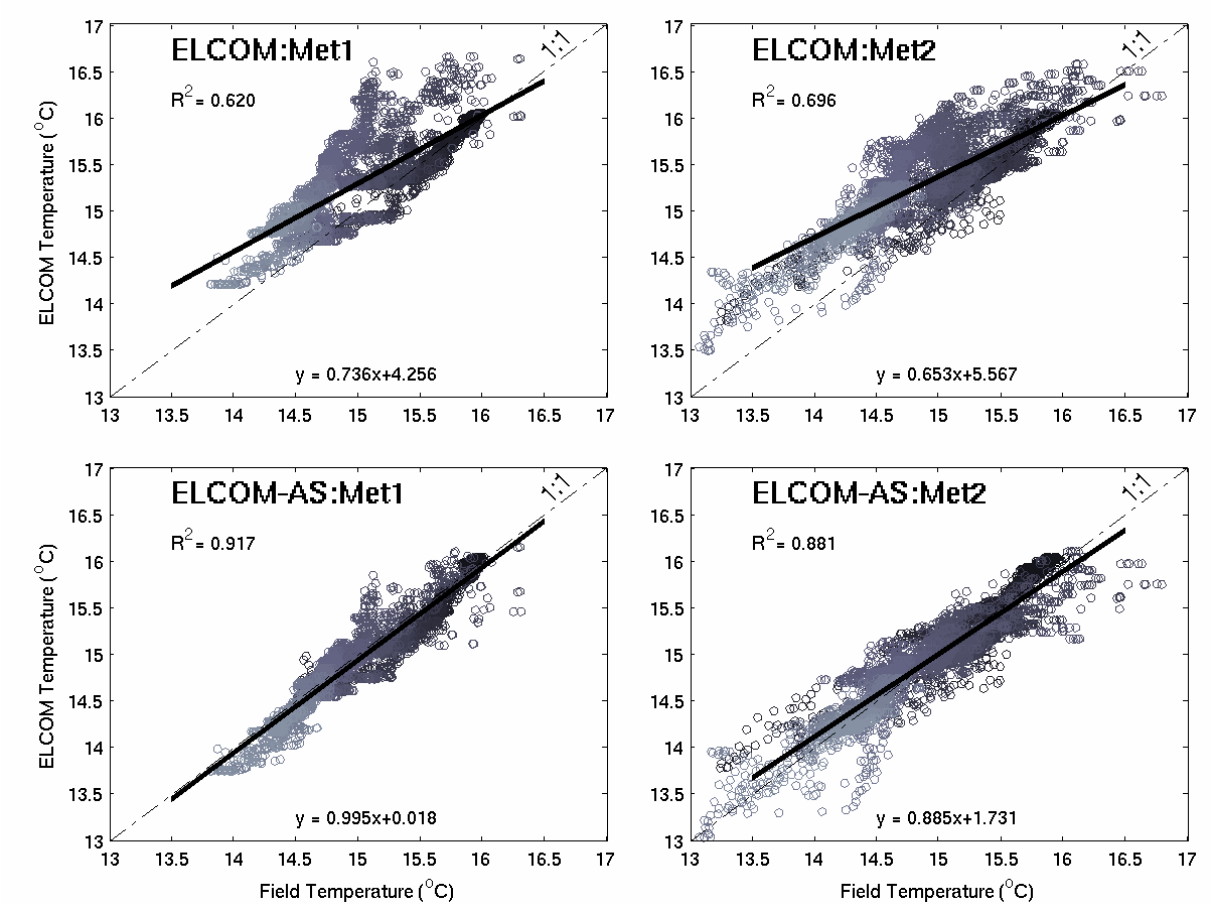

Figure A1.5: Comparison of all simulated (ELCOM and ELCOM-AS) and observed temperatures for Met1 and Met2. Shading reflects time within the simulation (dark at the beginning and light at the end). Comparison points were taken for each thermistor every hour for the entire simulation period.

Bibliography

Agrawal, Y. C., and Pottsmith, H. C., 2000. Instruments for particle size and settling velocity observations in sediment transport, *Mar. Geol.* 168: 89-114.

Allen, M. J., Clancy, J. L., and Rice, E. W., 2000. The plain, hard truth about pathogen monitoring, *J. Amer. Water Works Assoc.* 92(9): 64-76.

Allwood, P. B., Malik, Y. S., Hedberg, C. W., and Goyal, S. M., 2003. Survival of F-specific RNA coliphage, feline calcivius, and *Escherichia coli* in water: a comparative study, *Appl. Environ. Microbiol.* 69(9): 5707-5710.

Anderson, I. C., Rhodes, M. W., and Kator, H. I., 1979. Sublethal stress in *Escherichia coli*: a function of salinity, *Appl. Environ. Microbiol.* 38(6): 1147-1152.

Anderson, I. C., Rhodes, M. W., and Kator, H. I., 1983. Seasonal variation in survival of *Escherichia coli* exposed *in situ* in membrane diffusion chambers containing filtered and non-filtered water, *Appl. Environ. Microbiol.* 45(6): 1877-1883.

Antenucci, J. P., Brookes, J. D., and Hipsey, M. R., 2005a. Strategies for the effective sampling for pathogens in lakes and reservoirs, *J. Amer. Water Works Assoc.* 97(1): 86-93.

Antenucci, J. P., Whiteley, M., Devkota, B., Hipsey, M. R., and Imberger, J., 2005b. 'Mathematical model for the upper and middle Tiete River Basin in the metropolitan Sao Paulo area', Rep. No. ED1966. Centre for Water Research, University of Western Australia, Perth, Western Australia.

Arana, I., Muela, A., Iriberri, J., Egea, L., and Barcina, I., 1992. Role of hydrogen peroxide in loss of culturability mediated by visible light in *Escherichia coli* in a freshwater ecosystem, *Appl. Environ. Microbiol.* 58: 3903-3907.

Armon, R., and Kott, Y., 1995. Distribution comparison between coliphages and phages of anaerobic bacteria (*Bacteroides fragilis*) in water sources, and their reliability as faecal pollution indicators in drinking water, *Water Sci. Technol.* 31(5-6): 215-222.

Ashbolt, N., Dorsch, M. R., Cox, P. T., and Banens, B., 1995. 'Blooming *E. coli*, what do they mean?' *In* Coliforms and *E. coli*: problem or solution? (D. Kay and C. Fricker, eds.), pp. 78-85. The Royal Society of Chemistry, Cambridge, UK.

Ashbolt, N. J., Grabow, W. O. K., and Snozzi, M., 2001. 'Indicators of microbial water quality', *In* WHO | Water Quality: Guidelines, Standards and Health. Risk assessment and management for water-related infectious disease (L. Fewtrell and J. Bartram, eds.). IWA Publishing, London.

Atherholt, T. B., LeChevalier, M. W., Norton, W. D., and Rosen, J. S., 1998. Effect of rainfall on Giardia and Crypto, *J. Amer. Water Works Assoc.* 90(9): 66-80.

Atwill, E. R., Hou, L., Karle, B. M., Harter, T., Tate, K. W., and Dahlgren, R. A., 2002. Transport of *Cryptosporidium parvum* oocysts through vegetated buffer strips and estimated filtration efficiency, *Appl. Environ. Microbiol.* 68: 5517-5527.

Auer, M. T., Bagley, S. T., Stern, D. A., and Babiera, M. J., 1998. A framework for modelling the fate and transport of *Giardia* and *Cryptosporidium* in surface waters, *J. Lake Reserv. Manag.* 14(2-3): 393-400.

Auer, M. T., and Niehaus, S. L., 1993. Modeling fecal coliform bacteria – I. Field and laboratory determination of loss kinetics, *Water Res.* 27(4): 693-701.

Ayres, P. A., 1977. 'Coliphages in the marine environment', *In* Aquatic Microbiology (F. A. Skinner and J. M. Shewman, eds.), pp. 275-298. Academic Press, New York.

Barcina, I., Gonzalez, J. M., Iriberri, J., and Egea, L., 1991. Role of protozoa in the regulation of enteric bacteria populations in seawater, *Mar. Microb. Food Webs* 5: 179-187.

Barcina, I., Lebaron, P., and Vives-Rego, J., 1997. Survival of allochthonous bacteria in aqautic systems: a biological approach, *FEMS Microbiol. Ecol.* 23: 1-9.

Barnes, B., and Gordon, D. M., 2004. Coliform dynamics and the implications for source tracking, *Environ. Microbiol.* 6(5): 501-509.

Baudisova, D., 1997. Evaluation of *Escherichia coli* as the main indicator of faecal pollution, *Water Sci. Technol.* 35(11-12): 323-336.

Beach, R. A., and Sternberg, R. W., 1992. Suspended sediment transport in the surf zone: response to incident wave and longshore current interaction, *Mar. Geol.* 108: 275-294.

Belkin, S., and Colwell, R. R., eds., 2005. Oceans and health: pathogens in the marine environment, Springer, New York, 464p.

Bitton, G., 1975. Absorption of viruses onto surfaces in soil and water, *Water Res.* 9: 473-484.

Bitton, G., Farrah, S. R., Ruskin, R. H., Butner, J., and Chou, Y. J., 1983. Survival of pathogenic and indicator organisms in ground water, *Groundwater* 21(4): 405-410.

Bouteleux, C., Saby, S., Tozza, D., Cavard, J., Lahoussine, V., Hartemann, P., and Mathieu, L., 2005. *Escherichia coli* behavior in the presence of organic matter released by algae exposed to water treatment chemicals, *Appl. Environ. Microbiol.* 71(2): 734-740.

Boyer, D. G., and Kuczynska, E., 2003. Storm and seasonal distributions of fecal coliforms and *Cryptosporidium* in a spring, *J. Amer. Water Resour. Assoc.* 39: 1449-1456.

Bradford, S. A., and Schijven, J. F., 2002. Release of *Cryptosporidium* and *Giardia* from dairy calf manure: impact of solution salinity, *Environ. Sci. Technol.* 36: 3916-3923.

Brookes, J. D., Antenucci, J. P., Hipsey, M. R., Burch, M. D., Ashbolt, N., and Ferguson, C. M., 2004. Fate and transport of pathogens in lakes and reservoirs, *Environ. Intl.* 30: 741-759.

Brookes, J. D., Burch, M. D., and Tarrant, P., 2000. Artificial destratification: evidence for improved water quality, *Water* 27(4): 18-22.

Brookes, J. D., Davies, C. M., Hipsey, M. R., and Antenucci, J. P., 2006. Association of *Cryptosporidium* with bovine faecal particles and implications for risk reduction by settling within water supply reservoirs, *J. Water Health* 4(4): 87-98.

Brookes, J. D., Hipsey, M. R., Burch, M. D., Regel, R. H., Linden, L., Ferguson, C.M., and Antenucci, J. P., 2005. Relative value of surrogate indicators for detecting pathogens in lakes and reservoirs, *Environ. Sci. Technol.* 39(22): 8614-8621.

Bruce, L. C., Hamilton, D. P., Imberger, J., Gal, G., Gophen, M., and Zohary, T., 2006. A numerical simulation of the role of zooplankton in C, N and P cycling in Lake Kinneret, Israel., *Ecol. Model.* 193(3-4): 412-436.

Burkhardt, W., Calci, K. R., Watkins, W. D., Rippey, S. R., and Chirtel, S. J., 2000. Inactivation of indicator microorganisms estuarine waters, *Water Res.* 34(8): 2207-2214.

Businger, J. A., Wyngaard, J. C., Izumi, Y., and Bradley, E. F., 1971. Flux profile relationships in the atmospheric surface layer, *J. Atmos. Sci.* 28: 181-189.

Byappanahalli, M. N., Shively, D. A., Nevers, M. B., Sadowsky, M. J., and Whitman, R. L., 2003. Growth and survival of *Escherichia coli* and enterococci populations in the macro-alga *Cladophora* (Chlorophyta), *FEMS Microbiol. Ecol.* 46: 203-211.

Camper, A. K., McFeters, G. A., Characklis, W. G., and Jones, W. L., 1991. Growth kinetics of coliform bacteria under conditions relevant to drinking water distribution systems, *Appl. Environ. Microbiol.* 57(8): 2233-2239.

Canale, R. P., Patterson, R. L., Gannon, J. J., and Powers, W. F., 1973. Water quality models for total coliform, *J. Water Pollut. Control Fed.* 45(2): 325-336.

Carlucci, A. F., and Pramer, D., 1960a. An evaluation of factors affecting the survival of *Escherichia coli* in sea water – I. experimental procedures, *Appl. Microbiol.* 8: 243-246.

Carlucci, A. F., and Pramer, D., 1960b. An evaluation of factors affecting the survival of *Escherichia coli* in sea water – II. salinity, pH and nutrients, *Appl. Microbiol.* 8: 247-250.

Carlucci, A. F., and Pramer, D., 1960c. An evaluation of factors affecting the survival of *Escherichia coli* in sea water – III. antibiotics, *Appl. Microbiol.* 8: 251-254.

Carlucci, A. F., and Pramer, D., 1960d. An evaluation of factors affecting the survival of *Escherichia coli* in sea water – IV. Bacteriophages, *Appl. Microbiol.* 8: 254-256.

Carlucci, A. F., Scarpino, P. V., and Pramer, D., 1961. An evaluation of factors affecting the survival of *Escherichia coli* in sea water – V. studies with heat and filter-sterilized sea water, *Appl. Microbiol.* 9: 400-404.

Chamberlin, C. E., and Mitchell, R., 1978. 'A decay model for enteric bacteria in natural waters', *In* Water pollution microbiology (R. Mitchell, ed.), pp. 325-348. Wiley Interscience, New York.

Chan, T. U., Hamilton, D. P., Robson, B. J., Hodges, B. R., and Dallimore, C., 2002. Impacts of hydrological changes on phytoplankton succession in the Swan River, Western Australia, *Estuaries* 25: 1406-1415.

Considine, R. F., Dixon, D. R., and Drummond, C. J., 2000. Laterally-resolved force microscopy of biological microspheres: oocysts of *Cryptosporidium parvum*, *Langmuir* 16: 1323-1330.

Considine, R. F., Drummond, C. J., and Dixon, D. R., 2001. Force of interaction between a biocolloid and an inorganic oxide: complexity of surface deformation, roughness and brushlike behavior, *Langmuir* 17: 6325-6335.

Cornax, R., and Morinigo, M. A., 1991. Significance of several bacteriophage groups as indicator of sewage pollution in marine waters, *Water Res.* 25(6): 673-678.

Craig, D. L., Fallowfield, H. J., and Cromar, N. J., 2004. Use of microcosms to determine persistence of *Escherichia coli* in recreational coastal water and sediment and validation with in situ measurements, *J. Appl. Microbiol.* 96(5): 922-210.

Craik, S. A., Weldon, D., Finch, G. R., Bolton, J. R., and Belosevic, M., 2001. Inactivation of *Cryptosporidium parvum* oocysts using medium- and low-pressure ultraviolet radiation, *Water Res.* 35(6): 1387-1398.

Crane, S. R., and Moore, J. A., 1986. Modeling enteric bacterial die-off: a review, *Water Air Soil Pollut.* 27: 411-439.

Curtis, T. P., Mara, D. D., and Silva, S. A., 1992a. The effect of sunlight on faecal coliforms in ponds: implications for research and design, *Water Sci. Technol.* 26(7-8): 1729-1738.

Curtis, T. P., Mara, D. D., and Silva, S. A., 1992b. Influence of pH, oxygen and humic substances on ability of sunlight to damage fecal coliforms in waste stabilization pond water, *Appl. Environ. Microbiol.* 58(4): 1335-1343.

Dai, X., and Boll, J., 2003. Evaluation of attachment of *Cryptosporidium parvum* and *Giardia lamblia* to soil particles, *J. Environ. Qual.* 32: 296-304.

Dai, X., and Boll, J., 2006. Settling velocity of *Crytposporidium parvum* and *Giardia lamblia*, *Water Res.* 40: 1321-1325.

Dallimore, C. J., Hodges, B. R., and Imberger, J., 2003. Coupling an underflow model to a three-dimensional hydrodynamic model, *J. Hydraul. Engng.* 129(10): 748-757.

Dallimore, C. J., Imberger, J., and Hodges, B. R., 2004. Modeling a plunging underflow, *J. Hydraul. Engng.* 130(11): 1068-1076.

Darakas, E., 2002. *E. coli* kinetics - effect of temperature on the maintenance and respectively the decay phase, *Environ. Monit. Assess.* 78: 101-110.

Davies, C. M., and Evison, L. M., 1991. Sunlight and the survival of enteric bacteria in natural waters, *J. Appl. Bacteriol.* 70(3): 265-274.

Davies, C. M., Ferguson, C. M., Kaucnern, C., Altavilla, N., Deere, D. A., and Ashbolt, N. J., 2004. Dispersion and transport of *Cryptosporidium* oocysts from fecal pats under simulated rainfall events, *Appl. Environ. Microbiol.* 70: 1151-1159.

Davies, C. M., Long, J. A. H., Donald, M., and Ashbolt, N. J., 1995. Survival of fecal microorganisms in marine and freshwater sediments, *Appl. Environ. Microbiol.* 61(5): 1888-1896.

Davies-Colley, R. J., Bell, R. G., and Donnison, A. M., 1994. Sunlight inactivation of enterococci and fecal coliforms in sewage effluent diluted in seawater, *Appl. Environ. Microbiol.* 60(6): 2049-2058.

Davies-Colley, R. J., Donnison, A. M., Speed, D. J., Ross, C. M., and Nagels, J. W., 1999. Inactivation of faecal indicator micro-organisms in waste stabilization ponds: interactions of environmental factors with sunlight, *Water Res.* 33(5): 1220-1230.

Deen, A., Craig, R., and Antenucci, J. P., 2000. The Sydney Water contamination incident of 1998 — monitoring and modelling. *In* "Hydro 2000: 3rd International Hydrology and Water Resources Symposium". Institution of Engineers Australia, Perth, Australia.

Derajaguin, B. V., and Landau, L., 1941. Theory of the stability of strongly charged lyophobic sols and the adhesion of strongly charged particles in solutions of electrolytes, *Acta Physiocochim* 14: 628-633.

deRegnier, D. P., Cole, L., Schupp, D. G., and Erlandsen, S. L., 1989. Viability of *Giardia* cysts suspended in lake, river and tap water, *Appl. Environ. Microbiol.* 55: 1223-1229.

Desmarais, T. R., Solo-Gabriele, H. M., and Palmer, C. J., 2002. Influence of soil and fecal indicator organisms in a tidally influenced subtropical environment, *Appl. Environ. Microbiol.* 68(3): 1165-1172.

Drozd, C., and Schwartzbrod, J., 1996. Hydrophobic and electrostatic cell surface properties of *Cryptosporidium parvum*, *Appl. Environ. Microbiol.* 62(4): 1227-1232.

Dukan, S., Levi, Y., Piriou, P., Guyon, F., and Villon, P., 1996. Dynamic modelling of bacterial growth in drinking water networks, *Water Res.* 30(9): 1991-2002.

Dutka, B. J., 1984. Sensitivity of *Legionella pneumophila* to sunlight in fresh and marine waters, *Appl. Environ. Microbiol.* 48: 970-974.

Dyer, A. J., 1974. A review of flux-profile relationships, *Bound. Layer Meteor.* 7: 363-372.

Edzwald, J. K., and Kelley, M. B., 1998. Control of *Cryptosporidium* — from reservoirs to clarifiers to filters, *Water Sci. Technol.* 37(2): 1-8.

Enzinger, R. M., and Cooper, R. C., 1976. Role of bacteria and protozoa in the removal of *Escherichia coli* from estuarine waters, *Appl. Environ. Microbiol.* 31(5): 758-763.

Evison, L. M., 1988. Comparative studies on the survival of indicator organisms and pathogens in fresh and sea water, *Water Sci. Technol.* 20(11-12): 309-315.

Fayer, R., Graczyk, T. K., Lewis, E. J., Trout, J. M., and Farley, C. A., 1998a. Survival of infectious *Cryptosporidium parvum* oocysts in seawater and eastern oysters (*Crassostrea virginica*) in the Chesapeake Bay, *Appl. Environ. Microbiol.* 64(3): 1070-1074.

Fayer, R., and Trout, J. M., 2005. 'Zoonotic protists in the marine environment', *In* Oceans and health: pathogens in the marine environment (S. Belkin and R. R. Colwell, eds.), pp. 143-164. Springer, New York.

Fayer, R., Trout, J. M., and Jenkins, M. C., 1998b. Infectivity of *Cryptosporidium parvum* oocysts in water at environmental temperatures, *J. Parasitol.* 84(6): 1165-1169.

Fayer, R., Trout, J. M., Walsh, E., and Cole, R., 2000. Rotifers ingest oocysts of *Cryptosporidium parvum*, *Eukaryotic Microbiol.* 47(2): 161-163.

Ferguson, C. M., Coote, B. G., Ashbolt, N. J., and Stevenson, I. M., 1996. Relationships between indicators, pathogens and water quality in an estuarine system, *Water Res.* 30(9): 2045-2054.

Flint, K. P., 1987. The long-term survival of *Escherichia coli* in river water, *J. Appl. Bacteriol.* 63(3): 261-270.

Fong, T., and Lipp, E. K., 2006. Enteric viruses of humans and animals in aquatic environments: health risks, detection, and potential water quality assessment tools, *Microbiol. Mol. Biol. Rev.* 69(2): 357-371.

Francey, R. J., and Garratt, J. R., 1978. Eddy flux measurements over the ocean and related transfer coefficients, *Bound. Layer Meteor.* 14(2): 153.

Fujioka, R. S., Hashimoto, H. H., Siwak, E. B., and Young, R. H. F., 1981. Effect of sunlight on survival of indicator bacteria in seawater, *Appl. Environ. Microbiol.* 41(3): 690-696.

Fujioka, R. S., and Narikawa, O. T., 1982. Effect of sunlight on enumeration of indicator bacteria under field conditions, *Appl. Environ. Microbiol.* 44(2): 395-401.

Fujioka, R. S., Sian-Denton, C., Borja, M., Castro, J., and Morphew, K., 1999. Soil: the environmental source of *Escherichia coli* and enterococci in Guam's streams, *J. Appl. Microbiol.* 85: 83-89.

Gameson, A. L. H., and Saxon, J. R., 1967. Field studies on effect of daylight on mortality of coliform bacteria, *Water Res.* 1: 279-295.

Gannon, J. T., Manilal, V. B., and Alexander, M., 1991a. Relationship between cell surface properties and transport of bacteria through soil, *Appl. Environ. Microbiol.* 57(1): 190-193.

Gannon, J. T., Tan, Y., Baveye, P., and Alexander, M., 1991b. Effect of sodium chloride on transport of bacteria in a saturated aquifer material, *Appl. Environ. Microbiol.* 57: 2497-2501.

Gantzer, C., Gillerman, L., Kuzetsov, M., and Oron, G., 2001. Adsorption and survival of faecal coliforms, somatic coliphages and F-specific RNA phages in soil irrigated with wastewater, *Water Sci. Technol.* 43(12): 117-124.

Gartner, J. W., Cheng, R. T., Wang, P., and Richter, K., 2001. Laboratory and field evaluations of the LISST-100 instrument for suspended particle size determinations, *Mar. Geol.* 175: 199-219.

Gauthier, M. J., Flatau, G. N., Clement, R. L., and Munro, P. M., 1992. Sensitivity of *Escherichia coli* cells to seawater closely depends on their growth stage, *J. Appl. Bacteriol.* 73: 257-262.

Gauthier, M. J., Flatau, G. N., Le Rudulier, D., Clement, R. L., and Combarro, M. P., 1991. Intracellular accumulation of potassium and glutamate specifically enhances survival of *Escherichia coli* in seawater, *Appl. Environ. Microbiol.* 57: 272-276.

Geldreich, E. E., Best, E. C., Kenner, B. A., and Van Dosnsel, D. J., 1968. The bacteriological aspects of stormwater pollution, *J. Water Pollut. Control Fed.* 40(11): 1861-1872.

Geldreich, E. E., and Kenner, B. A., 1969. Concepts of fecal streptococci in stream pollution, *J. Water Pollut. Control Fed.* 41: 336-352.

George, I., Anzil, A., and Servais, P., 2004. Quantification of fecal coliform inputs to aquatic systems through soil leaching, *Water Res.* 38: 611-618.

Gerba, C. P., 2005. 'Survival of viruses in the marine environment', *In* Oceans and health: pathogens in the marine environment (S. Belkin and R. R. Colwell, eds.), pp. 133-142. Springer, New York.

Gerba, C. P., and McLeod, J. S., 1976. Effect of sediments on the survival of *Escherichia coli* in marine waters, *Appl. Environ. Microbiol.* 32(1): 114-120.

Gerba, C. P., and Schaiberger, G. E., 1975. Effect of particulates on virus survival in seawater, *J. Water Pollut. Control Fed.* 47(1): 93-103.

Ghoul, M., Bernard, T., and Cormier, M., 1990. Evidence that *Escherichia coli* accumulates Glycine Betaine from marine sediments, *Appl. Environ. Microbiol.* 56(2): 551-554.

Gibson, C. J., Haas, C. N., and Rose, J. B., 1998. Risk assessment of waterborne protozoa: current status and future trends, *Parasitol.* 117: 205-212.

Gonzalez, J. M., Iriberri, J., Egea, L., and Barcina, I., 1990. Differential rates of digestion of bacteria by freshwater and marine phagotrophic protozoa, *Appl. Environ. Microbiol.* 56: 1851-1857.

Gordon, C., and Toze, S., 2003. Influence of groundwater characteristics on the survival of enteric viruses, *J. Appl. Microbiol.* 95: 536-544.

Gould, D. J., and Munro, D., 1981. 'Relevance of microbial mortality to outfall design', *In* Coastal discharges, pp. 45-50. Thomas Telford Ltd., London.

Goyal, S. M., Gerba, C. P., and Melnick, J. L., 1978. Prevalence of human enteric viruses in coastal canal communities, *J. Water Pollut. Control Fed.* 50(10): 2247-2256.

Grabow, W. O. K., Taylor, M. B., and de Villiers, J. C., 2001. New methods for the detection of viruses: call for review of drinking water quality guidelines, *Water Sci. Technol.* 46(12): 1-8.

Grant, R. H., Heisler, G. M., and Gao, W., 1997. Clear sky radiance distributions in ultraviolet wavelength bands, *Theor. Appl. Climatol.* 56: 123–135.

Hanes, N. B., and Fragala, R., 1967. Effect of seawater concentration on survival of indicator bacteria, *J. Water Pollut. Control Fed.* 39(1): 97-104.

Harm, W., 1980. Biological effects of ultraviolet radiation, Cambridge University Press, London, 216p.

Hartke, A., Lemarinier, S., Pichereau, V., and Auffray, Y., 2002. Survival of *Enterococcus faecalis* in seawater microcosms is limited in the presence of bacterivorous zooflagellates, *Curr. Microbiol.* 44: 329-335.

Havelaar, A. H., van Olphen, M., and Drost, Y. C., 1993. F-specific RNA bacteriophages are adequate model organisms for enteric viruses in fresh water, *Appl. Environ. Microbiol.* 59(9): 2956-2962.

Hawkins, P. R., Swanson, P., Warnecke, M., Shanker, S. R., and Nicholson, C., 2000. Understanding the fate of *Cryptosporidium* and *Giardia* in storage reservoirs: a legacy of Sydney's water contamination inicident, *Aqua* 49(6): 289-306.

Hendricks, C. W., and Morrison, S. M., 1967. Multiplication and growth of selected enteric bacteria in clear mountain stream water, *Water Res.* 1: 567-576.

Herwaldt, B. L., Craun, G. F., Stokes, S. L., and Juranek, D. D., 1992. Outbreaks of waterborne disease in the United States: 1989-90, *J. Amer. Water Works Assoc.* 64(4): 129-135.

Hicks, B. B., 1975. A procedure for the formulation of bulk transfer coefficients over water, *Bound. Layer Meteorol.* 8(3-4): 515-524.

Hillmer, I., and Imberger, J., 2007. Influence of advection on time and space scales of ecological variables in a coastal equilibrium flow, *Continental Shelf Res.* 27: 134-153.

Hipsey, M. R., Antenucci, J. P., and Brookes, J. D., 2003. Coupling a *Cryptosporidium* fate model to a 3D hydrodynamic model: results from Myponga Reservoir, SA. *In* "AWA 20th OzWater Conference", Perth, Western Australia.

Hipsey, M. R., Antenucci, J. P., Brookes, J. D., Burch, M. D., and Regel, R. H., 2004a. Simulation tools for minimizing pathogen risk in drinking water reservoirs. *In* "6th International Conference on Hydroinformatics" (Liong, Phoon and Babovic, eds.), Vol. 2. World Scientific Publishing Company, Singapore.

Hipsey, M. R., Antenucci, J. P., Brookes, J. D., Burch, M. D., Regel, R. H., and Linden, L., 2004b. A three dimensional model of *Cryptosporidium* dynamics in lakes and reservoirs: a new tool for risk management, *Intl. J. River Basin Management* 2(3): 181-197.

Hipsey, M. R., Brookes, J. D., Antenucci, J. P., Burch, M. D., Regel, R. H., Davies, C.M., Ashbolt, N. J., and Ferguson, C.M., 2005. 'Hydrodynamic distribution of pathogens in lakes and reservoirs', Rep. No. 2752. Awwa Research Foundation (AwwaRF).

Hipsey, M. R., Brookes, J. D., Regel, R. H., Antenucci, J. P., and Burch, M. D., 2006a. In situ evidence for the association of total coliforms and *Escherichia coli* with suspended inorganic particles in an Australian reservoir, *Water Air Soil Pollut.* 170(1-4): 191-209.

Hipsey, M. R., Romero, J. R., Antenucci, J. P., and Hamilton, D. P., 2006b. The Computational Aquatic Ecosystem Dynamics Model (CAEDYM): v2.3 Science Manual. Centre for Water Research, University of Western Australia.

Hodges, B. R., Imberger, J., Saggio, A., and Winters, K. B., 2000. Modeling basin-scale internal waves in a stratified lake, *Limnol. Oceanogr.* 45(7): 1603-1620.

Hood, M. A., and Ness, G. E., 1982. Survival of *Vibrio cholerae* and *Escherichia coli* in estuarine waters and sediments, *Appl. Environ. Microbiol.* 43: 578-584.

Howe, A. D., Forster, S., Morton, S., Marshall, R., Osborn, K. S., and Wright, P., 2002. *Cryptosporidium* oocysts in a water supply associated with cryptosporidiosis outbreak, *Emerg. Infect. Dis.* 8(6): 619-624.

Howell, J. M., Coyne, M. S., and Cornelius, P. L., 1996. Effect of sediment particle size and temperature on fecal bacteria mortality rates and the fecal coliform/fecal streptococci ratio, *J. Environ. Qual.* 25: 1216-1220.

Hsu, B. M., Huang, C., Hsu, Y. F., and Hsu, C. L. L., 2000. Examination of *Giardia* and *Cryptosporidium* in water samples and faecal specimens in Taiwan, *Water Sci. Technol.* 41(7): 87-92.

Imberger, J., and Patterson, J. C., 1990. 'Physical Limnology', *In* Advances in Applied Mechanics (T. Wu, ed.), Vol. 27, pp. 303-475. Academic Press, Boston.

Imboden, D. M., and Wuest, A., 1995. 'Mixing mechanisms in lakes', *In* Physics and Chemistry of Lakes (A. Lerman, D. M. Imboden and J. R. Gat, eds.), pp. 83-138. Springer-Verlag.

Iriberri, J., Ayo, B., Artolozaga, I., Barcina, I., and Egea, L., 1994a. Grazing on allochthonous vs autochthonous bacteria in river water, *Lett. Appl. Microbiol.* 18: 12-14.

Iriberri, J., Azua, I., Labirua-Iturburu, A., Artolozaga, I., and Barcina, I., 1994b. Differential elimination of enteric bacteria populations in seawater, *J. Appl. Bacteriol.* 77: 476-483.

Jenkins, M. B., Anguish, L., Bowman, D., Walker, M., and Ghiorse, W., 1997. Assessment of a dye permeability assay for determination of inactivation rates of *Cryptosporidium parvum* oocysts, *Appl. Environ. Microbiol.* 63(10): 3844-3850.

Jenkins, M. B., Bowman, D., and Ghiorse, W., 1998. Inactivation of *Cryptosporidium parvum* oocysts by ammonia, *Appl. Environ. Microbiol.* 64(2): 784-788.

Jenkins, M. B., Bowman, D., and Ghiorse, W., 1999. Errata - Inactivation of *Cryptosporidium parvum* oocysts by ammonia, *Appl. Environ. Microbiol.* 65(3): 1362.

Jin, G., Englande, A. J., and Liu, A., 2003. A preliminary study on coastal water quality monitoring and modeling, *J. Environ. Sci. Health* A38(3): 493-509.

John, D. E., and Rose, J. B., 2004. Survival of fecal indicator bacteria, bacteriophage and protozoa in Florida's surface and ground waters: potential implications for aquifer storage and recovery. University of Florida Report.

Johnson, D. C., Enriquez, C. E., Pepper, I. L., Davis, T. L., Gerba, C. P., and Rose, J. B., 1997. Survival of *Giardia, Cryptosporidium*, poliovirus and *Salmonella* in marine waters, *Water Sci. Technol.* 35(11-12): 261-268.

Johnson, W. P., and Logan, B. E., 1996. Enhanced transport of bacteria in porous media by sediment-phase and aqueous-phase natural organic matter, *Water Res.* 30(4): 923-931.

Juranek, D. D., and Mackenzie, W. R., 1998. Drinking water turbidity and gastrointestinal illness, *Epidemiol.* 9(3): 228-231.

Kapuscinski, R. B., and Mitchell, R., 1980. Process controlling virus inactivation in coastal waters, *Water Res.* 17: 363-371.

Karunasagar, I., and Karunasagar, I., 2005. 'Retention of pathogenicity in viable but non-culturable pathogens', *In* Oceans and health: pathogens in the marine environment (S. Belkin and R. R. Colwell, eds.), pp. 69-92. Springer, New York.

Kaspar, C. W., and Tamplin, M. L., 1993. Effects of temperature and salinity on the survival of *Vibrio vulnificus* in seawater and shellfish, *Appl. Environ. Microbiol.* 59(8): 2425-2429.

Kay, D., and McDonald, A., 1980. Reduction of coliform bacteria in two upland reservoirs: the significance of distance decay relationships, *Water Res.* 14: 305-318.

Kelsey, H., Porter, D. E., Scott, G., Neet, M., and White, D., 2004. Using geographic information systems and regression analysis to evaluate relationships between land use and fecal coliform bacterial pollution, *J. Exp. Mar. Biol. Ecol.* 298: 197-209.

Khaengraeng, R., and Reed, R. H., 2005. Oxygen and photoinactivation of *Escherichia coli* in UVA and sunlight, *J. Appl. Microbiol.* 99(1): 39-50.

King, B. J., Hoefel, D., Daminato, D. P., Fanok, S., and Monis, P. T., 2006. Solar UV dramatically reduces *Cryptosporidium parvum* oocyst infectivity in environmental waters, *Appl. Environ. Microbiol.* in review.

King, B. J., Keegan, A. R., Monis, P. T., and Saint, C. P., 2005. Environmental temperature controls *Cryptosporidium* oocyst metabolic rate and associated retention of infectivity, *Appl. Environ. Microbiol.* 71(7): 3848-3857.

Kirk, J. T. O., 1994. Light and photosynthesis in aquatic ecosystems, (2nd ed). Cambridge University Press, London, 525p.

Kistemann, T., Claben, T., Koch, C., Dangendorf, F., Fischeder, R., Gebel, J., Vacata, V., and Exner, M., 2002. Microbial load of drinking water reservoir tributaries during extreme rainfall and runoff, *Appl. Environ. Microbiol.* 68(5): 2188-2197.

Klock, J. W., 1971. Survival of coliform bacteria in wastewater treatment lagoons, *J. Water Pollut. Control Fed.* 43(10): 2071-2083.

Korhonen, L. K., and Martikainen, P. J., 1991. Survival of *Escherichia coli* and *Campylobacter jejuni* in untreated and filtered lake water, *J. Appl. Bacteriol.* 71(379-382).

Kristian Stevik, T., Aa, K., Ausland, G., and Hanseen, J. F., 2004. Retention and removal of pathogenic bacteria in wastewater percolating through porous media: a review, *Water Res.* 38: 1355-1367.

LaBelle, R. L., and Gerba, C. P., 1979. Influence pH, salinity, and organic matter on the adsorption of enteric viruses to estuarine sediment, *Appl. Environ. Microbiol.* 38: 93-101.

LaBelle, R. L., and Gerba, C. P., 1980. Influence of estuarine sediment on virus survival under field conditions, *Appl. Environ. Microbiol.* 39(4): 749-755.

LaLiberte, P., and Grimes, D. J., 1982. Survival of *Escherichia coli* in lake bottom sediment, *Appl. Environ. Microbiol.* 43: 623-628.

Lantrip, B. M., 1983. The decay of enteric bacteria in an estuary, PhD thesis, John Hopkins University, Baltimore.

Launiainen, J., 1995. Derivation of the relationship between the Obukhov stability parameter and the bulk Richardson number for flux profile studies, *Bound. Layer Meteorol.* 76: 165-179.

Launiainen, J., and Cheng, B., 1998. Modelling of ice thermodynamics in natural water bodies, *Cold Reg. Sci. Tech.* 27: 153-178.

Launiainen, J., and Vihma, T., 1990. Derivation of turbulent surface fluxes – An iterative flux-profile method allowing arbitrary observing heights, *Environ. Softw.* 5(3): 113-124.

Laval, B. E., Hodges, B. R., and Imberger, J., 2003a. Reducing numerical diffusion effects with a pycnocline filter, *J. Hydraul. Engng.* 129(3): 215-224.

Laval, B. E., Imberger, J., Hodges, B. R., and Stocker, R., 2003b. Modeling circulation in lakes: spatial and temporal variations, *Limnol. Oceanogr.* 48(3): 983-994.

LeChevalier, M. W., 2003. 'Conditions favouring coliform and HPC bacterial growth in drinking-water and on contact water surfaces', *In* Heterotrophic plate counts and drinking-water safety (J. Bartram, J. Cotruvo, M. Exner, C. Fricker and A. Glasmacher, eds.), pp. 177-197. IWA Publishing, London, UK.

LeChevalier, M. W., Welch, N. J., and Smith, D. B., 1996. Full-scale studies of factors related to coliform regrowth in drinking water, *Appl. Environ. Microbiol.* 62(7): 2201-2211.

Leeming, R., Nichols, P. D., and Ashbolt, N. J., 1998. 'Distinguishing sources of faecal pollution in Australian inland and coastal waters using sterol biomarkers and microbial faecal indicators'. Water Services Association of Australia, Melbourne.

Lemckert, C. J., and Imberger, J., 1998. 'Turbulent benthic boundary layer mixing events in fresh water lakes', *In* Physical Processes in Lakes and Oceans (J. Imberger, ed.), Vol. 54, pp. 503-516. American Geophysical Union, Washington.

Lessard, E. J., and Sieburth, J. M., 1983. Survival of natural sewage populations of enteric bacteria in diffusion and batch chambers in the marine environment, *Appl. Environ. Microbiol.* 45(3): 950-959.

Linden, K. G., Shin, G., and Sobsey, M. D., 2001. Comparative effectiveness of UV wavelengths for the inactivation of *Cryptosporidium parvum* oocysts in water, *Water Sci. Technol.* 43(12): 171-174.

Lipson, S. M., and Stotzky, G., 1983. Adsorption of reovirus to clay minerals: effects of cation exchange capacity, cation saturation, and surface area, *Appl. Environ. Microbiol.* 46: 673-682.

Lisle, J. T., and Rose, J. B., 1995. *Crytposporidium* contamination of water in the USA and UK - a mini review, *Aqua* 44(3): 103-117.

Liu, S., 2002. Fecal coliform decay and regrowth kinetics in an anaerobic dairy wastewater environment. MSc thesis, Louisiana State University, Louisiana.

Lopez-Torres, A. J., Prieto, L., and Hazen, T. C., 1988. Comparison of the in situ survival and activity of *Klebsiella pneumoniae* and *Escherichia coli* in tropical marine environments, *Microb. Ecol.* 15: 41-57.

Lytle, D. A., Johnson, C. H., and Rice, E. W., 2002. Systematic comparison of the electrokinetic properties of environmentally important organisms in water, *Colloids Surf. B* 24: 91-101.

Lytle, D. A., Rice, E. W., Johnson, C. H., and Fox, K. R., 1999. Electrophoretic mobilities of *Escherichia coli* O157:H7 and wild-type *Escherichia coli* strains, *Appl. Environ. Microbiol.* 65: 3222-3225.

MacKenzie, W. R., Hoxie, N. J., Procter, M. E., Gradus, M. S., Blair, K. A., and Peterson, D. E., 1994. A massive outbreak of Milwaukee *Cryptosporidium* infection transmitted through the public water supply, *N. Engl. J. Med.* 331(3): 161-167.

Mancini, J. L., 1978. Numerical estimates of coliform mortality rates under various conditions, *J. Water Pollut. Control Fed.* 50(11): 2477-2484.

Marino, R. P., and Gannon, J. J., 1991. Survival of faecal coliforms and faecal streptococci in storm drain sediment, *Water Res.* 25: 1089-1098.

Marshall, K. C., 1971. 'Sorptive interactions between soil particles and microorganisms', *In* Soil biochemistry (A. D. McLaren and J. Skujins, eds.), Vol. 2, pp. 409-445. Marcel Dekker Inc., New York.

Marshall, K. C., Stout, R., and Mitchell, R., 1971. Mechanisms of the initial events in the sorption of marine bacteria to surfaces, *J. Gen. Microbiol.* 68: 337-348.

Matsumoto, J., and Omura, T., 1980. Some factors affecting the survival of fecal indicator bacteria in seawater, *Technol. Rep.* 45(2): 169-185.

Mawdsley, J. L., Brooks, A. E., Merry, R. J., and Pain, B. F., 1996. Use of a novel soil tilting table apparatus to demonstrate the horizontal and vertical movement of the protozoan pathogen *Cryptosporidium parvum* in soil, *Biol. Fertil. Soils* 23: 215-220.

Mayo, A. W., 1995. Modeling coliform mortality in waste stabilization ponds, *J. Environ. Engng.* 121(2): 140-152.

McCambridge, J., and McMeekin, T. A., 1980a. Effect of temperature on activity of predators of *Salmonella typhimurium* and *Escherichia coli* in estuarine waters, *Aust. J. Mar. Freshwater Res.* 31: 851-855.

McCambridge, J., and McMeekin, T. A., 1980b. Relative effects of bacterial and protozoan predators on survival of *Escherichia coli* in estuarine water samples, *Appl. Environ. Microbiol.* 40: 907-911.

McCambridge, J., and McMeekin, T. A., 1981. Effect of solar radiation and predacious microorganisms on survival of fecal and other bacteria, *Appl. Environ. Microbiol.* 41(5): 1083-1087.

McCorquodale, J. A., Georgiou, I., Carnelos, S., and Englande, A. J., 2004. Modeling coliforms in storm water plumes, *J. Environ. Eng. Sci.* 3: 419-431.

McDaniels, A. E., Cochran, K. W., Gannon, J. J., and Williams, G. W., 1983. Rotavirus and reovirus stability in microorganism-free distilled and wastewater, *Water Res.* 17(10): 1349-1353.

McFeters, G. A., Bissonnette, G. K., Jezeski, J. J., Thomson, C. A., and Stuart, D. G., 1974. Comparative survival of inidicator bacteria and enteric pathogens in well water, *Appl. Microbiol.* 27(5): 805-811.

McFeters, G. A., and Stuart, D. G., 1972. Survival of coliform bacteria in natural waters: field and laboratory studies with membrane-filter chambers, *Appl. Microbiol.* 24(5): 805-811.

Medema, G. J., Bahar, M., and Schets, F. M., 1997. Survival of *Cryptosporidium parvum*, *Escherichia coli*, Faecal Enterococci and *Clostridium perfringens* in river water: influence of temperature and autochthonous microorganisms, *Water Sci. Technol.* 35: 249-252.

Medema, G. J., Schets, F. M., Teunis, P. F. M., and Havelaar, A. H., 1998. Sedimentation of free and attached *Cryptosporidium* oocysts and *Giardia* cysts in water, *Appl. Environ. Microbiol.* 64(11): 4460-4466.

Medema, G. J., and Schijven, J. F., 2001. Modelling the sewage discharge and dispersion of *Cryptosporidium* and *Giardia* in surface water, *Water Res.* 35(18): 4307-4316.

Menon, P., Becquevort, S., Billen, G., and Servais, P., 1996. Kinetics of flagellate grazing in the presence of two types of bacterial prey, *Microb. Ecol.* 31: 89-101.

Menon, P., Billen, G., and Servais, P., 2003. Mortality rates of autochthonous and fecal bacteria in natural aquatic ecosystems, *Water Res.* 37(17): 4151-4158.

Mezrioui, N., Oufdou, K., and Baleux, B., 1995. Dynamics of non-01 *Vibrio cholerae* and faecal coliforms in experimental stabilization ponds in the arid region of Marrakesh, Morocco, and the effect of pH, temperature, and sunlight on their experimental survival, *Can. J. Microbiol.* 41(6): 489-498.

Michallet, H., and Ivey, G. N., 1999. Experiments on mixing due to internal solitary waves breaking on uniform slopes, *J. Geophys. Res.* 104(C6): 13467-13478.

Mills, A. L., Herman, J. S., Hornberger, G. M., and DeJesus, T. H., 1994. Effect of solution ionic strength and iron coatings on mineral grains on the sorption of bacterial cells to quartz sand, *Appl. Environ. Microbiol.* 60(9): 3300-3306.

Mills, S. W., Alabaster, G. P., Mara, D. D., Pearson, H. W., and Thitai, W. N., 1992. Efficiency of faecal bacteria removal in waste stabilization ponds in Kenya, *Water Sci. Technol.* 26(7): 1739-1748.

Mitchell, D. O., and Starzyk, M. J., 1975. Survival of *Salmonella* and other indicator microorganisms, *Can. J. Microbiol.* 21: 1420-1421.

Mitchell, R., and Jannagch, H. W., 1969. Processes controlling virus inactivation in seawater, *Environ. Sci. Technol.* 3: 941-943.

Moore, A. C., Herwaldt, B. L., Craun, G. F., Calderon, R. L., Highsmith, A. K., and Juranek, D. D., 1994. Waterborne disease in the United States, 1991-1992, *J. Amer. Water Works Assoc.* 86(2): 87-99.

Morowitz, H. J., 1950. Absorption effects in volume irradiation of microorganisms, *Science* 111: 229-230.

Morris, D. P., Zagarese, H., Williamson, C. E., Balseiro, E. G., Hargreaves, B. R., Modenutti, B., Moeller, R., and Queimalinos, C., 1995. The attenuation of solar UV radiation in lakes and the role of dissolved organic carbon, *Limnol. Oceanogr.* 40(8): 1381-1391.

Moss, S. H., and Smith, K. C., 1981. Membrane damage can be a significant factor in the inactivation of *Escherichia coli* by near ultraviolet radiation, *Photochem. Photobiol.* 33: 541-543.

Munro, P. M., Laumond, F., and Gauthier, M. J., 1987. A previous growth of enteric bacteria on salted medium increased their survival in seawater, *Lett. Appl. Microbiol.* 4: 121-124.

Murray, A. G., and Jackson, G. A., 1993. Viral dynamics II: a model of the interaction of ultraviolet light and mixing processes on virus survival in seawater, *Mar. Ecol. Prog. Series* 102: 105-114.

Murray, J. P., and Laband, S. J., 1979. Degradation of poliovirus by adsorption on inorganic surfaces, *Appl. Environ. Microbiol.* 37(3): 480-486.

Naik, S. R., Aggarwal, A., Sharma, G. L., and Vinayak, V. K., 1982. Effect of salinity, pH, and temperature on the survival of cysts of *Giardia lamblia*, *Indian J. Parasitol.* 6: 231-232.

Nasser, A. M., and Oman, S. D., 1999. Quantitative assessment of the inactivation of pathogenic and indicator viruses in natural water sources, *Water Res.* 33: 1748-1772.

Niemi, M., 1976. Survival of *Escherichia coli* phage T7 in different water types, *Water Res.* 10(9): 751-755.

Noble, R. T., Lee, I. M., and Schiff, K. C., 2004. Inactivation of indicator micro-organisms from various sources of faecal contamination in seawater and freshwater, *J. Appl. Microbiol.* 96: 464-472.

O'Brien, R. T., and Newman, J. S., 1977. Inactivation of polioviruses and coxsackieviruses in surface water, *Appl. Environ. Microbiol.* 33(2): 334-346.

O'Melia, C. R., and Tiller, C. L., 1993. 'Physicochemical aggregation and deposition in aquatic environments', *In* Environmental Particles (J. Buffle and H. P. van Leeuwen, eds.), Vol. 2, pp. 353-386. Lewis Publishers, Boca Raton.

Oliver, D. M., Clegg, C. D., Haygarth, P. M., and Heathwaite, A. L., 2003. Detemrining hydrological pathways for the transfer of potential pathogens from grassland soils to surface waters. *In* "7th International Conference on Diffuse Pollution and Basin Management", pp. 3.36-3.41, Dublin, Ireland.

Omura, T., Onuma, M., and Hashimoto, Y., 1982. Viability and adaptability of *E. coli* and enterococcus group to salt water with high concentration of sodium chloride, *Water Sci. Technol.* 14: 115-126.

Ongerth, J. E., and Pecoraro, J. P., 1996. Electrophoretic mobility of *Cryptosporidium* oocysts and *Giardia* cysts, *J. Environ. Eng.* 122(3): 228-231.

Ongerth, J. E., and Stibbs, H., 1989. Prevalence of *Cryptosporidium* infection in dairy calves in western Washington, *Am. J. Vet. Res.* 50: 1069-1070.

Orlob, G. T., 1956. Viability of sewage bacteria in seawater, *Sew. Indust. Wastes* 28: 1147-1167.

Ottosson, J., and Stenstrom, T. A., 2003. Growth and reduction of microorganisms in sediments collected from a greywater treatment system, *Lett. Appl. Microbiol.* 36: 168-172.

Palmer, M., 1988. Bacterial loadings from resuspended sediments in recreational beaches, *Can. J. Civ. Eng.* 15: 450-455.

Parhad, N. M., and Rao, N. U., 1974. Effect of pH on survival of *Escherichia coli*, *J. Water Pollut. Control Fed.* 46(5): 980-986.

Paulson, C. A., 1970. The mathematical representation of wind speed and temperature profiles in the unstable atmospheric surface layer, *J. Appl. Meteor.* 9: 857-861.

Payment, P., and Franco, E., 1993. *Clostridium perfringens* and somatic coliphages as indicators of the efficiency of drinking water treatment for viruses and protozon cysts, *Appl. Environ. Microbiol.* 59(8): 2418-2424.

Payment, P., Morin, E., and Trudel, M., 1988. Coliphages and enteric viruses in the particulate phase of river water, *Can. J. Microbiol.* 34: 907-910.

Pearson, H. W., Mara, D. D., Mills, S. W., and Smallman, D. J., 1987. Physico-chemical parameters influencing faecal bacterial survival in waste stabilization ponds, *Water Sci. Technol.* 18(10): 145-152.

Pommepuy, M., Guillaud, J. F., Dupray, E., Derrien, A., LeGuyader, F., and Cormier, M., 1992. Enteric bacteria survival factors, *Water Sci. Technol.* 25(12): 93-103.

Power, M. L., Littlefield-Wyer, J., Gordon, D. M., Veal, D. A., and Slade, M. B., 2005. Phenotypic and genotypic characterization of encapsulated *Escherichia coli* isolated from blooms in two Australian lakes, *Environ. Microbiol.* 7(5): 631-640.

Qian, S. S., Donnelly, M., Schmelling, D. C., Messner, M., Linden, K. G., and Cotton, C., 2004. Ultraviolet light inactivation of protozoa in drinking water: a bayesian meta-analysis, *Water Res.* 38: 317-326.

Rajala, R. L., and Heinonen-Tanski, H., 1998. Survival and transfer of faecal indicator organisms of wastewater effluents in receiving lake waters, *Water Sci. Technol.* 38(12): 191-194.

Redman, J. A., Walker, S. L., and Elimelech, M., 2004. Bacterial adhesion and transport in porous media: role of the secondary energy minimum, *Environ. Sci. Technol.* 38: 1777-1785.

Reynolds, C. S., 1984. The ecology of freshwater phytoplankton, Cambridge Univ. Press, Cambridge, 390p.

Rhodes, M. W., and Kator, H. I., 1988. Survival of *Escherichia coli* and *Salmonella* spp. in estuarine environments, *Appl. Environ. Microbiol.* 54(12): 2902-2907.

Rhodes, M. W., and Kator, H. I., 1990. Effects of sunlight and autochthonous microbiota on *Escherichia coli* survival in an estuarine environment, *Curr. Microbiol.* 21: 65-73.

Robertson, L. J., Campbell, A. T., and Smith, H. V., 1992. Survival of *Cryptosporidium parvum* oocysts under various environmental pressures, *Appl. Environ. Microbiol.* 58(11): 3494-3500.

Robson, B. J., and Hamilton, D. P., 2004. Three-dimensional modelling of a *Microcystis* bloom event in the Swan River estuary, Western Australia., *Ecol. Model.* 174: 203-222.

Romero, J. R., Antenucci, J. P., Dallimore, C. J., Horn, D. A., Imberger, J., Feaver, S., Lam, C., and Slawinski, D., 2002. 'Limnological Modeling Systems for Lake Burragorang and Prospect Reservoir: Progress Report 4', Rep. No. WP1717.4JR. Centre for Water Research, Perth, Australia.

Romero, J. R., Antenucci, J. P., and Imberger, J., 2004. One- and three- dimensional biogeochemical simulations of two differing reservoirs, *Ecol. Model.* 174(1): 143-160.

Romero, J. R., Hipsey, M. R., Antenucci, J. P., Hamilton, D. P., and Imberger, J., 2006a. Analysis of primary biogeochemical fluxes in two reservoirs using DYRESM-CAEDYM, manuscript in review.

Romero, J. R., Imberger, J., Antenucci, J. P., and Dallimore, C. J., 2006b. ARMS (Aquatic Real-time Management System): An automated decision support system for lakes, estuaries and coastal zones. *In* "2nd Intl. Symp. Mangt. Engin. Informatics (MEI)", Orlando, Florida.

Roper, M. M., and Marshall, K. C., 1978. Biological control agents of sewage bacteria in marine habitats, *Aust. J. Mar. Freshwater Res.* 29: 335-343.

Ross, T., Ratkowsky, D. A., Mellefont, T. A., and McMeekin, T. A., 2003. Modelling the effects of temperature, water activity, pH and lactic acid concentration on the growth rate of *Escherichia coli*, *Intl. J. Food Microbiol.* 82: 33-43.

Rossi, P., and Aragno, M., 1999. Analysis of bacteriophage inactivation and its attenuation by adsorption onto colloidal particles by batch agitation techniques, *Can. J. Microbiol.* 45: 9-17.

Rozen, Y., and Belkin, S., 2005. 'Survival of enteric bacteria in seawater: Molecular aspects', *In* Oceans and health: pathogens in the marine environment (S. Belkin and R. R. Colwell, eds.), pp. 93-108. Springer, New York.

Salomon, J. C., and Pommepuy, M., 1990. Mathematical model of bacterial contamination of the Morlaix Estuary (France), *Water Res.* 24(8): 983-994.

Salter, M. A., Ratkowsky, D. A., Ross, T., and McMeekin, T. A., 2000. Modelling the combined temperature and salt (NaCl) limits for growth of a pathogenic *Escherichia coli* strain using nonlinear logistic regression, *Intl. J. Food Microbiol.* 61: 159-167.

Sarikaya, H. Z., and Saatchi, A. M., 1995. Bacterial die-away rates in Red Sea waters, *Water Sci. Technol.* 32(2): 45-52.

Savage, H. P., and Hanes, N. B., 1971. Toxicity of seawater to coliform bacteria, *J. Water Pollut. Control Fed.* 43(5): 855-861.

Scarce, L. E., Rubenstein, S. H., and Megregian, S., 1964. Survival of indicator bacteria in receiving waters under various conditions. *In* "7th Conference on Great Lakes Research", Vol. 11, pp. 130-139. Great Lakes Research Institute, Ann Arbor, Michigan.

Scholl, M. A., Mills, A. L., Herman, J. S., and Hornberger, G. M., 1990. The influence of mineralogy and solution chemistry on the attachment of bacteria to representative aquifer materials, *J Contam. Hydrol.* 6: 321-336.

Scott, D. M., 2000. Fecal coliform decay in an anaerobic dairy wastewater environment, MSc thesis, Louisiana State University, Louisiana.

Shirais, M. P., Rex, A. C., Pettibone, G. W., Keay, K., McManus, P., Rex, M. A., Ebersole, J., and Gallagher, E., 1987. Distribution of indicator bacteria and *Vibrio parahaemolyticus* in sewage-polluted intertidal sediments, *Appl. Environ. Microbiol.* 53: 1756-1761.

Sinton, L. W., 2005. 'Biotic and abiotic effects', *In* Oceans and health: pathogens in the marine environment (S. Belkin and R. R. Colwell, eds.), pp. 69-92. Springer, New York.

Sinton, L. W., Davies-Colley, R. J., and Bell, R. G., 1994. Inactivation of enterococci and fecal coliforms from sewage and meatworks effluent in seawater chambers, *Appl. Environ. Microbiol.* 60(6): 2040-2048.

Sinton, L. W., Finlay, R. K., and Lynch, P. A., 1999. Sunlight inactivation of fecal bacteriophages and bacteria in sewage-polluted seawater, *Appl. Environ. Microbiol.* 65(8): 3605-3613.

Sinton, L. W., Hall, C. H., Lynch, P. A., and Davies-Colley, R. J., 2002. Sunlight inactivation of fecal indicator bacteria and bacteriophages from waste stabilization pond effluent in fresh and saline waters, *Appl. Environ. Microbiol.* 68(3): 1122-1131.

Slifko, T. R., Raghubeer, E., and Rose, J. B., 2000. Effect of high hydrostatic pressure on *Cryptosporidium parvum* infectivity, *J. Food Protect.* 63(9): 1262-1267.

Solic, M., and Krstulovic, N., 1992. Separate and combined effects of solar radiation, temperature, salinity and pH on the survival of faecal coliforms in seawater, *Mar. Pollut. Bull.* 24(8): 411-416.

Solo-Gabriele, H. M., Wolfert, M. A., Desmarais, T. R., and Palmer, C. J., 2000. Sources of *Escherichia coli* in a coastal subtropical environment, *Appl. Environ. Microbiol.* 66(1): 230-237.

Spillman, C. M., Imberger, J., Hamilton, D. P., Hipsey, M. R., and Romero, J. R., 2007. Modelling the effects of Po River discharge, internal nutrient cycling and hydrodynamics on biogeochemistry of the Northern Adriatic Sea, *J. Mar. Sys.* in press.

Steets, B. M., and Holden, P. A., 2003. A mechanistic model of runoff-associated fecal coliform fate and transport through a coastal lagoon, *Water Res.* 37: 589-608.

Stetler, R. E., 1984. Coliphages as indicators of enteroviruses, *Appl. Environ. Microbiol.* 48(3): 668-676.

Stott, R., May, E., Matsushita, E., and Warren, A., 2001. Protozoan predation as a mechanism for the removal of *Cryptosporidium* oocysts from wastewaters in constructed wetlands, *Water Sci. Technol.* 44(11-12): 191-198.

Strub, P. T., and Powell, T. M., 1987. Surface temperature and transport in Lake Tahoe: inferences from satellite (AVHRR) imagery, *Continental Shelf Res.* 7: 1001-1013.

Struck, P. H., 1998. The relationship between sediment fecal coliform levels in a Puget Sound estuary, *J. Environ. Health* 50: 403-407.

Tartera, C., Lucena, F., and Jofre, J., 1989. Human origin of *Bacteroides fragilis* bacteriophage present in the environment, *Appl. Environ. Microbiol.* 55: 2696-2701.

Thomas, D., Kotz, S., and Rixon, S., 1999. 'Watercourse survey and management recommendations for the Myponga River catchment'. Environmental Protection Agency, Adelaide, Australia.

UNESCO, 1981. 'Oceanographic tables and standards', Rep. No. 36, Sidney, Canada.

van der Kooij, D., 2003. 'Managing regrowth in drinking-water distribution systems', *In* Heterotrophic plate counts and drinking-water safety (J. Bartram, J. Cotruvo, M. Exner, C. Fricker and A. Glasmacher, eds.), pp. 199-232. IWA Publishing, London, UK.

Van Donsel, D. J., and Geldreich, E. E., 1971. Relationship of salmonellae to fecal coliforms in bottom sediments, *Water Res.* 5: 1079-1087.

Vasconcelos, G. J., and Swartz, R. G., 1976. Survival of bacteria in seawater using a diffusion chamber apparatus *in situ*, *Appl. Environ. Microbiol.* 31(6): 913-920.

Vaze, J., and Chiew, F. H. S., 2004. Nutrient loads associated with different sediment sizes in urban stormwater and surface pollutants, *J. Environ. Eng.* 130: 391-396.

Verwey, E. J. W., and Overbeck, J. T. G., 1948. Theory of the stability of lyophobic colloids, Elsevier, Amsterdam, 205p.

Walker, F. R., and Stedinger, J. R., 1999. Fate and transport model of *Cryptosporidium*, *J. Environ. Eng.* 125(4): 325-333.

Walker, M., Leddy, K., and Hagar, E., 2001. Effects of combined water potential and temperature stresses on *Cryptosporidium parvum* oocycts, *Appl. Environ. Microbiol.* 67(12): 5526-5529.

Walker, M. J., Montemagno, C. D., and Jenkins, M. B., 1998. Source water assessment and non-point source of acutely toxic contaminants: A review of research related to survival and transport of *Cryptosporidium parvum*, *Water Resour. Res.* 34(12): 3383-3392.

Walker, S. G., Flemming, C. A., Ferris, F. G., Beveridge, T. J., and Bailey, G. W., 1989. Physiochemical interaction of *Escherichia coli* cell envelopes and *Bacillus subtilis* cell walls with two clays and ability of the composite to immobilize heavy metals from solution, *Appl. Environ. Microbiol.* 55(11): 2976-2984.

Webb, R. B., and Brown, M. S., 1979. Action spectra for oxygen-dependent and independent activation of *Escherichia coli* WP2s from 254 to 460 nm, *Photochem. Photobiol.* 29: 407-409.

Webb, R. B., and Lorenz, J. R., 1970. Oxygen dependence and repair of lethal effects of near ultraviolet and visible light, *Photochem. Photobiol.* 12: 383-389.

Weiss, C. M., 1951. Adsorption of *Escherichia coli* on river and estuarine silts, *Sew. Indust. Wastes* 23: 227-237.

Whitman, R. L., and Nevers, M. B., 2003. Foreshore sand as a source of *Escherichia coli* in nearshore water of a Lake Michigan beach, *Appl. Environ. Microbiol.* 69(9): 5555-5562.

Wilkinson, J., Jenkins, A., Wyer, M., and Kay, D., 1995. Modelling faecal coliform dynamics in streams and rivers, *Water Res.* 29(3): 847-855.

Withers, N., and Drikas, M., 1998. Bacterial regrowth potential: quantitative measure by acetate carbon equivalents, *Water* 25: 19-23.

Yates, M. V., Stetzenbach, L. D., Gerba, C. P., and Sinclair, N. A., 1990. The effect of indigenous bacteria on virus survival in ground water, *J. Environ. Sci. Health* A25: 81-100.

Yee, N., Fein, J. B., and Daughney, C. J., 2000. Experimental study of the pH, ionic strength, and reversibility behavior of bacteria-mineral adsorption, *Geochemica et Cosmochimica Acta* 64(4): 609-617.

Zanoni, B., Garzaroli, C., Anselmi, S., and Rondinini, G., 1993. Modeling the growth of *Enterococcus faecium* in bologna sausage, *Appl. Environ. Microbiol.* 59(10): 3411-3417.

Zuckerman, U., Gold, D., Shelef, G., and Armon, R., 1997. The presence of *Giardia* and *Cryptosporidium* in surface waters and effluents in Israel, *Water Sci. Technol.* 25(11-12): 381-384.